Effect of Liquid Drop-out on the Productivity of a Rich Gas Condensate Reservoir

by

Olalekan Kayode Fawumi

A Thesis Presented to the

FACULTY OF THE COLLEGE OF GRADUATE STUDIES

KING FAHD UNIVERSITY OF PETROLEUM & MINERALS

DHAHRAN, SAUDI ARABIA

In Partial Fulfillment of the
Requirements for the Degree of

MASTER OF SCIENCE

In

PETROLEUM ENGINEERING

December, 1999

INFORMATION TO USERS

This manuscript has been reproduced from the microfilm master. UMI films the text directly from the original or copy submitted. Thus, some thesis and dissertation copies are in typewriter face, while others may be from any type of computer printer.

The quality of this reproduction is dependent upon the quality of the copy submitted. Broken or indistinct print, colored or poor quality illustrations and photographs, print bleedthrough, substandard margins, and improper alignment can adversely affect reproduction.

In the unlikely event that the author did not send UMI a complete manuscript and there are missing pages, these will be noted. Also, if unauthorized copyright material had to be removed, a note will indicate the deletion.

Oversize materials (e.g., maps, drawings, charts) are reproduced by sectioning the original, beginning at the upper left-hand corner and continuing from left to right in equal sections with small overlaps.

Photographs included in the original manuscript have been reproduced xerographically in this copy. Higher quality 6" x 9" black and white photographic prints are available for any photographs or illustrations appearing in this copy for an additional charge. Contact UMI directly to order.

Bell & Howell Information and Learning
300 North Zeeb Road, Ann Arbor, MI 48106-1346 USA

UMI®
800-521-0600

Effect of Liquid Drop-out on the Productivity of a Rich Gas Condensate Reservoir

BY

OLALEKAN KAYODE FAWUMI

A Thesis Presented to the

DEANSHIP OF GRADUATE STUDIES

KING FAHD UNIVERSITY OF PETROLEUM & MINERALS

DHAHRAN, SAUDI ARABIA

In Partial Fulfillment of the
Requirements for the Degree of

MASTER OF SCIENCE

In

PETROLEUM ENGINEERING

DECEMBER 1999

KING FAHD UNIVERSITY OF PETROLEUM AND MINERALS, DHAHRAN, SAUDI ARABIA

COLLEGE OF GRADUATE STUDIES

This thesis, written by Mr. Olalekan kayode Fawumi under the direction of his Thesis Advisor and approved by his Thesis Committee, has been presented to and accepted by the Dean of the College of Graduate Studies, in partial fulfillment of the requirements for the degree of MASTER OF SCIENCE in Petroleum Engineering.

Thesis Committee:

Dr. Hasan S. Al-Hashim
Thesis Advisor

Dr. Hasan Y. Al-Yousef
Member

Dr. Abdulaziz A. Al-Majed
Member

Dr. Habib Menouar
Member

Dr. Abdulaziz A. Al-Majed
Department Chairman

29-12-09

Dr. Abdulla A.M. Al-Shehri
Dean, College of Graduate Studies

Dedicated to my family and friends.

ACKNOWLEDGEMENTS

I am grateful to God for granting me the grace to complete this thesis.

I acknowledge the financial support provided to me by King Fahd University of Petroleum and Minerals throughout the period of my study. My sincere appreciation goes to Dr. Hasan S. Al-Hashim for serving as my thesis advisor and committee chairman. He went to any length to make this research fruitful and gave me all necessary support required. He is always available and he offered useful suggestions throughout the period of the research. I am indeed grateful.

I am taking this opportunity to thank the committee members, Dr. Hasan Al-Yousef, Dr. Habib Menouar and Dr. Abdulaziz A. Al-Majed, for the assistance, guidance and useful suggestions they gave throughout the time I was working on this thesis.

I appreciate the assistance of Dr. Don Chan and Faith McKnew of Chevron Petroleum Technology U.S.A., Hsu Ho-Jeen of Chevron Kuwait, Dr. Hasan Al-Yousef, Mr. Bin Fuseni and Mr. Wajid of the Research Institute at King Fahd University of Petroleum and Minerals. They provided me with technical assistance on CHEARS compositional reservoir simulator.

I am also grateful for the patience and understanding of my family in Nigeria, my friends, staff and all faculty of Petroleum Engineering Department.

TABLE OF CONTENTS

LIST OF TABLES

LIST OF FIGURES

THESIS ABSTRACT

NAME OF STUDENT	OLALEKAN KAYODE FAWUMI
TITLE OF STUDY	Effect of Liquid Drop-out on the Productivity of a Rich Gas Condensate Reservoir
MAJOR FIELD	PETROLEUM ENGINEERING
DATE OF DEGREE	DECEMBER, 1999

A 2-D radial compositional simulator was used to investigate the effect of liquid drop out on the productivity of a rich gas condensate reservoir. A seven layer reservoir model was constructed based on well logs and core analysis data. A two phase relative permeability model was used to generate the relative permeability curves for the oil and gas phases assuming the initial water saturation is immobile. The pore size distribution index required in the relative permeability model was calculated by finding the slope of the log-log plot of the J-function versus normalized water saturation obtained from the air displacing brine experiment. Major objective of this study includes identification of parameter controlling the productivity of the gas condensate well, evaluation of the effect of condensate drop-out near the wellbore on well productivity, determination of optimum production rate and investigation of the extent of condensate banks in different layers. It was concluded that gas condensate well productivity is reduced as the critical condensate saturation increases. Gas production rate more than 40MMSCF/D offers no significant improvement on cumulative gas and condensate produced, Ninety one percent (91%) reduction in gas flow productivity was observed for all production rates investigated. The percent liquid condensed near the wellbore in all layers ranged between 37 to 44 percent and there are noticeable changes in pressure distribution near the wellbore in all layers though it remains the same at a distance more than 100 ft away from the wellbore.

ملخص الرسالة

الاســـــــــم : أوليكان كايودى فايومى

عنوان الرسالة : تأثير تساقط على إنتاجية مكامن المتكثفات الغازية الغنية

التخصـــــــص : هندسة البترول

تاريخ الدرجـة : ديسمبر ١٩٩٩م

استخدم محاكى قطرى ثنائي الأبعاد لدراسة تأثير تساقط السوائل على إنتاجية مكامن المتكثفات الغازية ذات التشبع العالي . وأنشئ نموذج لمكن سباعي الطبقات بناء على سجلات الآبار وبيانات تحليل العينات . واستخدم نموذج النفاذية النسبية ثنائي الأطوار لتوليد منحنيات النفاذية النسبية لطورى الغاز والزيت بفرض أن تركيز الماء الأولي غير قابل للإنتاج ، وتم حساب دليل توزيع حجم المسام المطلوب في نموذج النفاذية النسبية بايجاد ميل دالة – J عند رسمها على محاور لوغاريثم – لوغاريثم مع تركيز الماء المعدل والمتحصل عليه من تجربة إزاحة الماء بالهواء . ومن أهم أهداف الدراسة هو تحديد المتغيرات التي تتحكم في إنتاجية بئر المتكثف الغازي ، تحديد معدل الإنتاج الأمثل ، تقييم تأثير تساقط المتكثف بالقرب من قاع البئر على إنتاجية البئر ، والبحث في امتداد ضفاف المتكثفات في الطبقات المختلفة . وقد لوحظ أن إنتاجية بئر المتكثف الغازي يقل بزيادة تركيز المتكثف الحرج ، كما وأن معدل إنتاج الغاز بأعلى من ٤٠ مليون قدم مكعب في اليوم لا يعطي تحسن ملحوظ في إنتاج الغاز التراكمي ، وقد لوحظ انخفاض في إنتاجية الغاز الساري بمقدار ٩١% مع جميع معدلات الإنتاج قيد الدراسة ، وكما لوحظ بأن النسبة المئوية للمتكثف السائل بالقرب من قاع البئر في كل الطبقات تتراوح بين ٣٧% – ٤٤% أما الضغط بالقرب من قاع البئر فقد وجد أنه يتغير بتغير المسافة في كل الطبقات مع أنه يظل ثابت على مسافة أكثر من ١٠٠ قدم بعيد عن قاع البئر .

CHAPTER 1

INTRODUCTION

The depletion of a rich or lean gas condensate reservoir to pressures below the dew point has become a research interest to reservoir engineers as deeper and hotter hydrocarbon reservoirs are being exploited [1,2]. Predicting the recovery of gas and liquids from a rich gas condensate field requires the understanding of the thermodynamics of the fluid systems and the law governing their flow through the porous medium [3].

Well productivity loss is a critical issue in the development of many gas condensate reservoirs when the reservoir pressures fall below the dew point pressure. Pressure decline below the dew point pressure causes condensation to occur and liquid hydrocarbon saturation builds up around the wellbore leading to significant reduction in the inflow performance of gas condensate well even if the reservoir fluid is lean [4,5]. Several examples of severe productivity loss are available in the literature [2].

Predictions of gas condensate well performance require accurate modeling of the gas condensate relative permeability in the two phase region near the wellbore with the relative permeability often modeled as a function of interfacial tension, capillary number, bond number or it's generalization, trapping number [6]. Improvement in mobility at high capillary number is the most significant of the special phenomena affecting the near

Reservoir simulation studies have been used to predict the performance of many gas condensate reservoirs using compositional reservoir simulators. The effect of fluid velocities, viscosity's, interfacial tensions, and permeability of the reservoir rock on the saturation required to initiate condensate flow from the reservoir, has not been extensively investigated [20]. The reservoir fluid description is an important factor that affects the accuracy of a reservoir simulation study because of the complexity of the mass transfer between phases. To cope with the complicated phase behavior of gas normally encountered in gas condensate reservoir, an equation of state is often used in the simulator. Examples of equations of state commonly used are the Peng Robinson and Redlich Kwong equations of state.

The main Objective of this study is to investigate the effect of condensate liquid drop out on the productivity of a layered, tight, and rich condensate reservoir in the Kingdom of Saudi Arabia. Apart from the main objective, the following specific objectives will be investigated:

1. Identification of the parameters controlling the productivity of the gas condensate well.
2. Evaluate the effect of condensate drop out near the wellbore on the productivity of the gas condensate well.
3. Determination of the optimum production rate to achieve the optimum phase production from the gas condensate reservoir.

4. Investigate the extent of the condensate banks in different layers.

In order to achieve the above objectives, a multi-layer single well radial compositional model will be used to carry out this study.

In the next chapter, a review of the previous work related to gas condensate reservoir will be presented. The current methods used to predict the gas condensate well performance is also reviewed. In chapter 3, the petrophysical and core analysis is done with the aim of obtaining the reservoir geological model while chapter 4 is centered on the condensate fluid samples analysis. The relative permeability models considered are discussed in chapter 5. The results, interpretations, conclusions and recommendations are presented in chapters 6 and 7.

CHAPTER 2

LITERATURE REVIEW

The prediction of the performance of gas condensate reservoir especially when the flowing bottom hole pressure is below the dew point has been studied widely in recent years. These studies were aimed at accurately predicting the productivity impairment due to the near well bore build up of condensate liquid saturation. In this chapter, a thorough literature review is done and discussed.

Morel et al [1] conducted experimental investigation to understand the behavior of gas condensate fluid in the far field region. He used three long composite cores for the study at reservoir condition but the rate is low. This depletion test was done to measure the critical condensate saturation, relative permeability and to model the mobility of the condensed phase. The three tests were simulated with Eclipse E300 compositional reservoir simulator with the Peng Robinson equation of state used for the PVT behavior of the fluid. He concluded that the critical condensate saturation and the relative permeability, inverse of the bond number and the variation of the relative permeability with interfacial tension are the key parameters to be measured in order to evaluate the possible recovery of the deposited condensed phase in gas condensate reservoirs.

Barnum et al [2] studied gas condensate reservoir by evaluating the historical frequency and severity of productivity impairment due to near wellbore condensate buildup and identification of reservoir parameters associated with severe productivity and recovery reduction. They used a single well fully coupled semi-implicit volatile oil model

to simulate the performance of gas condensate well during pressure depletion. They concluded that condensation of hydrocarbon liquids in the gas condensate reservoirs can severely restricts gas productivity and that the potential for significant loss in gas recovery exist when the initial permeability thickness (kh) is less than 1000 md-ft over a range of condensate yields.

Morel et al [3] conducted a depletion experiment at bottom hole condition on vertically stacked composite core at a continuous withdrawal rate of 2 cc/day and a pressure of 1 bar/day at the beginning and 0.5 bar/day at the end. The depletion experiment was simulated using the Peng Robinson equation of state in $\sum CORE$ compositional reservoir simulator. They concluded from the study that knowing the mobility of the condensate phase is important in deciding the field recovery scheme.

Boom et al [4] conducted mobility experiment and a single well radial compositional reservoir simulation using MORES (shell group simulator) on gas condensate reservoir. They concluded that condensate mobility improvement is the main uncertainty in the prediction of well deliverability for a gas/condensate reservoir. In addition, the mobility experiment clearly shows that the controlling parameter for the mobility improvement is the bond number and it is the equivalent of capillary number in the field and not interfacial tension alone.

Robert Mott [5] used single well radial compositional simulation model to study the near well condensation behavior of a lean North Sea gas condensate reservoir. He found that liquid drop out in the near wellbore region causes significant loss in productivity even for lean condensate fluids. The most important parameters determining productivity loss in a gas condensate reservoir are the gas-oil relative permeability curves and high capillary number. The high capillary number can affect the relative permeability so the effect should be considered in the simulation model. He suggested that the relative permeability should be measured at conditions representative of the near well region and that pseudopressure technique provides a convenient and accurate means of modeling the well productivity in full field simulations.

Pope et al [6] showed that the relative permeability and productivity index of gas condensate wells can be significantly reduced if condensate builds up near the wellbore thus accurate modeling of relative permeability is important for the prediction of gas/gas condensate well performance. A compositional reservoir simulator "UTCOMP" was used to study the effect of trapping number on the productivity of a single well in a gas condensate reservoir with a solution domain of two dimensional vertical cross-section (x-z) and a fan shape at an angle of 36^0. They concluded that residual saturation, end point relative permeability and relative permeability of gas/gas condensate should be modeled as a function of trapping number rather than interfacial tension. The study did not consider non-Darcy flow effect in the simulation despite the fact that non-Darcy effect becomes significant at high flow rate.

Fussel [7] described the use of the modified version of 1-D radial compositional model developed by Roebuck et al [53-55] to study long term single well performance in three gas condensate reservoirs. He concluded that the productivity of a gas condensate well can be reduced owing to condensate accumulation in the near wellbore region and that the radial model has advantage over the steady state predictions for many predictions.

Leemput et al [8] conducted full field compositional simulation studies of the central Oman gas condensate field using the Shell in house Simulator "MoRes". They concluded that not all the physical processes in gas condensate fields could be represented in full field models especially near the wellbore. Well parameters generation and well test matching indicate that well deliverability reduce significantly due to near wellbore condensate precipitation. Capillary number dependent relative permeability modeled in single well can also be applied in full field model. The most important parameters determining recovery and productivity decline in the Barik and Saih Rawl reservoirs are reservoir permeability, Well productivity and fluid composition.

Boom et al [9] found limited field documented cases of productivity impairment due to condensate drop out in the literature and they attributed this to enhancement of the gas/gas condensate mobility in the near wellbore conditions. The focus of their research is on the experimental quantification of the mobility enhancement, identification of the controlling parameter(s) and incorporation of this mobility enhancement in the reservoir model that will lead to a better assessment of the productivity impairment due to

condensate build up near the wellbore. A model experiment was used to assess the enhanced gas/gas condensate mobility under near wellbore flow conditions. In addition, results from a fine grid reservoir simulation were shown to highlight the impact of enhancement on condensate banking and gas/gas condensate production forecast. They concluded that enhancement in condensate mobility at near wellbore conditions is caused by capillary number and not interfacial tension alone.

Malachowski et al [10] proposed an alternative simulation method which accurately computes condensate blockage effects in multi-well, full-field simulations without local grid refinement. The method used correlations of pseudoskins that can be combined with the general well function to capture the effect of well productivity losses. In all the simulations they did, the ARKES equations of state was used and they concluded that the pseudoskins correlations are useful in computing the well productivity losses in field scale simulations hence there is no need of local grid refinement of the near wellbore.

Fevang and Whitson [11] proposed a pseudopressure deliverability model that can reproduce the fine grid well simulations almost exactly. A simple method was developed to solve the pseudopressure integrals according to the approach proposed by Evinger and Muskat [56] for solution gas drive wells. The producing GOR is needed to calculate the pseudopressure. The gas condensate rate is calculated using the proposed pseudopressure method and they have successfully tested it for radial, vertically fractured and horizontal wells. They concluded that there are three flow regions in a gas condensate well and that

region1 is the main source of deliverability loss in a gas condensate well. In addition, they found out that local grid refinement near wells is not necessary in gas condensate wells and that critical oil saturation has no effect on gas condensate well deliverability.

Clark [12] studied Anschutz Ranch East retrograde condensate reservoir. The west lobe unit is the productive zone of interest where the flowing bottom hole pressure was limited to 3500 psi and the unit is also undergoing injection program to maximize hydrocarbon liquid recovery. There was a breakthrough of the injection gas at the producing wells complicating the analysis of the well producing behavior. A simulation work was done to understand the producing characteristics of wells in the west lobe using a two dimensional (2-D) compositional, single well radial model. The system comprises of nine components fluids description with the modified Redlich-Kwong equation of state used in the simulator to predict the phase equilibra. The eleven layer reservoir description used in the single well model was base on stratigraphy and other reservoir parameters derived from core analysis. They concluded that there would be no detrimental effect on condensate recovery if the unit imposed 3500psi flowing bottom hole pressure is removed and that the gas breakthrough is the result of lower gas viscosity and higher gas relative permeability in the breakthrough layer.

Novosad [13] analyzed the depletion of two retrograde gas reservoirs; a tight formation bearing a lean saturates fluid and a high-permeability reservoir with a rich undersaturated fluid. He used a 1D, single well radial compositional model to investigate the changes in well performance due to liquid drop out. He found out that the

thermodynamic path of depletion in a gas condensate reservoir is quite complex involving transition from a retrograde gas to an oil and back to a gas. A near well liquid accumulation forms within hours of bottom hole flowing pressure falling below the dew point pressure (this is true for both lean and rich fluids) and that in low formation permeability, the transient rate decline can mask the productivity decline caused by condensate drop out.

Mohammadi et al [14] developed mathematical models to investigate the process of pressure depletion for a gas condensate system and the development of relative permeability's for a gas and condensate fluids in the absence of gravitational effects. They concluded that impairment to the gas relative permeability due to condensate dropout follows the imbibition oil relative permeability closely and that no significant hysteresis is observed for the gas or condensate liquid relative permeability in the condensate/vaporization cycle. In addition, they found out that both gas and liquid relative permeability moved to higher total wetting phase saturation when the liquid phase trapping is incorporated into the model.

Dyung et al [15] examined the behavior of a gas condensate reservoir both above and below the dew point pressure by applying the result of the work of Jones and Raghavan [57]. They examined the applicability of the conventional material balance equation to predict reserves, the methods to compute the well deliverability in condensate reservoirs and the changes in saturation and composition that takes place during build up tests. They showed that the average reservoir pressure and total skin factor computed

with single phase gas analog can be used to predict well deliverability and correlated the radius of the two phase region as a function of time in terms of the Aronofsky-Jenkins drainage radius concept. The radius of the two phase region can be estimated from the pressure build up data. In addition, a practical procedure to compute the appropriate two phase compressibility factor was presented and they concluded, on the basis of β model simulations, that the phase behavior of gas condensate systems in the vicinity of the well is similar to that of solution gas reservoir.

Hidde [16] studied the effect of low interfacial tensions on the relative permeabilities in some gas condensate systems. He showed that a C_1-C_3 near critical fluid system goes through a cahn transition. He used simple flow model to see how the wetting transition affects the relative permeability curves in the near critical domain. Two flow models were used namely the Poiseulle flow model for big pores under film flow conditions and the Bingham formalism model for the small pores. He concluded that a cahn transition takes place for a C_1-C_3 at σ = 0.3 mN/m leading to core annular flow regime for pores with a channel radius greater than 0.1E-6m. Straightening of relative permeability curves for a near-critical fluid starts around the cahn transition. Einstein Emulsion contribution to relative permeability is identifiable at the saturation extremes leading to asymmetric straightening of relative permeability curves in the core annular flow regime and that capillary condensation might occur in the milli-darcy range for near critical fluids.

Kim [17] studied a rich gas condensate reservoir located in lower permian wolfcamp and upper Pennsylvanian strawn formations at a depth of 10,000ft. Mobil Corporation devised an optimal depletion plan for the reservoir and a compositional simulation model was chosen to study the Coyanosa Wolcamp Field Gas cycling Operation. The objective of the study being optimization of condensate liquid recovery. The sensitivity of the liquid recovery to pressure, rate and degree of cycling was investigated. Depletion plans such as added compression, immediate blow down and partial cycling were evaluated. The phase behavior of a unit member of the gas reservoir fluid in Cayonosa Wolfcamp filed was accurately characterized with the fluid analysis of the Sibley No.1 well in Wolfcamp field in 1963. The characterization indicates a rich gas condensate system at a reservoir temperature of 175°F, dew point pressure of 6,179 psia and initial reservoir pressure of 6,700 psia. They were able to match the past twenty-three years' reservoir performance of the field and used the compositional simulation study to predict the future performance of the reservoir. They concluded that gas injection with selective zonal perforations will yield more condensate reserve compared to a base depletion plan though 7% to 16% of initial gas condensate remains for all scenarios considered hence an economic evaluation of the study results was required to determine an optimum depletion plan.

Lindeberg et al [18] measured the low interfacial tension and the sum of gas and liquid viscosity's in a low IFT real gas condensate system at high pressure and temperature using a laser light scattering technique. The measured IFT values were

found to be three to six times as large as the values predicted by a PVT simulator using compositional data and the Weinaug-Katz correlation. They concluded that procedures often used to predict the IFT's perform rather badly at low IFT's hence there is need for good experimental data on low IFT gas condensate systems. This confirms the conclusions drawn from previous measurements on synthetic gas condensate systems at lower pressure and temperature conditions. They also found that the interface laser-light scattering technique has measurement accuracy within 4%. This 4% uncertainty was due mainly to the uncertainties in the density values used as input parameters in the data analysis. Therefore, accurate density data are required to reduce the uncertainty in accuracy of the technique.

Phillip [19] worked on the engineering applications of phase behavior of crude oil and gas condensate reservoirs and identified that surface/separator and subsurface are the two basic methods of collecting the fluid samples required for compositional analysis of gas condensate systems. He emphasized that great care must be taken in preparing a well for sampling and that a reservoir must be sampled before a significant loss in pressure is experienced by the reservoir. The two conditions must be adhered to if representative sample of reservoir fluids must be obtained. He concluded that the reservoir fluid studies performed in the laboratory require that laboratory personnel and reservoir engineer are sure of character of reservoir fluids. This is important because he must not treat a near critical fluid sample as a black oil else the result that will be obtained will under-estimate the producing potential of the field.

Henderson et al [20] carried out vertical and horizontal long core experiments at reservoir conditions to study the flow of gas and condensate in the area of the reservoir close to the wellbore and the region of the reservoir away from the producing wells. The gas and condensate flow rates are increased from capillary dominated to viscous dominated in order to observe the effect of flow rate on flow and recovery. They investigated the effect of rate on equilibrium gas injection, fluid distribution, and permeability on the gas/condensate recovery. They observed that as flow of gas approach the area around the wellbore, the flow rate of gas and condensate would be determined by the production rate. The flow in this region being increasingly viscous dominated as opposed to increasingly capillary and gravity dominated with distance from the wellbore. The results of the horizontal core tests shows that mobility of condensate in the area around the wellbore may be greater than previously assumed and while the vertical core tests shows that the reduction of the condensate saturation by drainage can be considerable in the gravity/capillary dominated flow regime.

Gerard et al [21] identified that the process of evaluating and assessing a reservoir early in its development is difficult and uncertain though the results of the evaluation may have far reaching consequences for the reservoir. They proposed, described and applied a methodology for enhancing this assessment for a gas condensate reservoir whose choice of recovery process (depletion or gas cycling) has not yet been determined. They proposed identification and quantification of key heterogeneity's, development of models representing the full breadth of variations in heterogeneity, the detailed modeling of limited areas of the reservoir to assess the effects of the model and geologic uncertainties,

and the use of these results for calibrating up-scaled full-field models. They concluded that key heterogeneity is different since they depend on the recovery process adopted.

Hsu and Ponting [22] did a field wide compositional simulation for a high pressure and high temperature gas condensate reservoirs in the Central Graben region of the North Sea using an adaptive implicit method. The recovery mechanisms of the gas condensate reservoir consist of pressure depletion, rock compaction and condensate banking near a wellbore. The main challenges in simulating the HPHT gas condensate reservoir are to account for the permeability reduction due to rock compaction and the productivity loss due to condensate drop out near a wellbore when the reservoir pressure falls below the dew point pressure. They concluded that the degree of condensate banking depends on the relative permeability and the impact of rock compaction is more profound at lower rock permeability.

Guo et al [23] identified the contradiction in the literature on the effect of porous media on the dew point pressure of a gas condensate system in the laboratory or a real gas formation. They think the influence of porous media on phase behavior is different in real gas reservoir and laboratory PVT cells. The phenomenon was explained through the use of a new theory model that considers the effect of capillary pressure and adsorption in porous media. They concluded that in a real formation, there could be an increase, decrease and no influence at all of capillary pressure and adsorption on the dew point pressure of a gas condensate system. Meanwhile, in the laboratory, the effect of porous

decrease and no influence at all of capillary pressure and adsorption on the dew point pressure of a gas condensate system. Meanwhile, in the laboratory, the effect of porous media is not evident because the permeability and porosity of the media used are generally high.

Kalaydjian et al [24] conducted experimental studies on alterations that occur to flow parameters of a gas condensate reservoir as the wellbore is being approached. The parameter studied includes the critical liquid saturation, relative permeability's, Darcy and Non-Darcy flow effects. They concluded that the capillary number dependence of relative permeability near the wellbore is probably not valid, that the critical liquid saturation's and gas condensate relative permeability's were found to be comparable justifying using analog instead of real fluids. They also concluded that the critical liquid saturation increases with interfacial tension and that the gas relative permeability was found to exhibit hysteresis between drainage and imbibition. In addition, they found that the dependence of gas condensate relative permeability's on flow rates is based on the competition between capillary and viscous forces and that flow regimes near the wellbore region are characterized by local turbulence-like effects which involves macroscopic non-Darcy flow terms.

Henderson et al [25] conducted steady state relative permeability experiments to study the sensitivity of relative permeability to velocity, rate hysteresis and end effects. They concluded that the relative permeability is rate sensitive. The gas and condensate relative permeability increased as the velocity increased. They also observed that the rate

high IFT though the relative permeabilities are reduced and that hysteresis becomes pronounced with increasing IFT.

Ali, McGauley and Wilson [26] conducted studies to evaluate the characteristic effects of immobile and mobile condensate saturation's on the mobility of gas in the near wellbore region. The gas flow rates studied span both the Darcy and non-Darcy flow regimes but they developed correlation's that can be used to model the effect of high velocity flow in gas condensate reservoir. The methods of study are both experimental and numerical simulation. The laboratory measurements were done using a coreflooding rig while the simulation work was done using the three cell variable model derived from the work of Al-Majed and Dougherty. In addition, the authors constructed a conventional 1-D single well radial model on Eclipse E300 compositional simulator for comparison. They concluded that the non-Darcy gas coefficient, β is dependent on the saturation and distribution of the immobile liquid and that significant errors will result if published correlations for dry cores or immobile water saturation are used to predict the β value for gas flow in the presence of gas condensate. They also observed that the β value obtained on several core samples for heterogeneous or layered reservoirs need to be averaged before being applied in the radial flow equations.

Thomas et al [27] described the phenomena at work in rich gas condensate reservoirs. The study is a summary of the authors five years experience gained while working on many of the phenomena that must be accounted for in optimizing production from a gas condensate system. They recommended that appropriate characterization of

condensate fluid, determination of the extent of retrograde condensation and retrograde condensate relative permeability reduction. They also recommend the determination of the efficiency of cycled gas in ameliorating gas productivity in the presence of retrograde effects, quantification of the influences of gas cycling including composition and pressure effects and simulation must be done to optimize the production strategy of a gas condensate reservoir.

Thomas et al [28] identified three main areas that must be adequately addressed in order to adequately develops an exploitation strategy. These areas are the characterization of the gas condensate fluids, the coupling of the inherent phase behavior and the fluid flow in porous media and the implementation into a simulator for forecasting capability. They employed the experience gained while studying a number of gas condensate reservoirs over the years to provide a summary of important characteristics that must be considered in each of these areas. They concluded that knowing the controlling parameter of a gas condensate reservoir and how to include it in the simulators would help in providing a better exploitation strategy.

Chen, Wilson and Monger-McClure [29] conducted laboratory experiments, under reservoir conditions, on gas condensate flow behavior to determine the relative permeability and recovery for North Sea gas condensate reservoirs. The study also involves the investigation of the effects of rock and fluid characteristics on critical condensate saturation (CCS), gas and condensate relative permeability during in situ-condensation, hydrocarbon recovery and trapping by water injection and incremental hydrocarbon recovery by subsequent blowdown. They found out that the critical

condensate saturation and the relative permeability were rate sensitive. This indicate that gas productivity can be improved if the production rate is increased, that phase behavior and interfacial tension influence the extents of gas relative permeability reduction and condensate mobility and that condensate mobility under gas injection could be recovered by water injection.

Narayanaswamy, Sharma and Pope [30] studied the effect of heterogeneity on the Non-Darcy flow coefficient and presented an analytical method for calculating the effective non-Darcy flow coefficient for a heterogeneous formation and/or heterogeneous grid blocks in reservoir simulator. It was confirmed using numerical simulations, that non-Darcy flow coefficients of a heterogeneous formation is larger than the non-Darcy flow coefficient of an equivalent homogeneous formation. Furthermore, they found that non-Darcy flow coefficient obtained from well tests are significantly larger than those predicted from experimental correlation's. They concluded that permeability heterogeneity is a likely reason for differences in non-Darcy flow coefficients often seen in the lab and field data.

Coats [31] presented a generalized equation of state obtained by the manipulation of Martin's equation of state and also a pseudoization procedure that reduces the multicomponent condensate fluid to pseudo two component mixture of surface gas and oil. The pseudoization process allows the use of a less expensive black oil model instead of compositional model. The study investigated that if the black oil model will truly represent the compositional phenomena active during the depletion or the cycling of gas

condensate reservoirs by comparing the simulation results of black oil model to compositional model. He observed that the black oil simulations of reservoir depletion for a number of condensate systems have shown close agreement with results obtained from compositional modeling except for gas cycling below the dew-point pressures. He concluded that full compositional modeling is necessary for accuracy in cycling of condensates below the dewpoint pressure.

Bourbiaux [32] did a parametric study of gas condensate reservoir behavior during depletion using a single well 2-D radial model with a multipurpose compositional reservoir simulator, ∑CORE. Three gas condensate fluid compositions (lean, reference and rich) with exactly the same dew point pressure were considered. He analyzed and quantified the effects of changing various parameters such as the role of non-Darcy flow, the permeability, relative permeabilities as a function of IFT on productivity, recoveries and fluid distribution. It was observed that productivity of a gas condensate well is controlled by the permeability of the formation above the dew point pressure. The gas viscosity and non-Darcy effects are secondary factors here. Below the dew point pressure, the drop in gas productivity is linked to the formation of a near wellbore condensate ring which is controlled by relative permeability curves. He concluded that sensitivity study on gas condensate reservoirs should be done to reduce field development uncertainties.

Al-Majed and Dougherty [33] developed a variable cell model for simulating gas condensate reservoir performance. The model was used to study the effect of liquid flow on well stream fluid composition and investigate the influence of reservoir fluid phase

equilibria data on two-phase flow region. He concluded that the model closely approximates the conventional compositional models and it requires a fraction of computation time.

Sanger and Hargoot [34] conducted both experimental and simulation studies on the recovery of gas condensate by nitrogen injection with methane injection. The study objective is to assess the feasibility of flooding gas condensate by nitrogen flooding as compared to methane flooding. Methane injection or gas cycling has been the choice for gas condensate reservoir but economic limitations may not allow this hence the need to consider an alternative injection gas like Nitrogen. They observed that recoveries was over 90% for a gas condensate reservoir when Nitrogen is injected which is slightly less than methane flooding and concluded that Nitrogen is a potential alternative to gas cycling in condensate reservoirs.

Wei-jr et al [36] assess the effect of non-equilibrium mass transfer on the productivity of a single well producing from a gas condensate field. They used the non-equilibrium mass transfer model of the Wilkins et al [59] implemented in the equations of state compositional reservoir simulator developed by University of Texas at Austin. Peng-Robinson equation of state was used to compute equilibrium mass transfer for hydrocarbon components and phase volumes while the diffusion coefficients for each component were calculated using the correlation of Wilkee and Lee [58]. The simulation was done using a layered single well radial model and they concluded that non-

equilibrium phase behavior lead to a reduction in the condensate saturation in the region near the wellbore.

Killough and Kossack [40] presented the results of comparisons between the fully compositional and four-component miscible flood reservoir simulation models from seven different participants for a series of three test cases. These cases varied from scenarios dominated by immiscible conditions to scenarios in which the minimum miscibility pressure was maintained or exceeded throughout the simulations. Seven companies participated in this comparative solution project. The simulation results obtained by the seven companies are in good agreement. However, it was concluded that the compositional formulation give more accurate results for a case in which some of the reservoir oils is volatilized into gaseous phase.

CHAPTER 3

PETROPYSICAL AND CORE ANALYSIS

3.1 PETROPHYSICAL ANALYSIS

Petrophysical analysis is usually done to identify permeable and hydrocarbon bearing formation and calculate parameters such as porosity, water saturation, layering, layers thickness, shale volume, water resistivity, mechanical properties and net pay per foot. Well logs obtained from logging include gamma ray, spontaneous potential, resistivity, lithodensity, borehole-compensated sonic, caliper and production logs [52]. The required data for the zone of interest (14342-14572ft) was used as input parameters into the open-hole well log interpretation software.

3.1.1 Water saturation and effective porosity

A major objective of logging is the determination of the quantity $\phi(1\text{-}Sw)$ or the pore volume. However, water saturation calculated through the open hole log interpretation software model(s) is not encouraging due to the poor readings from the resistivity logs. The models used to calculate water saturation includes Archie, Alger dispersed, Simandoux, Waxman Smit, Dual water and Simplified Dual water model [47].

The estimated water saturation computed by each model is presented in figures 3.1 to 3.7. The Alger-laminated model broke-down at the high resistivity zone. The reason for this is that the software has to find the square root of a negative number and this is outside the domain of the square root function. The effective porosity calculated

per foot using the cross-plot model of the density and neutron log readings is presented in figure 3.8

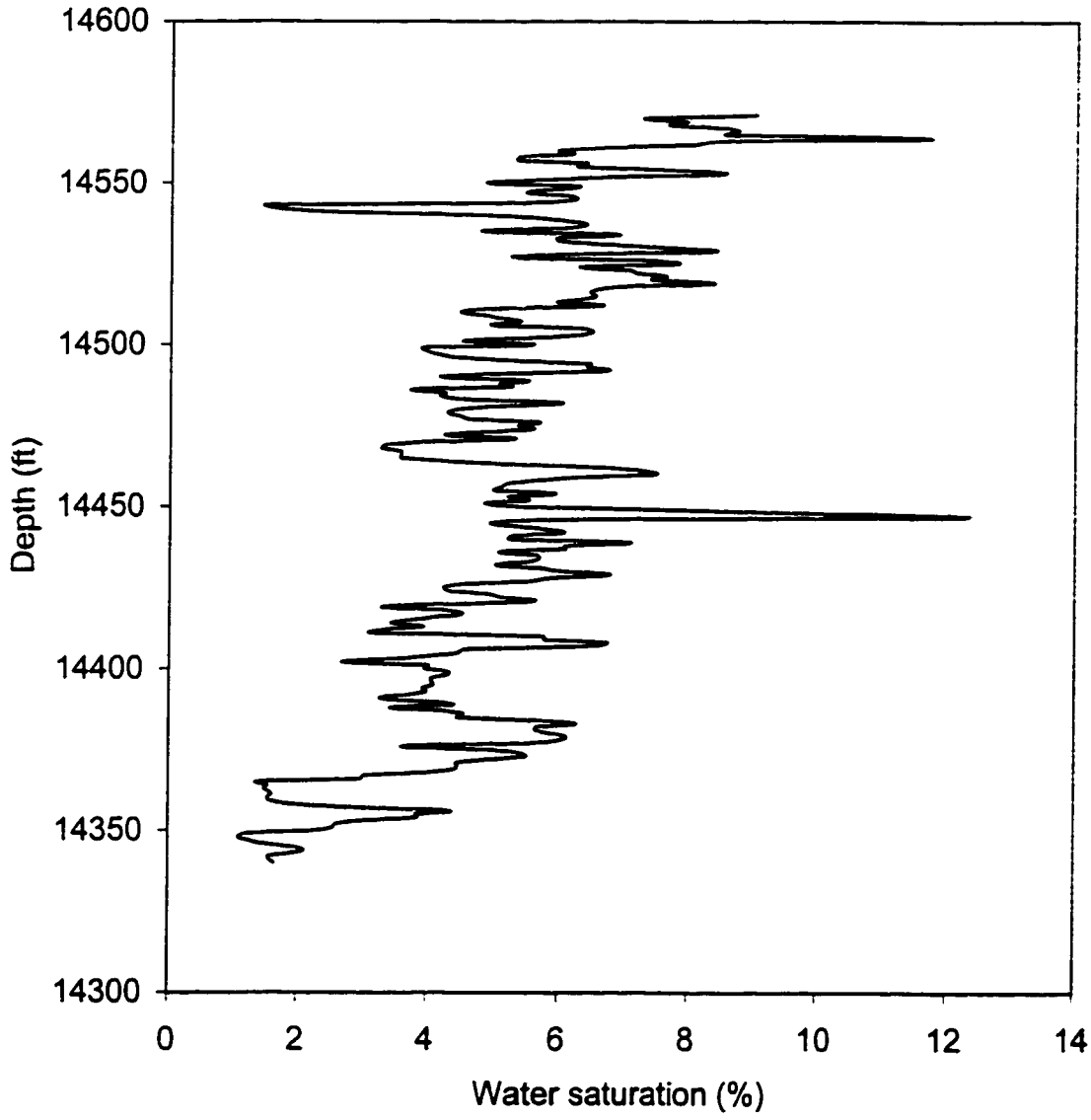

Fig 3.1: Water saturation estimated using Archie model

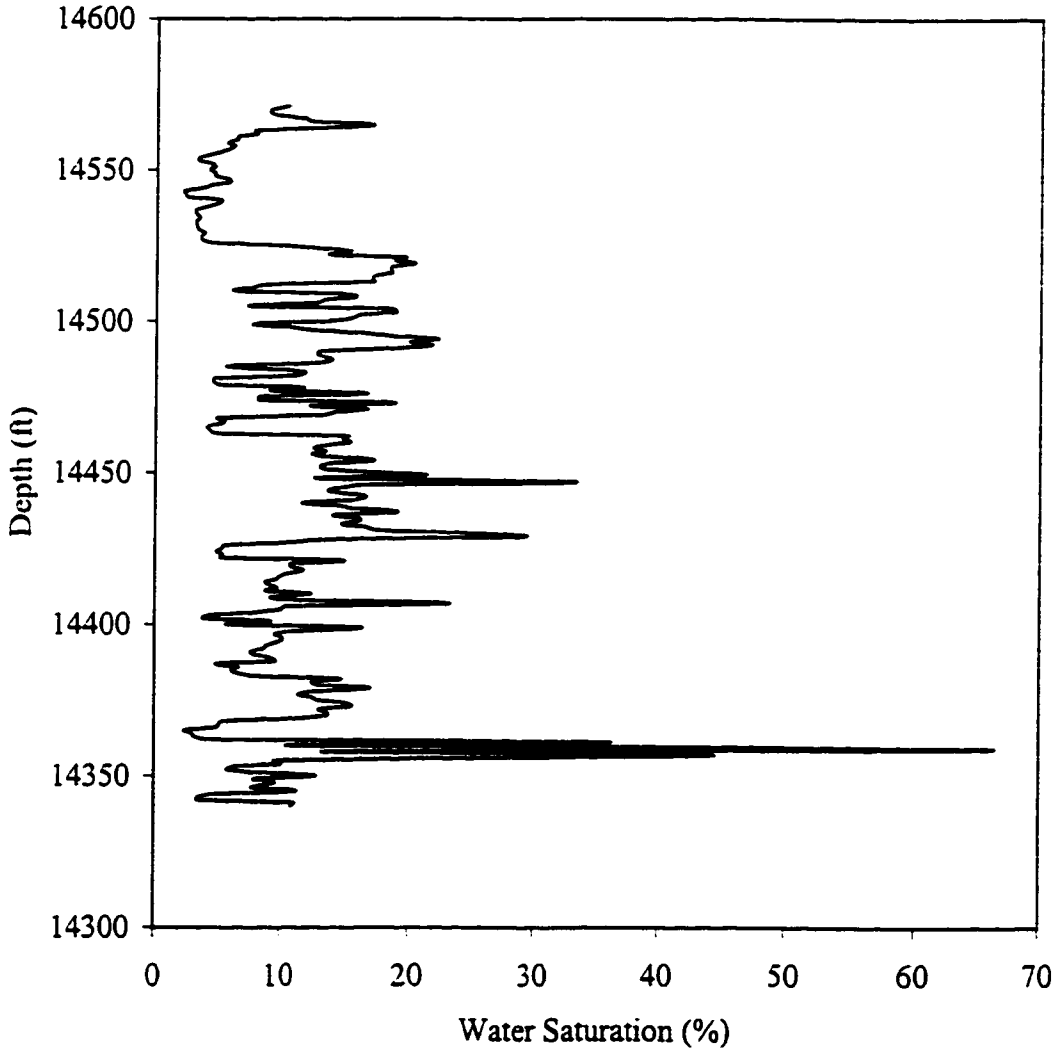

Fig 3.2 : Water saturation estimated using alger dispersed model

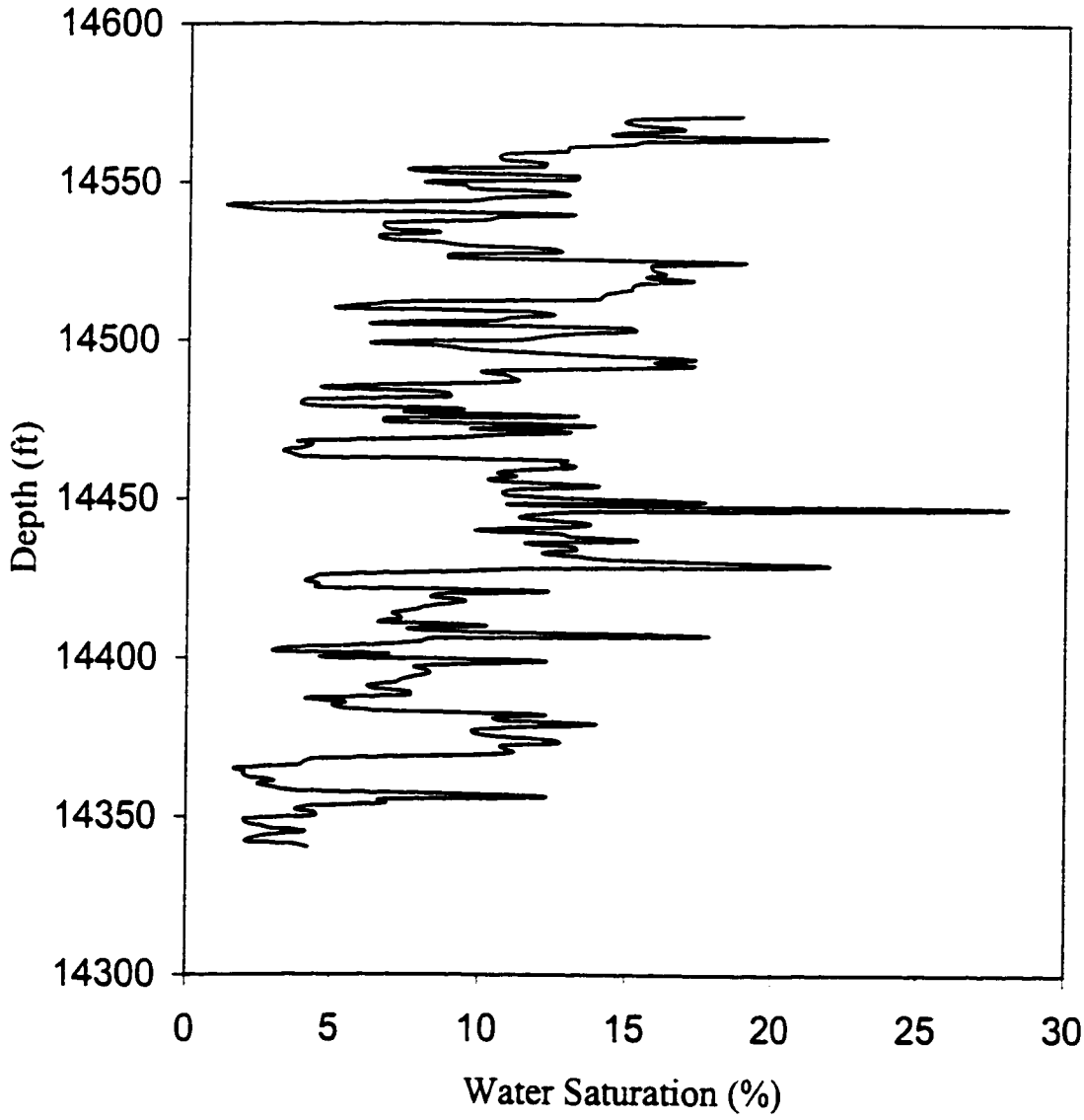

Fig 3.3: Water Saturation estimated using Simandoux model

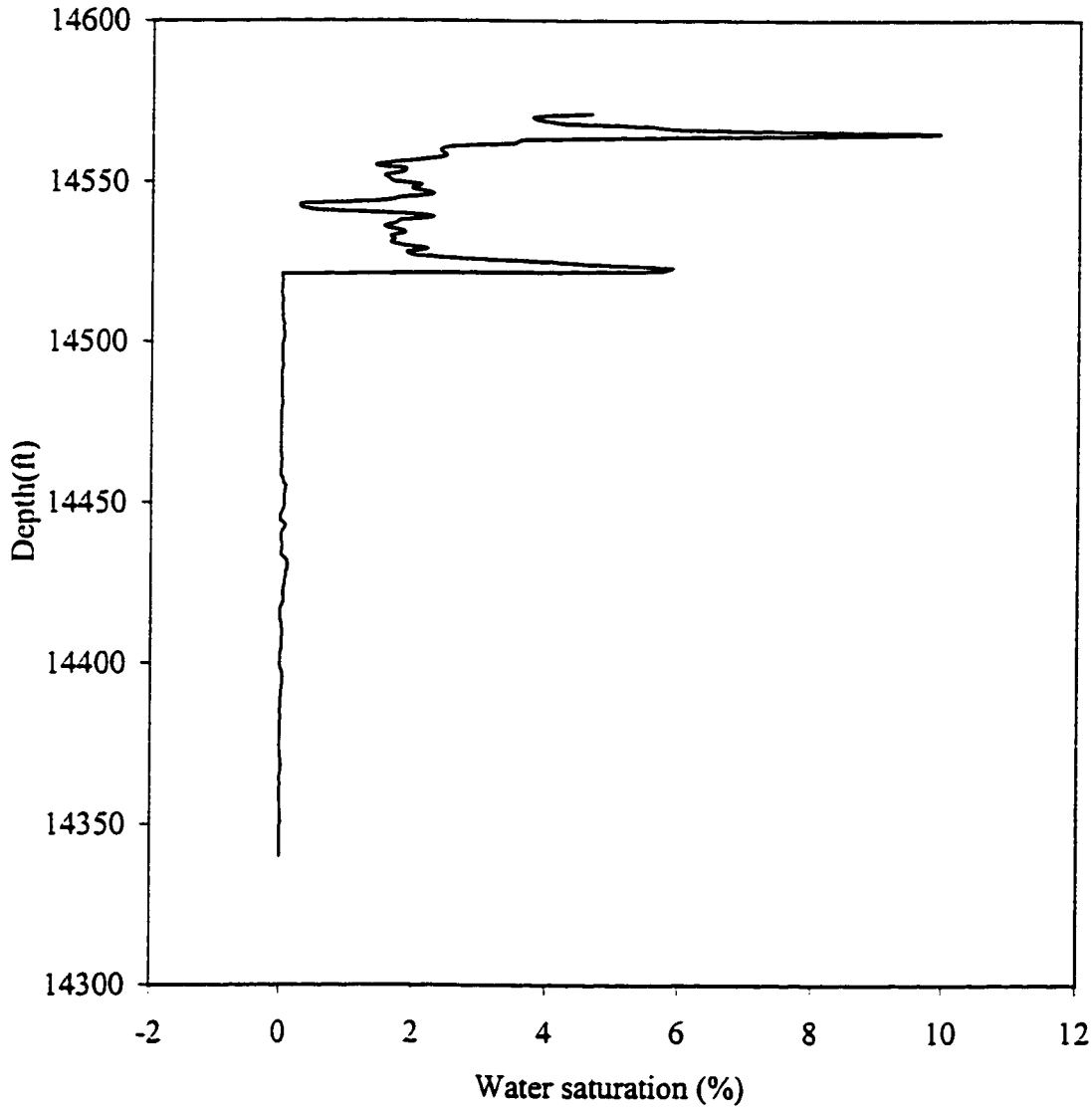

Fig 3.4 : Water saturation estimated using alger's laminated model

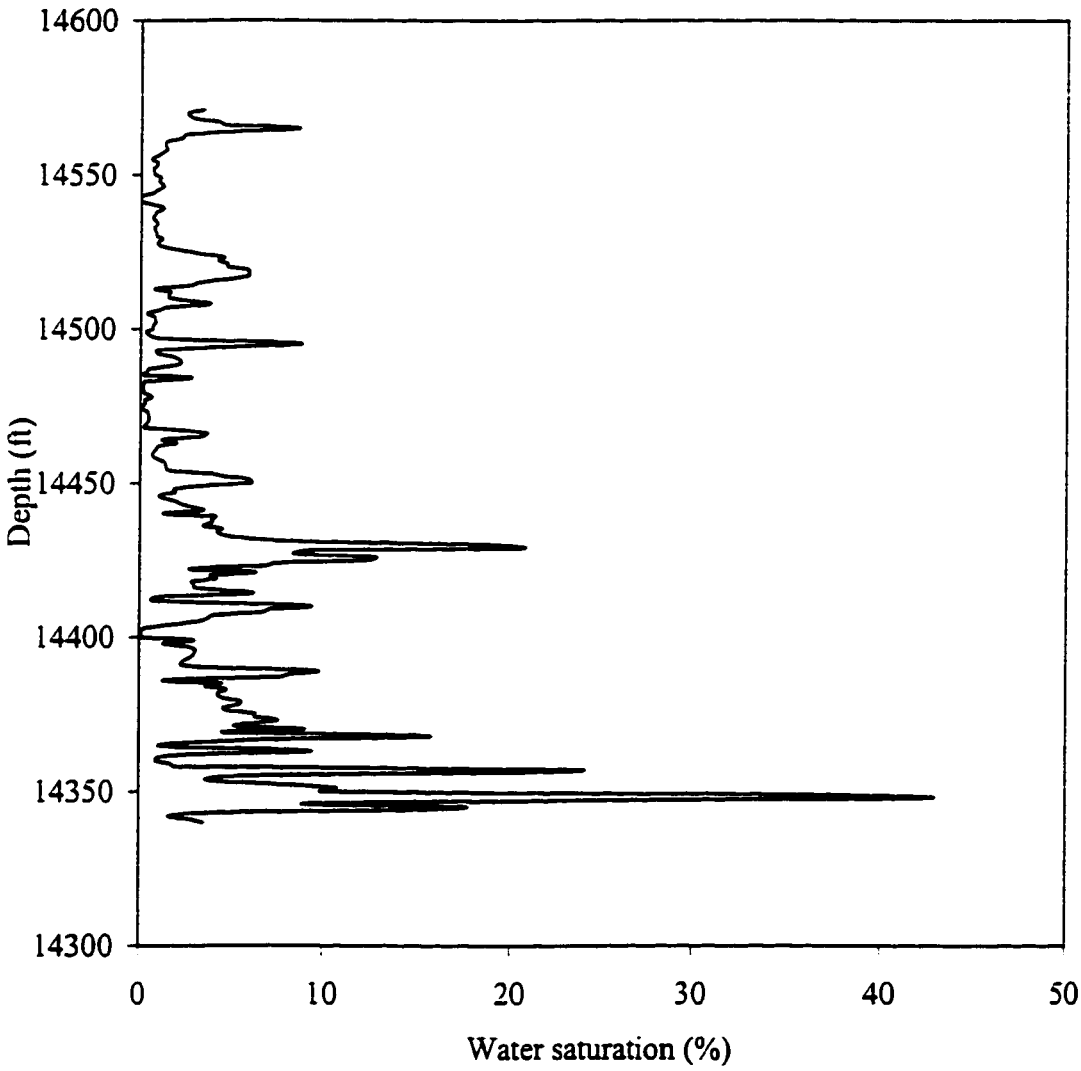

Fig 3.5 : Water saturation estimated using waxman smit model

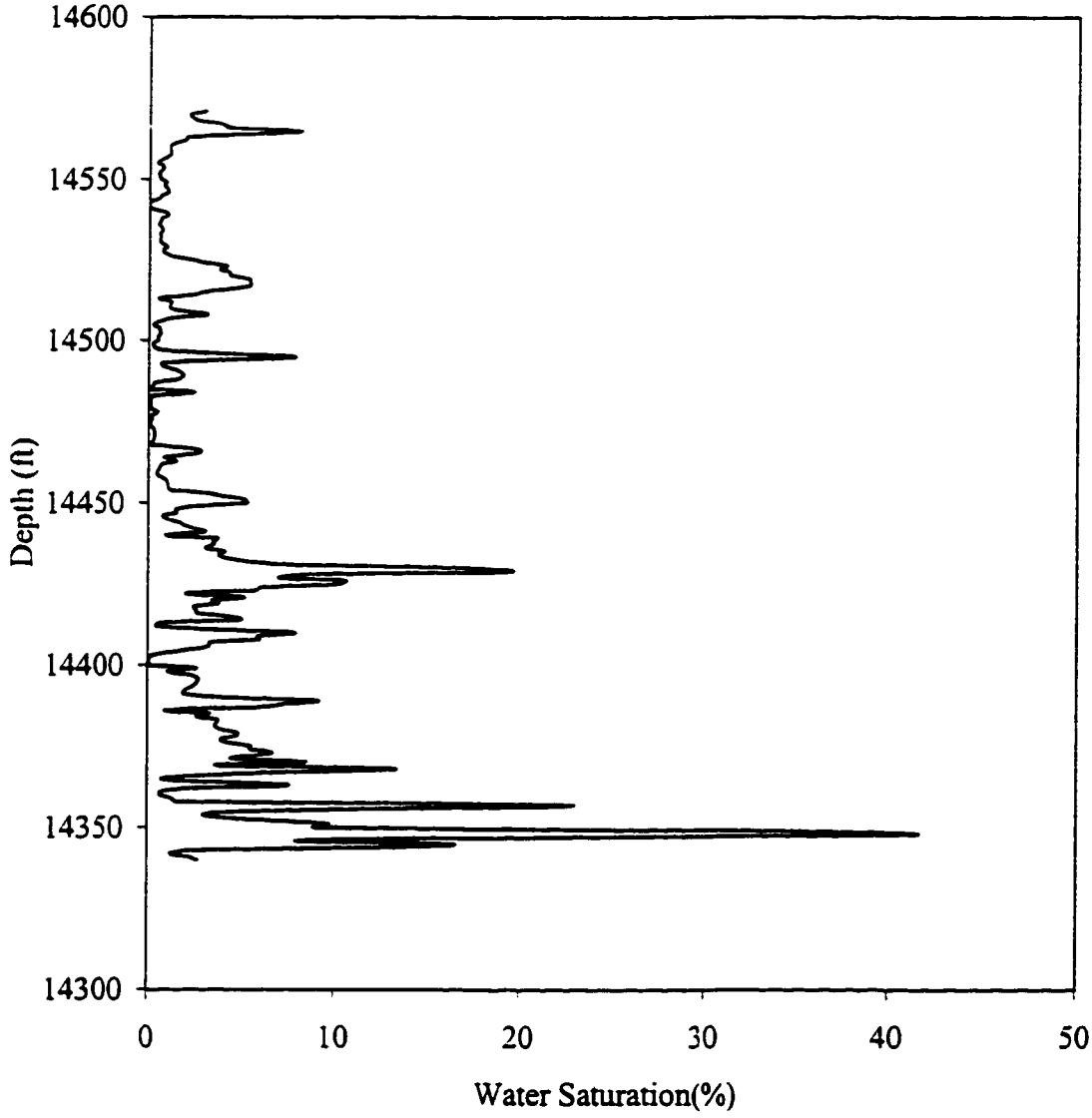

Fig 3.6: Water Saturation estimated using dual water model

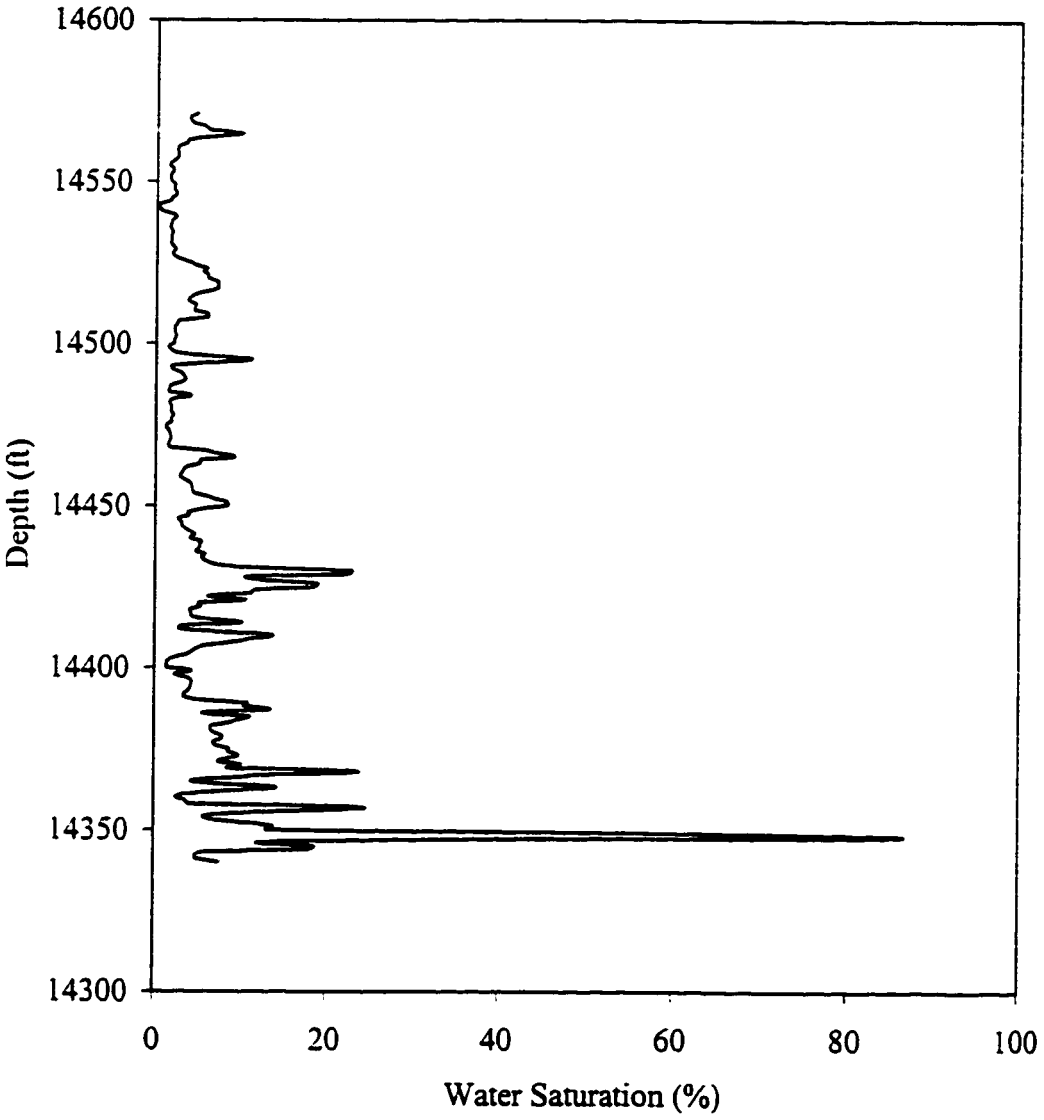

Fig 3.7: Water saturation estimated using for Simplified dual water model

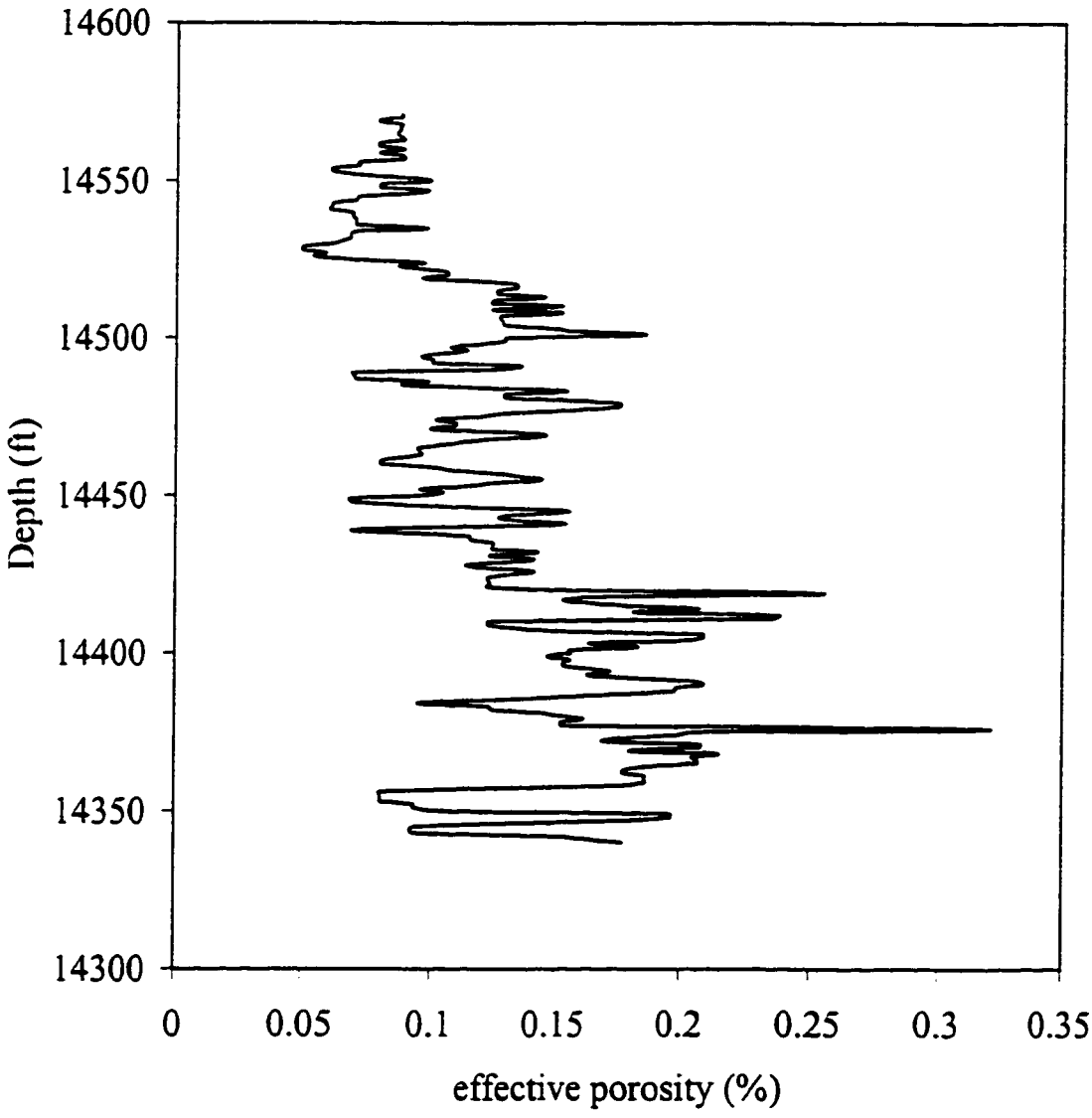

Fig 3.8 : variation of effective porosity with depth

3.1.2 Reservoir description

After the interpretation of well logs [52], seven productive layers have been identified. A weighted average of the petrophysical parameters such as porosity was determined. The reservoir permeability was calculated from core samples obtained per foot from the well. Like the porosity, a weighted average was found for each layer. The reservoir description is presented in Table 3.1.

TABLE 3.1: Reservoir description

Layering	Depth (ft)	Thickness(ft)	Porosity (%)	Permeability (md)
Layer 1	14342-14360	18	12.56	0.1992
Shale	14360-14370	10		
Layer 2	14370-14384	14	17.88	0.3333
Shale	14384-14390	6		
Layer 3	14390-14400	10	17.29	115.66
Shale	14400-14415	15		
Layer 4	14415-14422	7	17.57	21.68
Shale	14422-14432	10		
Layer 5	14432-14464	32	12	0.0852
Shale	14464-14490	26		
Layer 6	14490-14510	20	12.41	0.0085
Shale	14510-14514	4		
Layer 7	14514-14572	58	8.44	0.0009

3.2 CORE ANALYSIS

3.2.1 Absolute permeability

The absolute permeability per foot for the zone of interest was available [52] and was used along with other data to identify the number of layers.

3.2.2 Pore size distribution index λ

The pore size distribution index can be obtained from a capillary-pressure curve or, a group of curves, or from the Leverett J-function curve. Below is the theory behind each approach.

(a) Capillary pressure curve

Brooks and Corey showed that the ratio of capillary pressure to capillary entry pressure, P_c/P_e, and the effective wetting phase saturation, S^*_{wt}, can be represented by:

$$S^*_{wt} = \left(\frac{P_c}{P_e} \right)^{-\lambda} \tag{3-1}$$

Or

$$\log P_c = -\left(\frac{1}{\lambda}\right) \log S^*_{wt} + \log P_e \tag{3-2}$$

$$S^*_{wt} = \frac{S_{wt} - S_{wtr}}{1 - S_{wtr}} \tag{3-3}$$

where:

S_{wt} = Wetting phase saturation (S_w for a water-wet reservoir)

S_{wtr} = residual wetting –phase saturation (S_{wi} for a water-wet reservoir)

P_c = capillary pressure, which is a function of S_{wt} and therefore of S_{wt}^*

Equation (3-2) above is a straight line on log P_c vs. log S_{wt}^* coordinates. The pore size distribution index λ is obtained from the slope of the straight line, $-(1/\lambda)$.

(b) Leverett J-function curve

The leverett J- function is mathematically defined by equation (3-4)

$$J_1(S_w) = (0.217*P_c)*(\sigma\cos\theta)^{-1}*(k/\varphi)^{1/2} \qquad (3\text{-}4)$$

Where

P_c = Capillary pressure (psi)

σ = Interfacial tension in dynes/cm

θ = Contact angle in degrees

k = permeability, md

ϕ = Porosity, fraction

0.217 = constant needed to make $J(S_w)$ dimensionless

A log- log plot of the J-function with the normalized water saturation gives a slope that is equal to the inverse of $-\lambda$ as shown in equation (3-5)

$$\log J_1(S_w^*) = -\frac{1}{\lambda}\log(S_w^*) + \log(J_1) \qquad (3\text{-}5)$$

Many types of reservoirs studied by Brooks and Corey [50] led to the conclusion that a λ greater than 6 is not common. Most natural sandstone and limestone can be represented by pore-size distribution indices between 0.5 and 4 [49, 50].

APPLICATION OF THE THEORY TO DETERMINE λ

Available capillary pressure data determined using air displacing water experiment on core samples taken at a formation depth of 14364.9, 14370.8, 14390.5, 14393.7 and 14395.6 ft was used to determine λ [51]. Samples corresponding to the above depths are defined as A, B, C, D and E respectively. The most important parameters we needed from the experimental results are water saturation, capillary pressure or J-function. The above data was used to calculate the pore size distribution index of the rock samples. Figure 3.9 present the J-function versus normalized water saturation for samples A, B, C, D and E. The inverse of the slope of the line passing through the clustered data points in figure 3.9 provide a single value for the pore size distribution index λ of the reservoir rock. The slope of this line is calculated to be -1.365 and the inverse of the slope or the pore size distribution index λ is equal to 0.73. The initial water saturation for the reservoir rock is 0.33 based on the arithmetic average of initial water saturation the samples. Table 3.2 presents the initial water saturation of each sample. In this study the value of pore size distribution index and initial water saturation used is 0.73 and 0.33 respectively.

TABLE 3.2: Rock properties of core samples

Samples	Swi	Permeability k(md)	Porosity (%)
A	0.3443	1012.2	22.57
B	0.3498	30.5	15.3
C	0.3102	177.1	17.46
D	0.233	839.3	18.72
E	0.4542	19.2	19.86

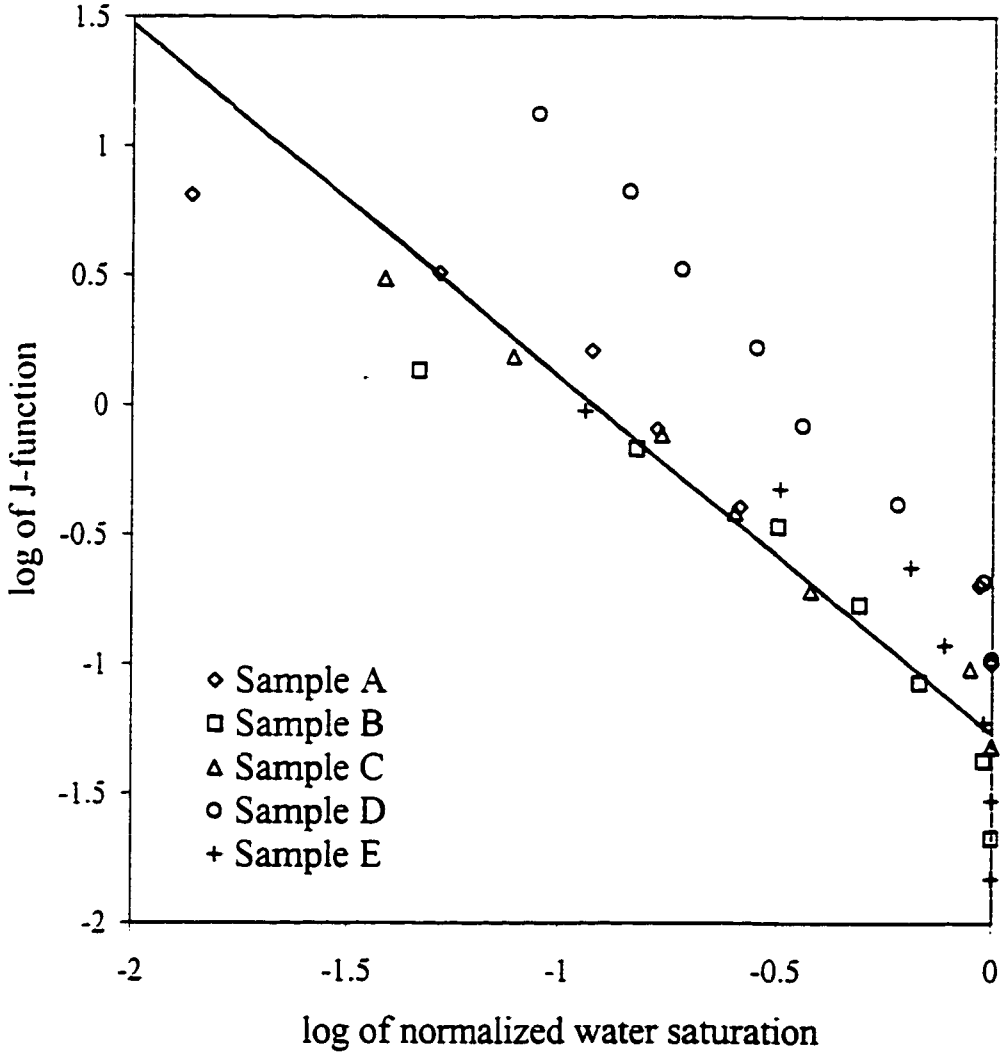

Fig 3.9: J-Function versus normalized water saturation for samples A,B,C,D and E

3.3 GEOLOGICAL MODEL

The petrophysical and core analysis was done in order to construct the geological model. The geological model shown in Table 3.3 obtained by averaging petrophysical parameters (except water saturation) per layer. The initial water saturation and pore size distribution index are obtained through the air displacing water capillary pressure experiments.

TABLE 3.3: Geological model

Layering	Depth (ft)	Thickness(ft)	Porosity (%)	K (md)	λ	Swi
Layer 1	14342-14360	18	12.56	0.1992	0.73	0.33
Shale	14360-14370	10				
Layer 2	14370-14384	14	17.88	0.3333	0.73	0.33
Shale	14384-14390	6				
Layer 3	14390-14400	10	17.29	115.66	0.73	0.33
Shale	14400-14415	15				
Layer 4	14415-14422	7	17.57	21.68	0.73	0.33
Shale	14422-14432	10				
Layer 5	14432-14464	32	12	0.0852	0.73	0.33
Shale	14464-14490	26				
Layer 6	14490-14510	20	12.41	0.0085	0.73	0.33
Shale	14510-14514	4				
Layer 7	14514-14572	58	8.44	0.0009	0.73	0.33

CHAPTER 4

INPUT PVT DATA

4.1 Chevron Phase Calculation Program

The Chevron phase calculation program is designed to calculate the phase compositions, densities, viscosity's, thermal properties and interfacial tension between phases for liquid and vapors in equilibrium [48]. Such phase calculations conducted through an equation of state model can be used to generate the fluid properties needed for applications such as CHEARS, material balance calculations and well test analysis.

Important parameters such as the binary interaction parameters, parachor, interfacial tension, gas and liquid viscosity, constant composition expansion and constant volume depletion data were obtained from the fluid analysis numerical calculation. In addition to this the program generated the input data required by the compositional simulator.

Available PVT data of fluid samples from the reservoir of interest was used to generate the input data. To do this, parameters such as the dew point pressure have to be matched. Matching dew point pressure may involve tuning of some parameters of the equations of state. Examples of such equations of state parameters are molecular weight, density and binary interaction parameters. Once the dew point pressure is matched, calculations such as the constant composition expansion, constant volume depletion, the envelope calculation, critical pressure and temperature are made. The phase diagram generated by the chevron phase calculation program for the gas condensate fluid is presented in figure 4.1

To validate the phase behavior calculation program result, a comparison is made between the experimental and numerically determined PVT data as shown in figures 4.2 to 4.9. The numerically determined fluid properties matched the experimental data very well except for the relative liquid volume that required optimization of the experimental determined relative liquid volume data before it could be matched. Table 4.1 shows the composition of the gas condensate fluid used in the simulation study.

TABLE 4.1 : Gas condensate composition

Laboratory		*Simulation (PVT package)*	
Component	(Mole %)	Component	(Mole %)
N2	3.49	N2	3.49
CO2	2.7	CO2	2.7
H2S	0	CH4	65.07
CH4	65.07	C2H6	10.5
C2H6	10.5	C3H8	4.97
C3H8	4.97	n-C4H10	0.95
n-C4H10	0.95	i-C4H10	1.87
i-C4H10	1.87	i-C5H12	0.77
i-C5H12	0.77	n-C5H12	0.78
n-C5H12	0.78	n-C6H14	1.25
C6H14	1.25	C10	6.44
C7H16	1.49	C25	1.205
C8H18	1.56		
C9H20	1.08		
C10H22	0.78		
Undecanes	0.38		
Dodecanes	2.36		

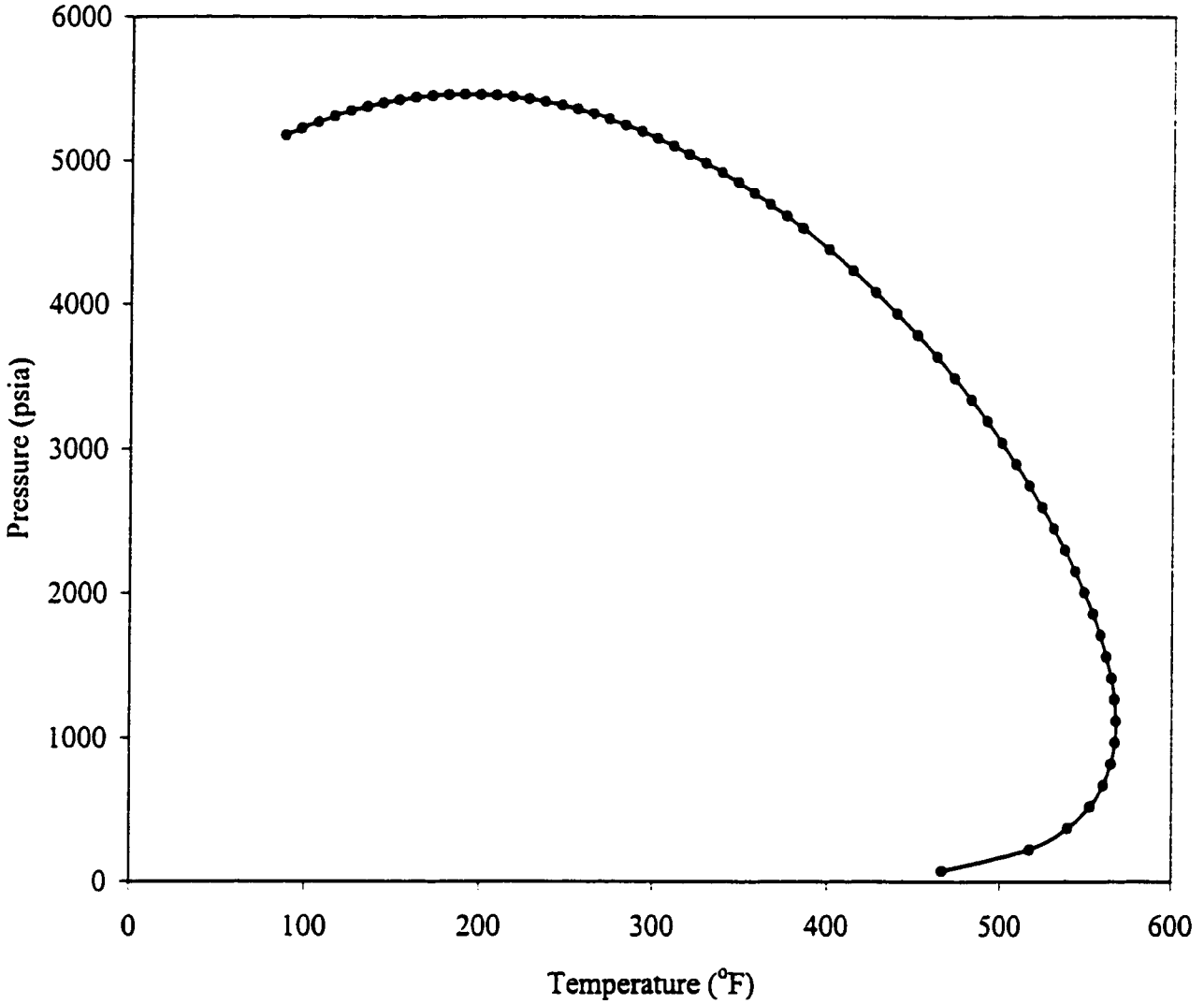

Fig 4.1: The phase diagram for the gas condensate fluid system with critical temperature Tc = 87.250F, ciritical pressure Pc = 4527.18 psia and dew-point pressure = 5153 psia

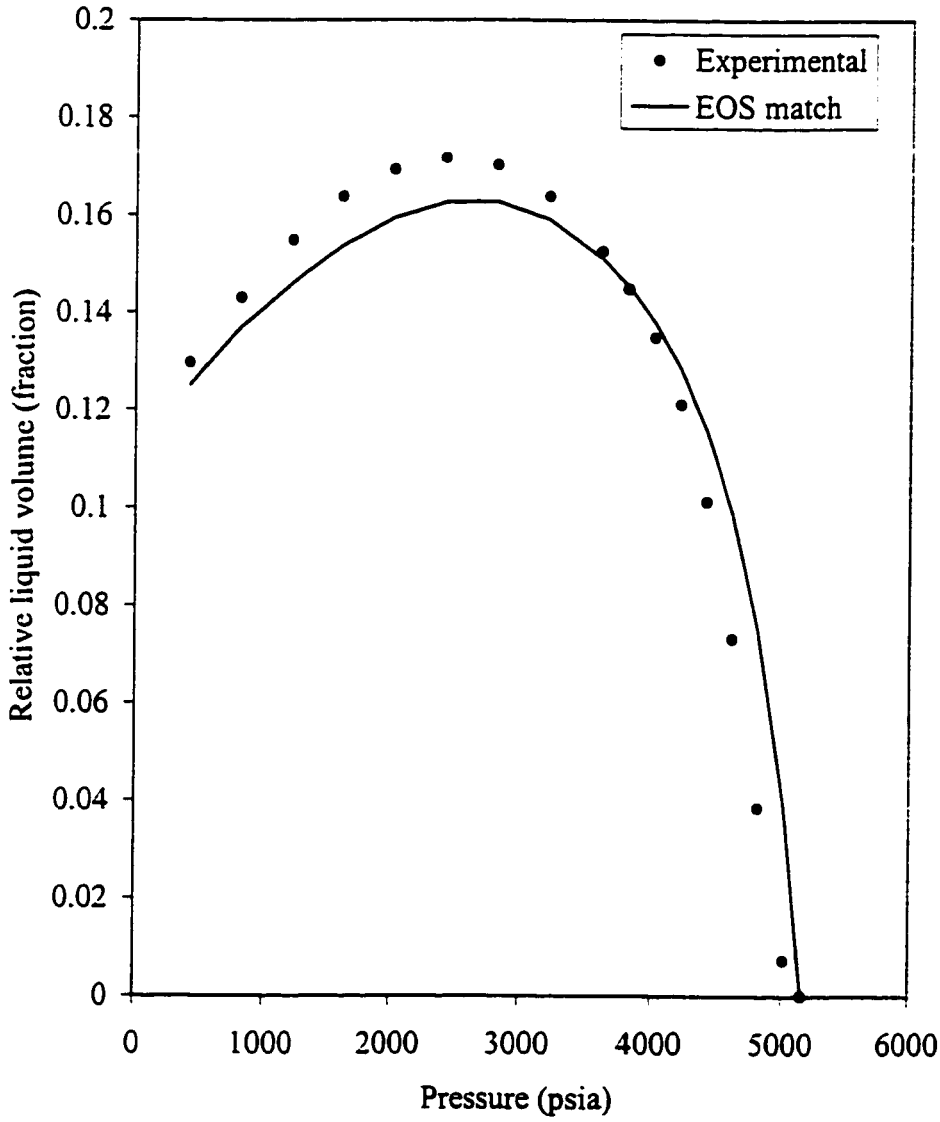

Fig 4.2: Constant volume depletion curve

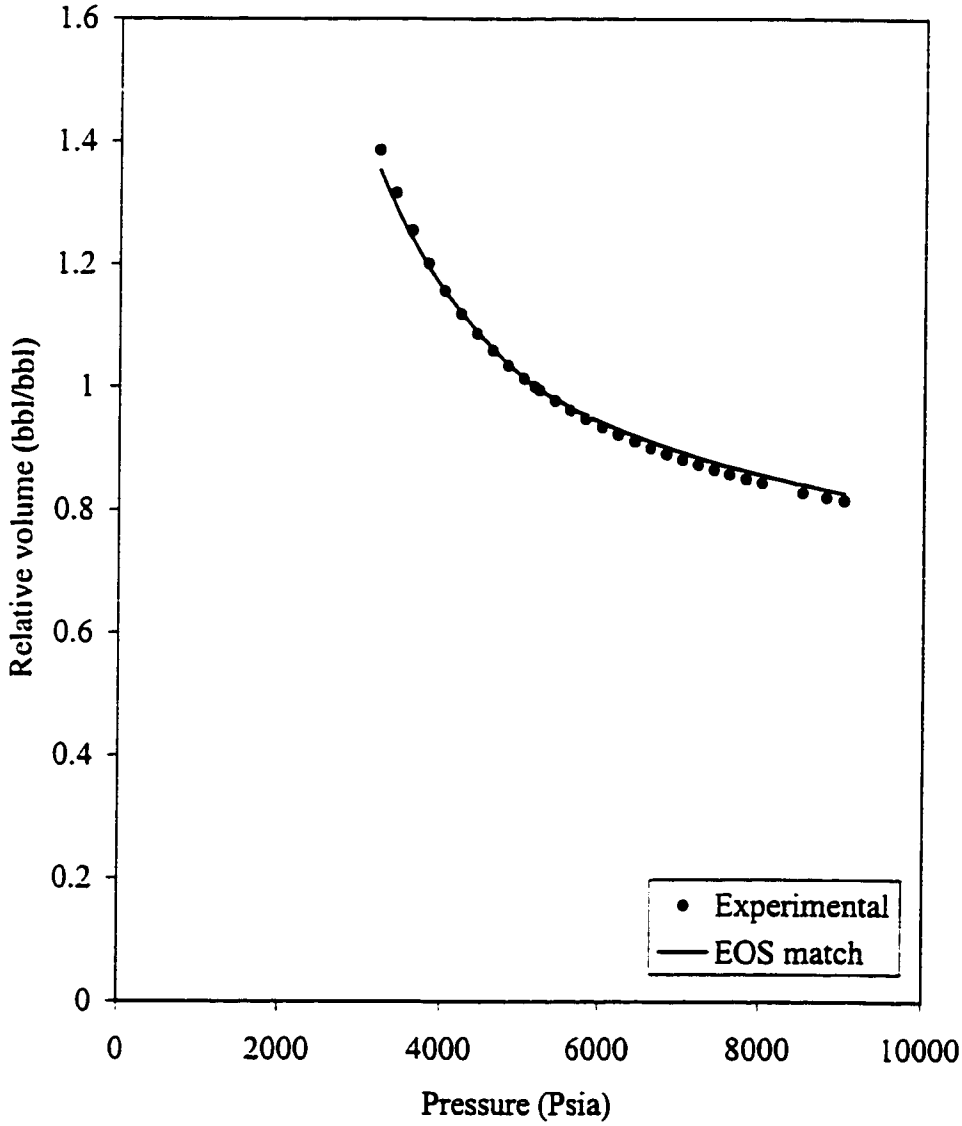

Fig 4.3: Relative volume versus pressure

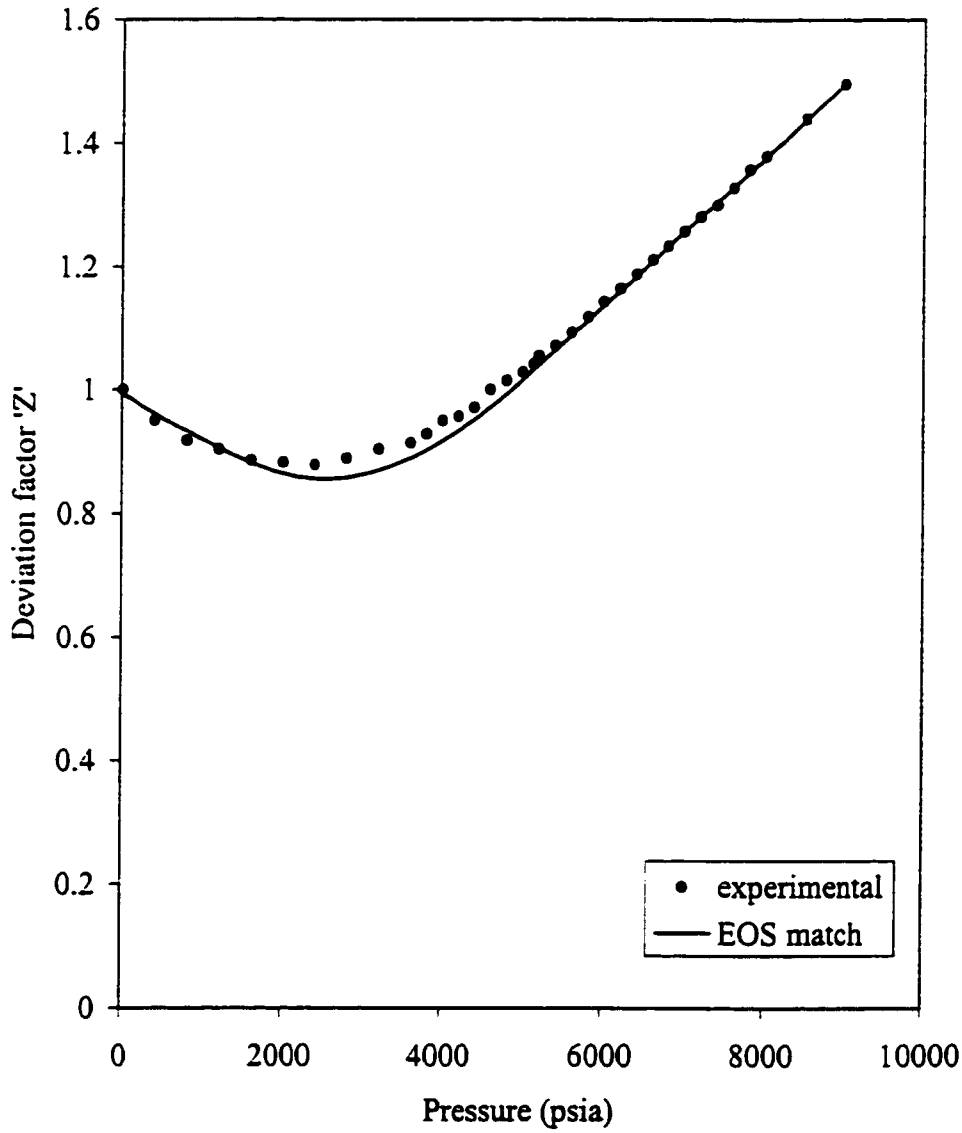

Fig 4.4: Deviation factor 'Z' versus pressure

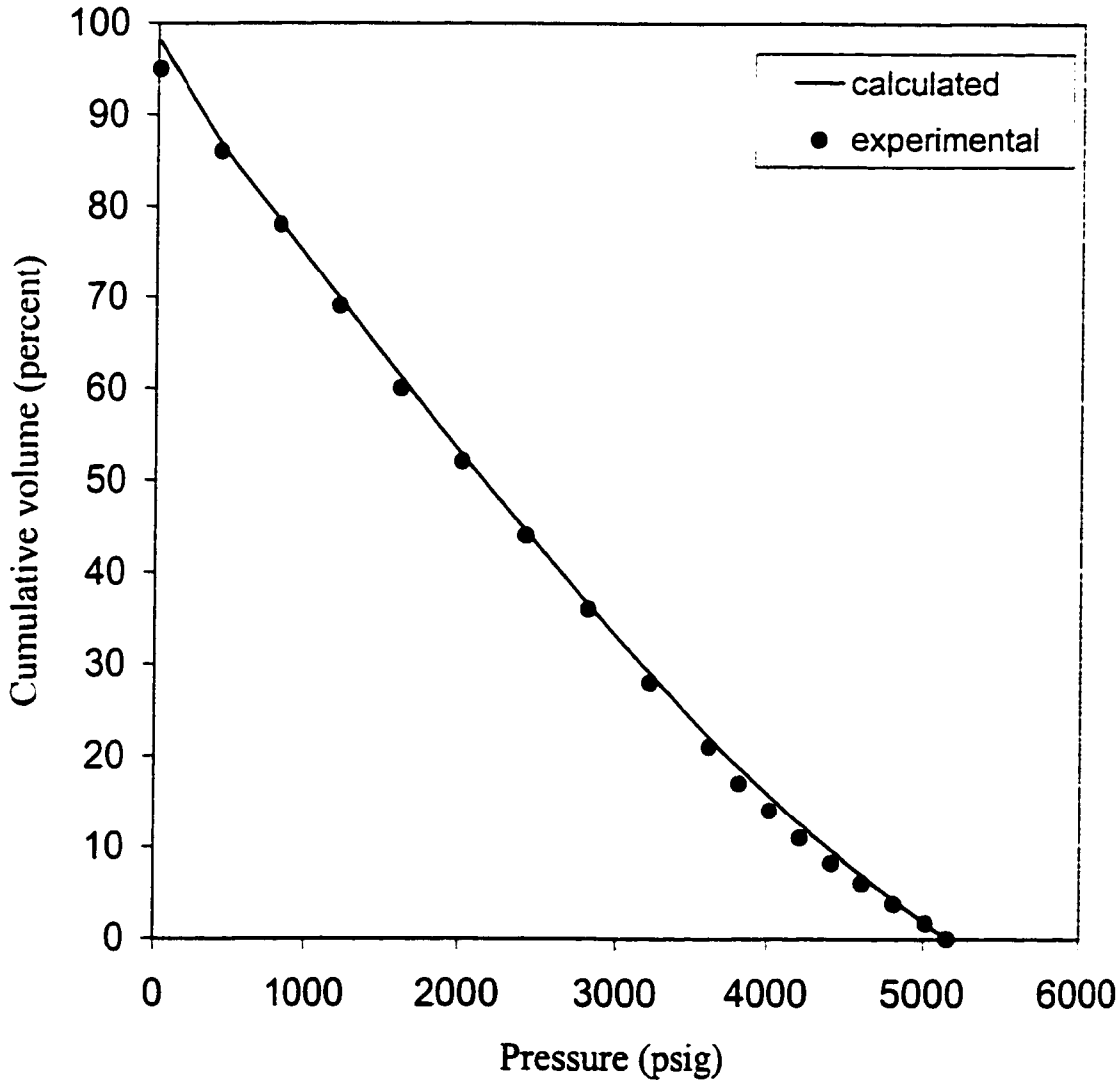

Fig 4.5: Cumulative volume of wellstream produced during depletion versus pressure

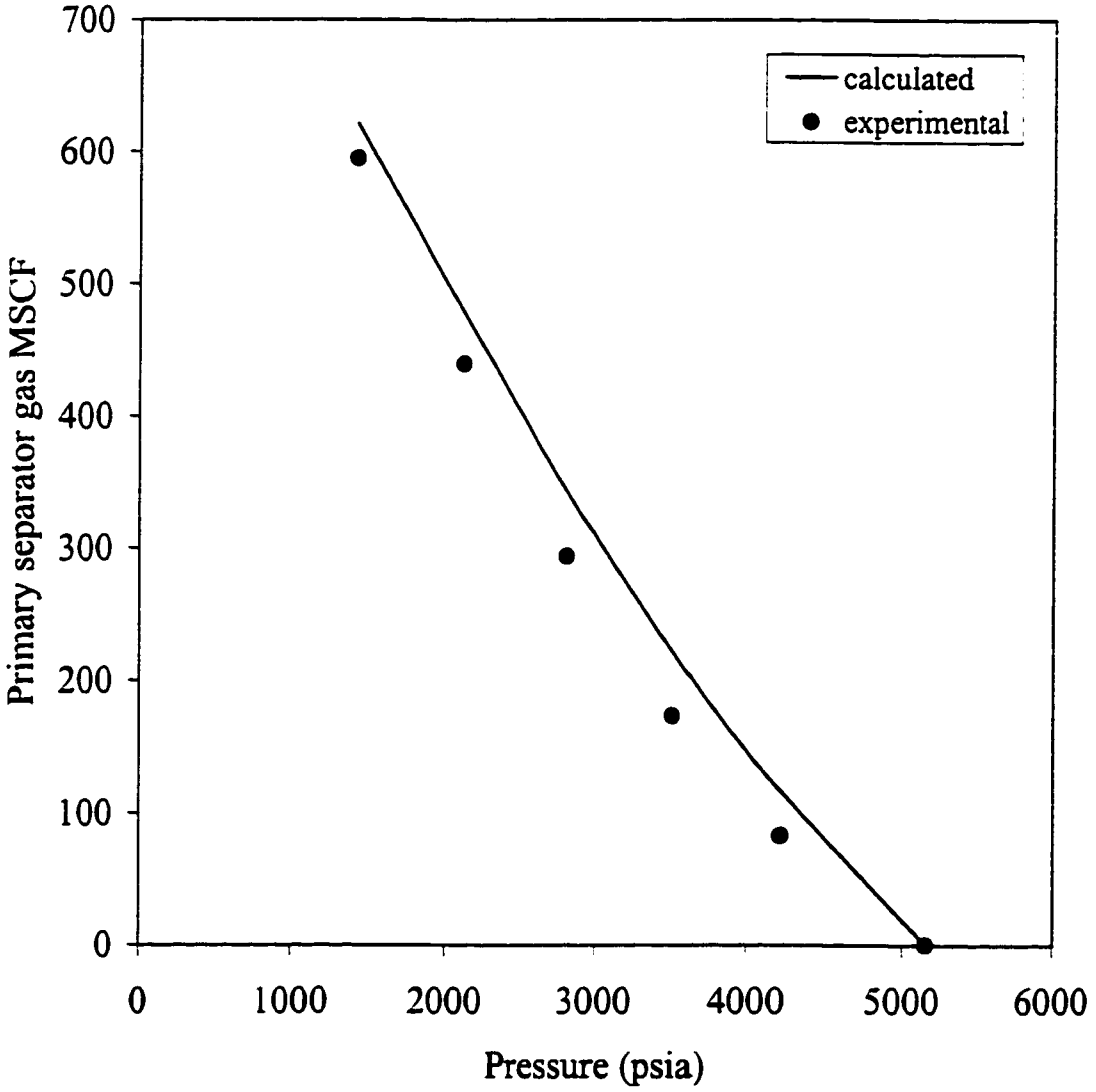

Fig 4.6: Cumulative recovery per MSCF of original reservoir fluid

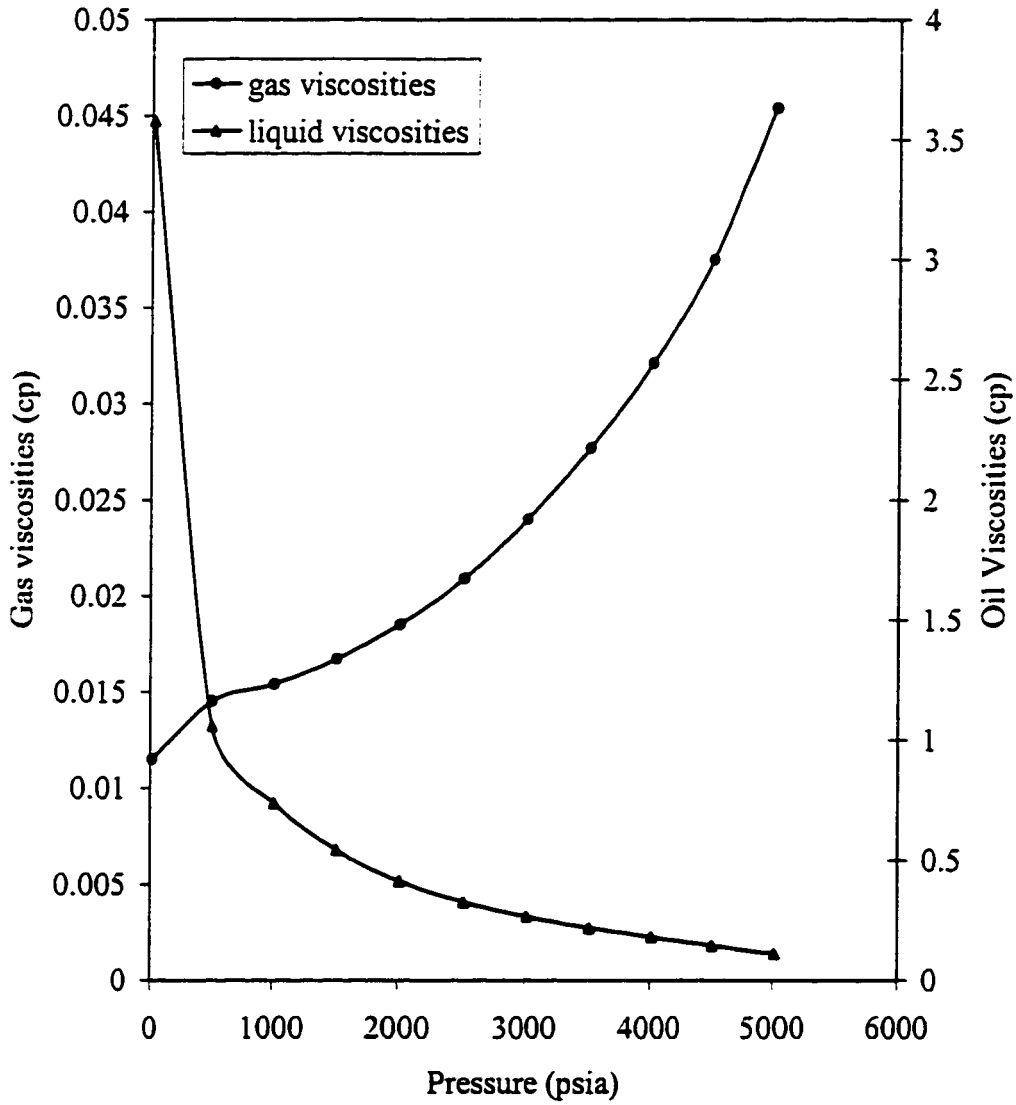

Fig 4.7: Gas and oil viscosities versus Pressure

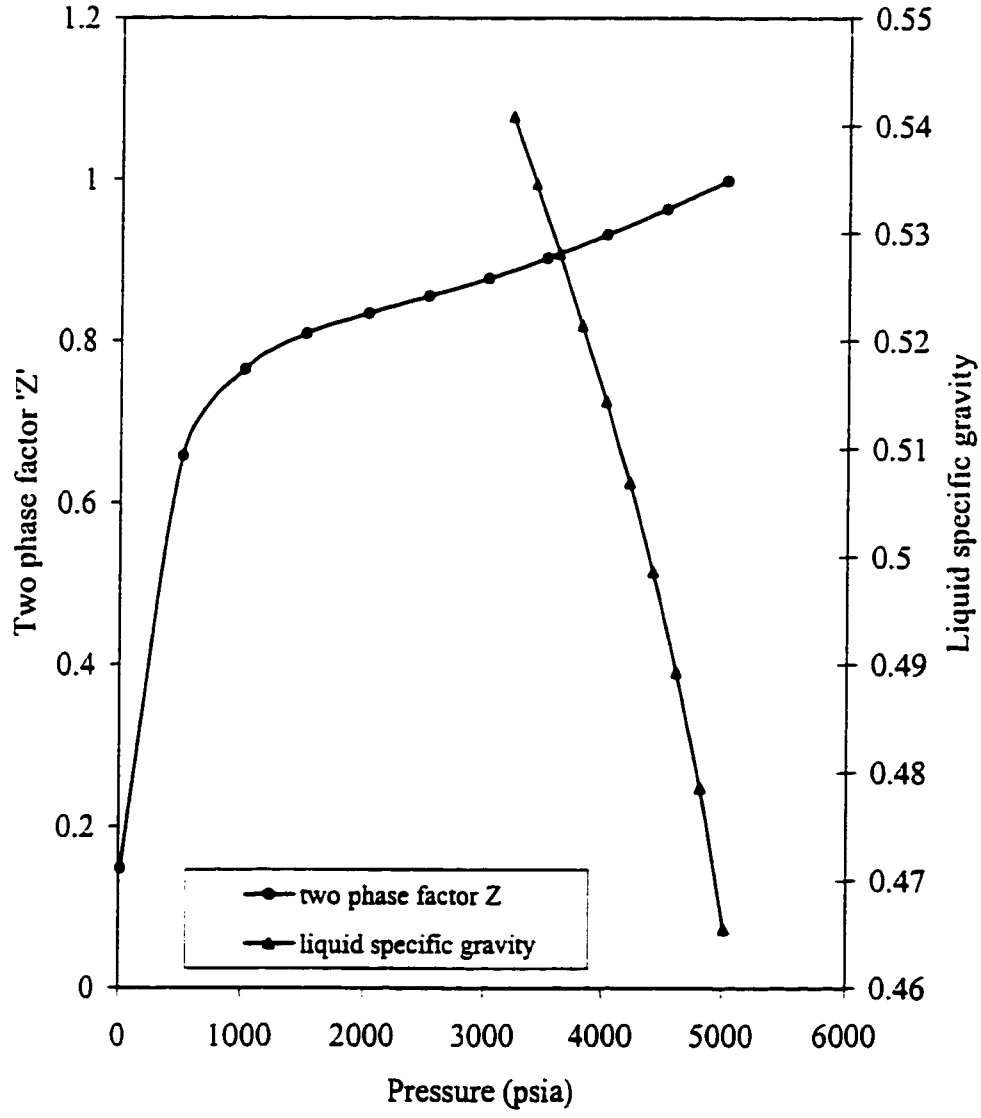

Fig 4.8 : Two phase factor 'Z' versus pressure

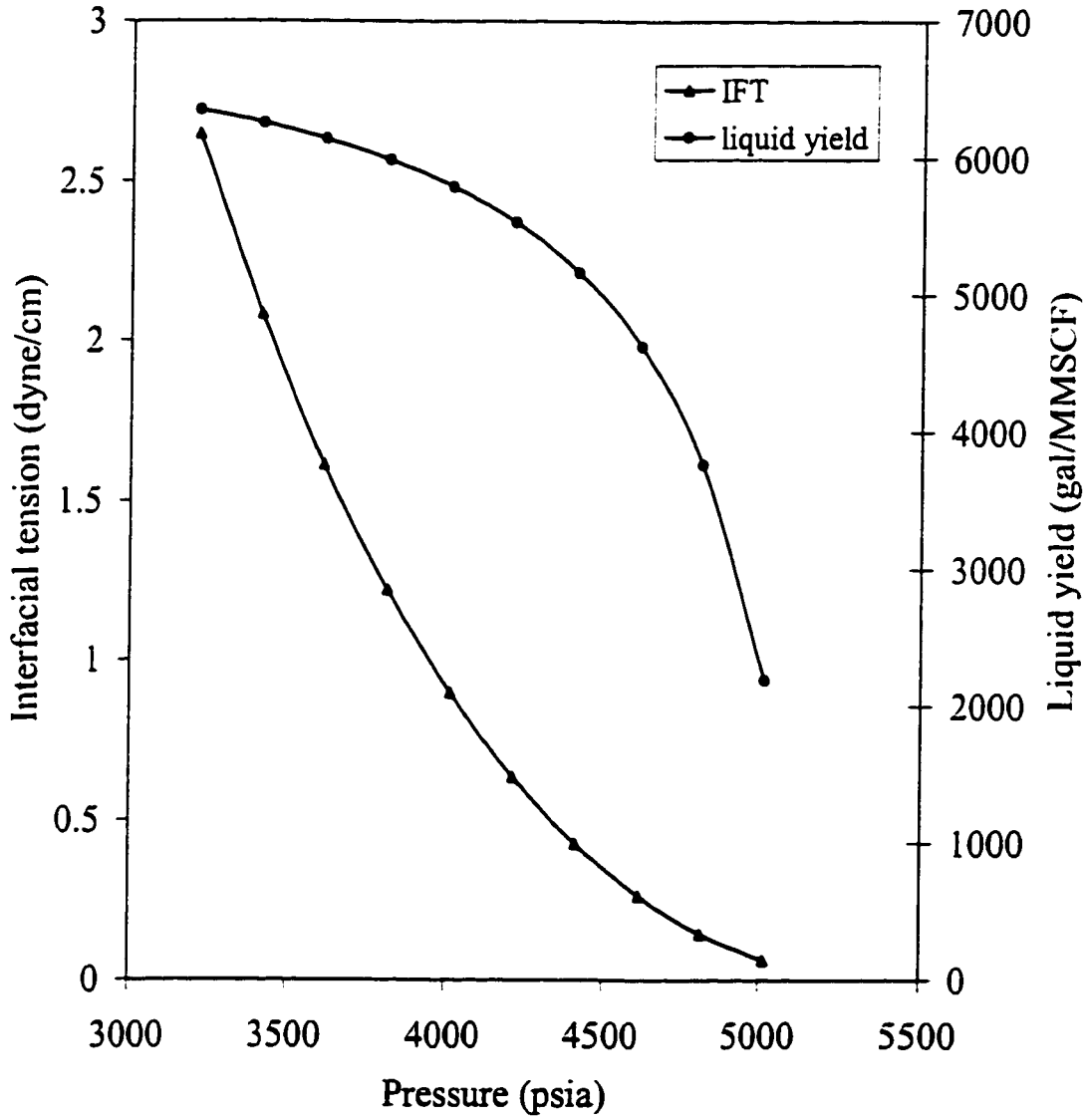

Fig 4.9: IFT and liquid yield versus pressure

4.2 Matching of Drill Stem Test (DST) Pressure response

Well test such as the drill stem, build up and drawdown tests are performed on gas condensate wells to determine formation and well characteristics [43,46]. The DST pressure response data for the gas condensate well was matched for the single-phase flow of the gas above the dew point pressure. The matching of the DST pressure response can be interpreted as a confirmation that the simulation model is capable of predicting the pressure transient behavior and that the constructed geological model reasonably represents the reservoir under study. Some difficulties were encountered while trying to match the pressure response due to high-pressure drop during the DST. Figure 4.10 shows a good match of the pressure response from the DST. The match was obtained by reducing the drainage area indicating that the well from which the DST was obtained is located in a small compartment.

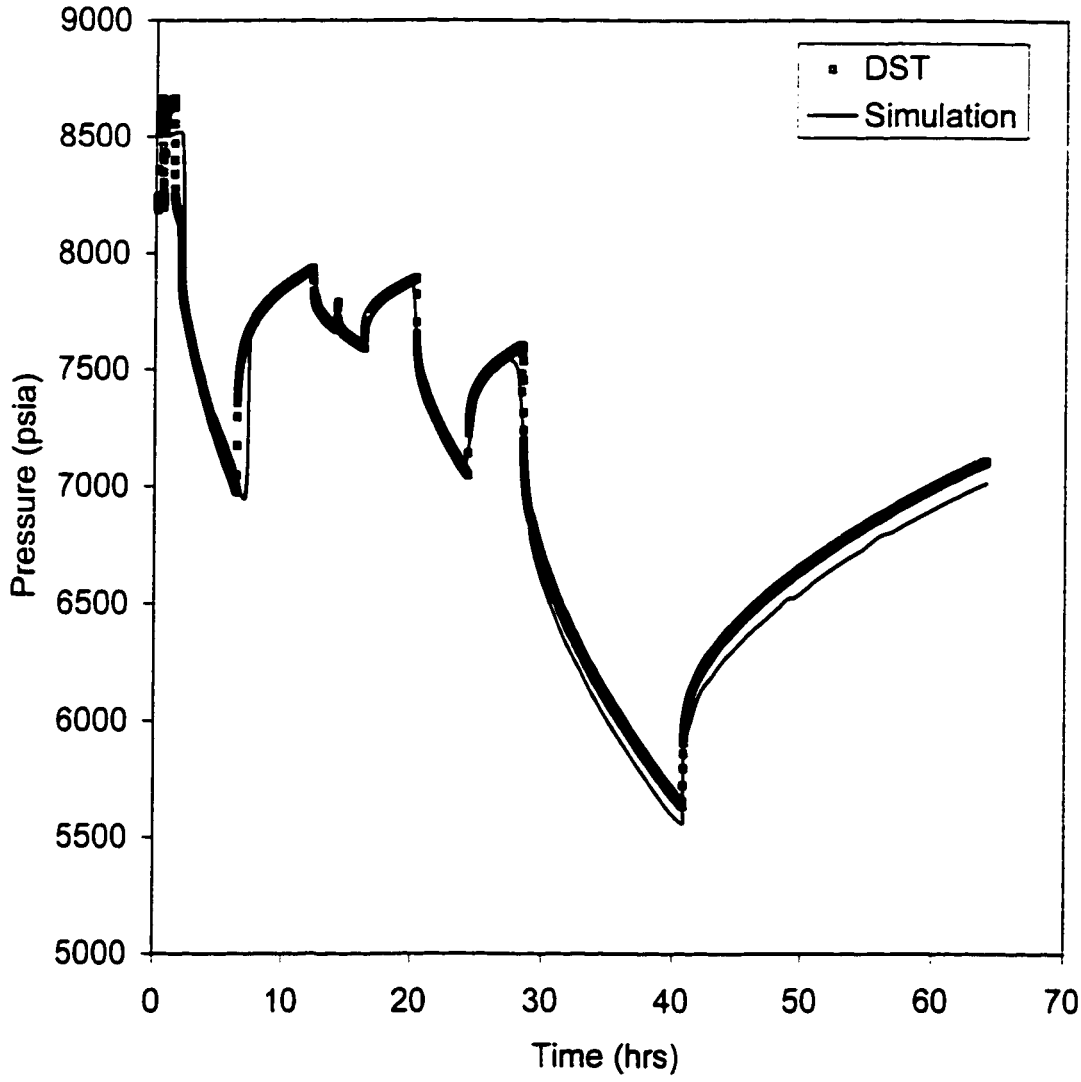

Fig 4.10: Comparison between DST pressure response and simulation results for a gas condensate well.

CHAPTER 5

RELATIVE PERMEABILITY

5.1 Relative permeability model

Due to non-availability of an experimentally determined relative permeability for the zones of interest, it was decided to search for a suitable relative permeability model from literature. There are many relative permeability models or correlation that were obtained through experimental investigations while some are empirical. Such correlation or models includes power law [60], Settari et al [45], Corey [50], and the two-phase relative permeability model. In this study, the two-phase relative permeability model is used.

5.1.1 Two phase relative permeability model

The gas/oil relative permeability equations are:

$$k_{rog} = \left(\frac{S_o - S_{org}}{1 - S_{wi} - S_{org}} \right)^{\frac{2+3\lambda}{\lambda}} \tag{5-1}$$

$$k_{rg} = \left(\frac{S_g - S_{gc}}{1 - S_{wi} - S_{gc}} \right)^{2} \left[1 - \left(\frac{S_o}{1 - S_{wi}} \right)^{\frac{2+\lambda}{\lambda}} \right] \tag{5-2}$$

Water is immobile but we need to input relative permeability data for it in the simulator. The data was generated using the gas/water relative permeability equations

presented below or the water equation in the power law model can be used but the polynomial index must be the same.

$$k_{rw} = \left(\frac{S_w - S_{wrg}}{1 - S_{wrg}} \right)^{\frac{2+3\lambda}{\lambda}} \tag{5-3}$$

$$k_{rg} = \left(\frac{S_g - S_{gc}}{1 - S_{gc}} \right)^{2} \left[1 - (S_w)^{\frac{2+\lambda}{\lambda}} \right] \tag{5-4}$$

λ is the pore size distribution index of the formation and if λ=2, the equations become Corey correlation.

5.1.2 Steps required to generate the k_{rg} and k_{rog} curves

1. Plot a log-log plot of capillary pressure versus normalized water saturation curve or log-log of J-Function versus normalized water saturation.

2. Determine the pore size distribution index λ from the log-log plot of capillary pressure or J-Function versus water saturation curve by calculating the inverse of the slope of the straight line passing through the clustered points. The slope of the straight line is equal to $-(1/\lambda)$.

3. Estimate the end points of the relative permeability curves. The end points are the critical gas saturation and the critical condensate saturation.

4. Calculate k_{rg} and k_{rog} using equations (5-1) and (5-2).

5. Plot k_{rg} and k_{rog} as a function of gas saturation.

It should be noted that S_{gc} is assumed to be 10% and the critical condensate saturation is varied from 0 to 40 % to study its effect on the performance of the productivity of the gas condensate well. The oil-gas relative permeability plot generated using the relative permeability equations when critical condensate saturation is varied from 0 to 40 % is shown in figure 5.1

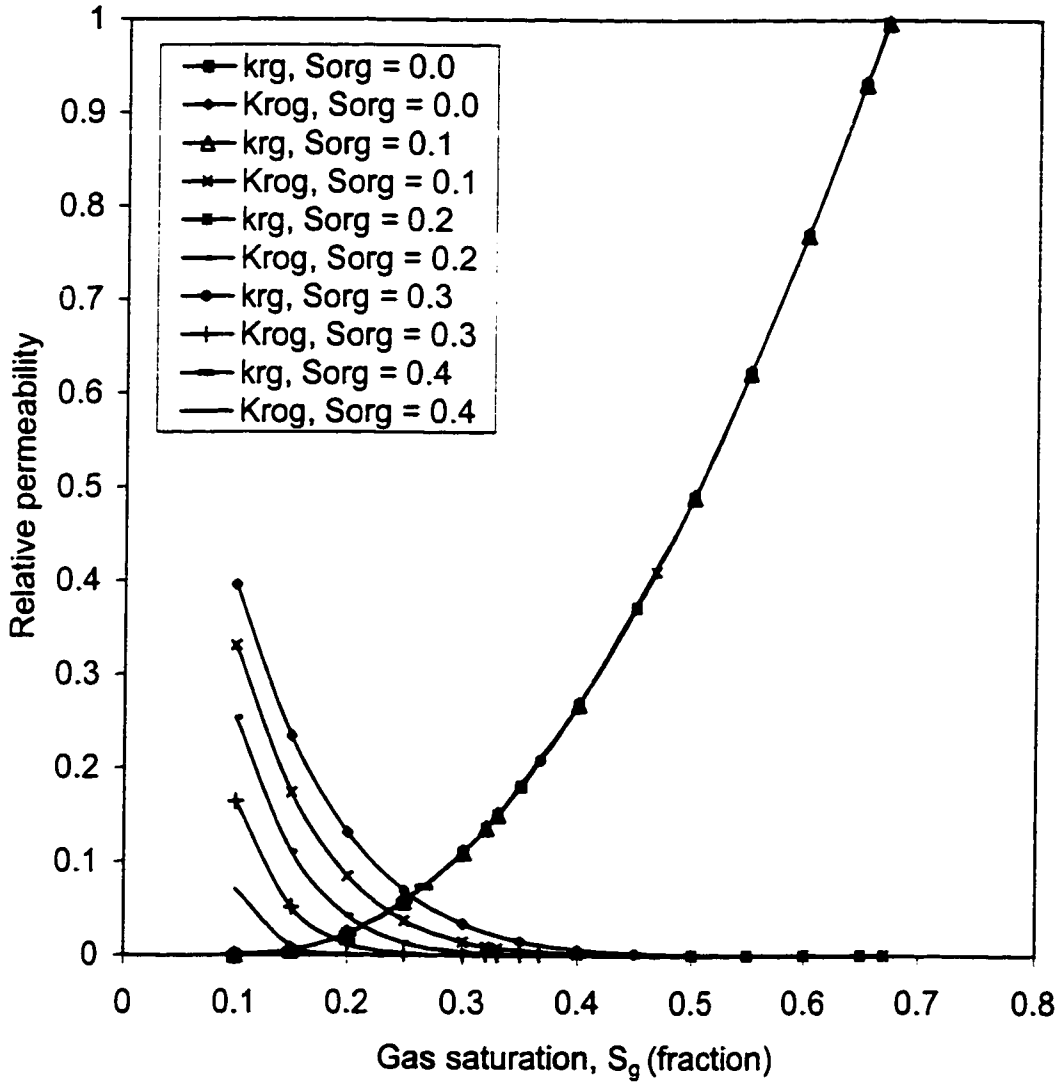

Fig 5.1 Relative permeability curves for the gas condensate system generated using $\lambda = 0.73$, $S_{wi} = 0.33$, $S_{gc} = 0.1$

CHAPTER 6

RESULTS AND DISCUSSION

The main objective of this study is to understand the effect of liquid drop out on the productivity of a multi-layer, tight and rich gas condensate reservoir. In order to achieve the study objectives, we build a single well radial compositional model utilizing "CHEARS" simulator developed by Chevron Petroleum Technology Company.

In this study, we imposed a minimum bottom hole pressure of 500 psia on the well. Setting minimum BHFP constraint is reported in the literature [11]. Fevang and Whitson [11] imposed a minimum BHFP of 250psia on the well in order to see if low oil saturation near the wellbore due to vaporization will lead to significant improvement in the well deliverability.

The following parameters will be investigated and discussed in this chapter.

1. Number of grid cells away from the wellbore
2. Size of the first grid cell in the radial model
3. Critical condensate saturation
4. Production rate
5. Gas flow productivity index
6. Condensate saturation distribution
7. Pressure distribution

6.1 SENSITIVITY OF WELL PERFORMANCE TO NUMBER OF GRID CELLS AWAY FROM THE WELLBORE

In order to eliminate the effect of grid system on the performance of the gas condensate well, several runs were made with different grid system. Figures 6.1 and 6.2 show the sensitivity of the well performance to the number of radial grid cells away from the wellbore. The model was run for production rates of 20 and 50 MMSCF/D. Similar results were also obtained for production rates of 30, 40 and 60 MMSCF/D. The literature reported similar attempts made by Affidick et al [44], Clark [12], Hsu et al [22], Fevang and whitson [11] and Barnum et al [2] and Bourbiax, B.J [24].

In this study, it is obvious from figures 6.1 and 6.2 that there is a need to use more than 20 grid cells but there exist almost no difference on the results if 30, 40 or 50 grid cells are used. This observation is true for all gas production rates used. The observation that using 20, 30, 40, 50 or more grid cells away from the wellbore has very minimal effect on production supports the findings of Morel et al [1]. He conducted sensitivity to gridding and found out that extending the number of grid blocks from 112 to 200 or reducing it to 50 did not modify the well productions. Since this study is carried out at 20, 30, 40 50 and 60 MMSCF/D, 30 radial grid cells away from the wellbore were used to capture the condensation effects accurately for all rates.

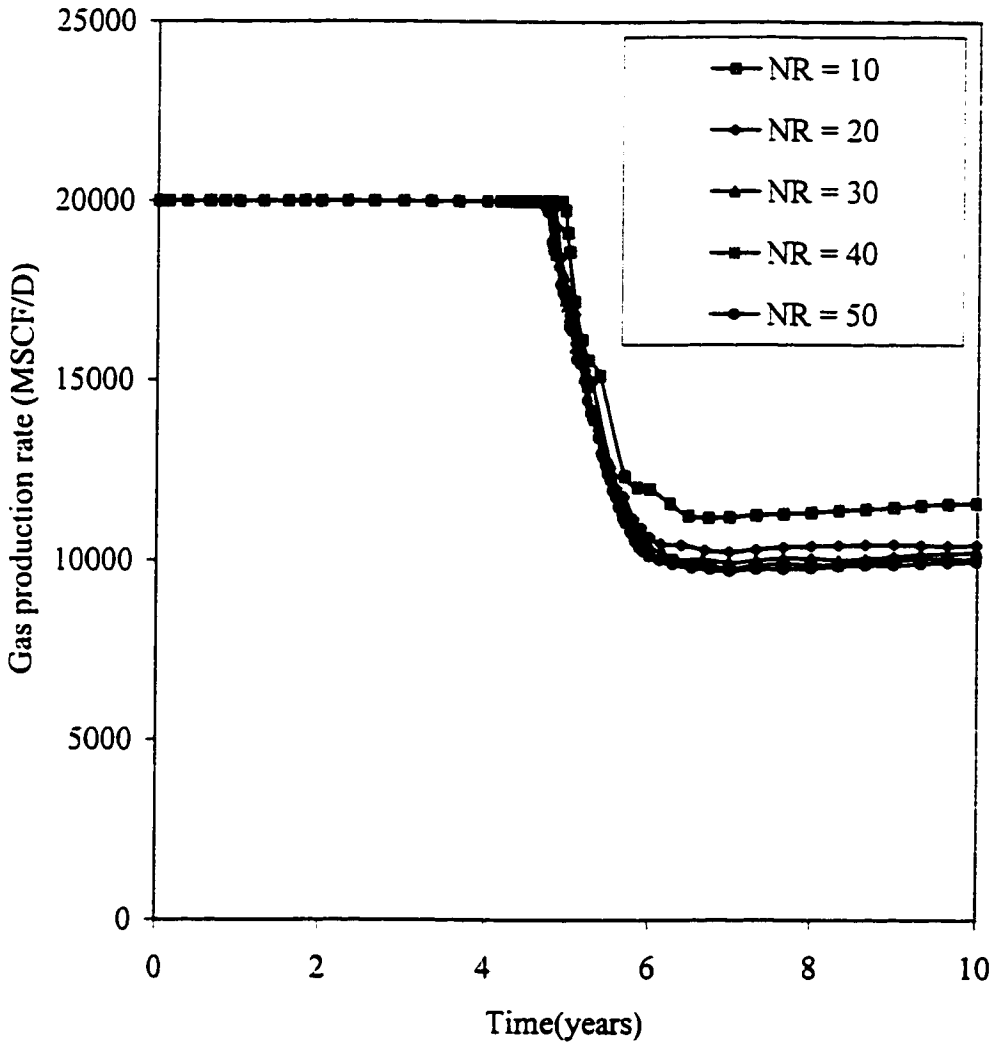

Fig 6.1: Effects of the number of radial grid cells away from the wellbore on well performance predictions when gas production rate is 20MMSCF/D

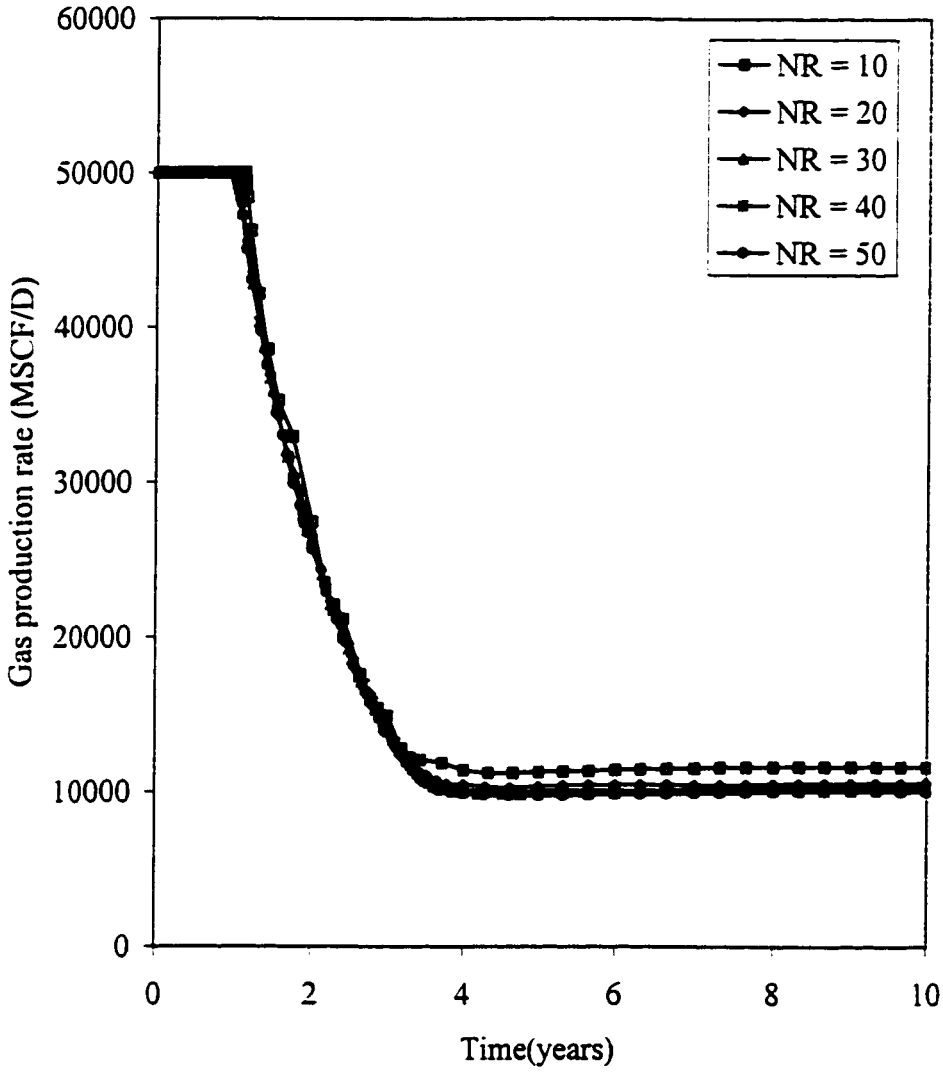

Fig 6.2: Effect of the number of radial grid cells away from the wellbore on well performance when gas production rate is 50MMSCF/D

6.2 SENSITIVITY OF WELL PERFORMANCE TO THE SIZE OF FIRST GRID CELL IN THE RADIAL MODEL

The size of the inner grid blocks in a radial model has been reported to influence pressure and saturation profiles in the wellbore region [33].

Choosing a small radii around the wellbore allows accurate modeling of pressure drop in the near wellbore region. If a large grid cell size is used it will give higher grid block pressure which will under-predict the amount of hydrocarbon liquid that will condense at lower pressure hence lower hydrocarbon saturation will be predicted or rather over-predicting well productivity [2].

The size of the first grid cell in a radial simulation is important in modeling well deliverability of a gas condensate well [11]. Bourbiaux [24], Barnum et al [2], Hsu et al [22], Afidick et al [44], Fevang and Whitson [11] and Wu et al [36] found that the size of first grid cell in a radial model must be small. The above investigators used a grid size of 6m, 0.2 ft, 1ft, 10ft, 1ft and 0.7ft respectively.

In this study, a sensitivity of the size of the first radial grid cell on the production performance of the gas condensate well was investigated. Figures 6.3 and 6.4 show the result obtained for the effects of different values of r_1 on the well performance when gas production rates are 20 and 50 MMSCF/D. Similar results were also obtained when 30, 40 and 60 MMSCF/D were used. The results confirm that the size of the first cell must be small and that there is no significant difference between using 0.4, 0.5, 0.6, 0.7, 0.8, 0.9 or 1.0ft for r_1 especially at higher production rates. 0.4 ft is the size of r_1 used in this study.

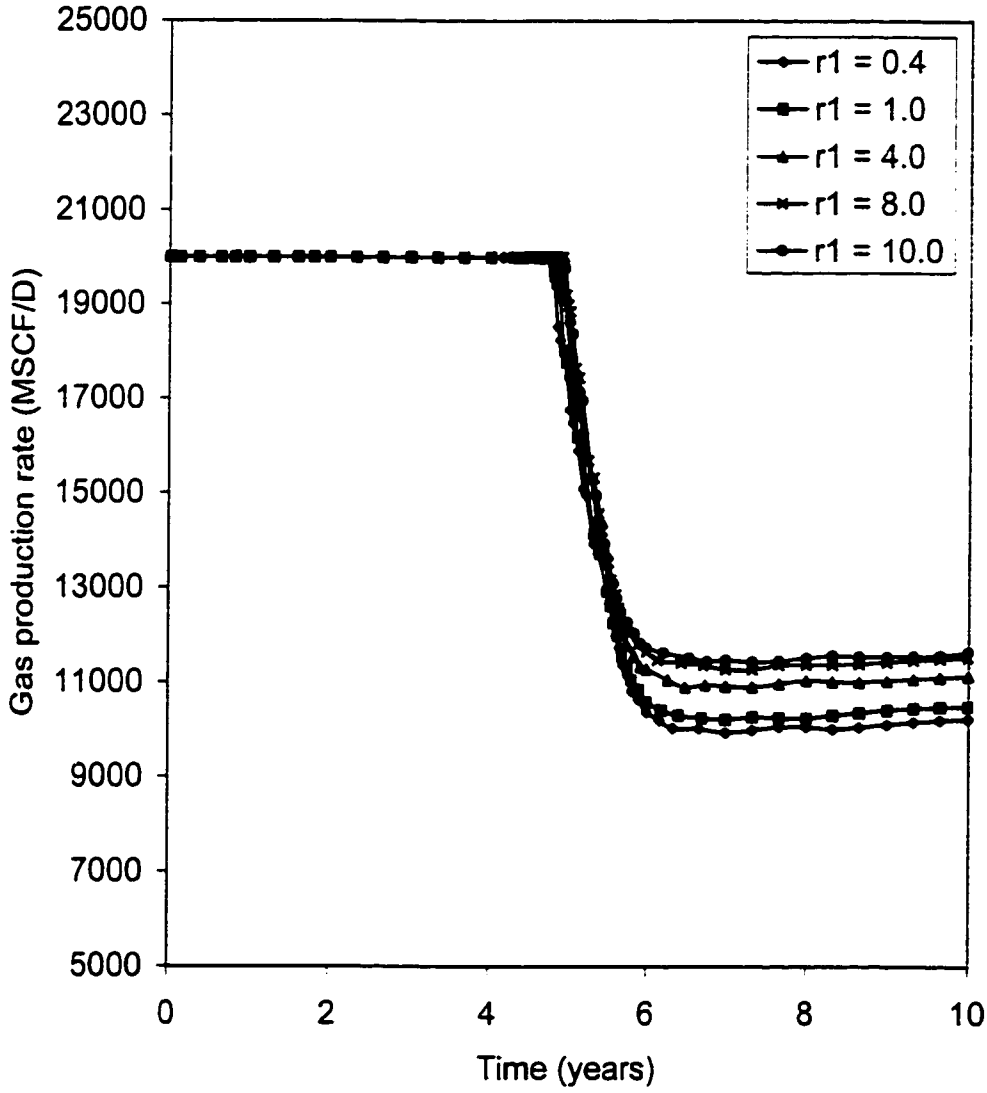

Fig 6.3: Sensitivity of r1 on the gas condensate well perfomance prediction when gas production rate is 20MMSCF/D

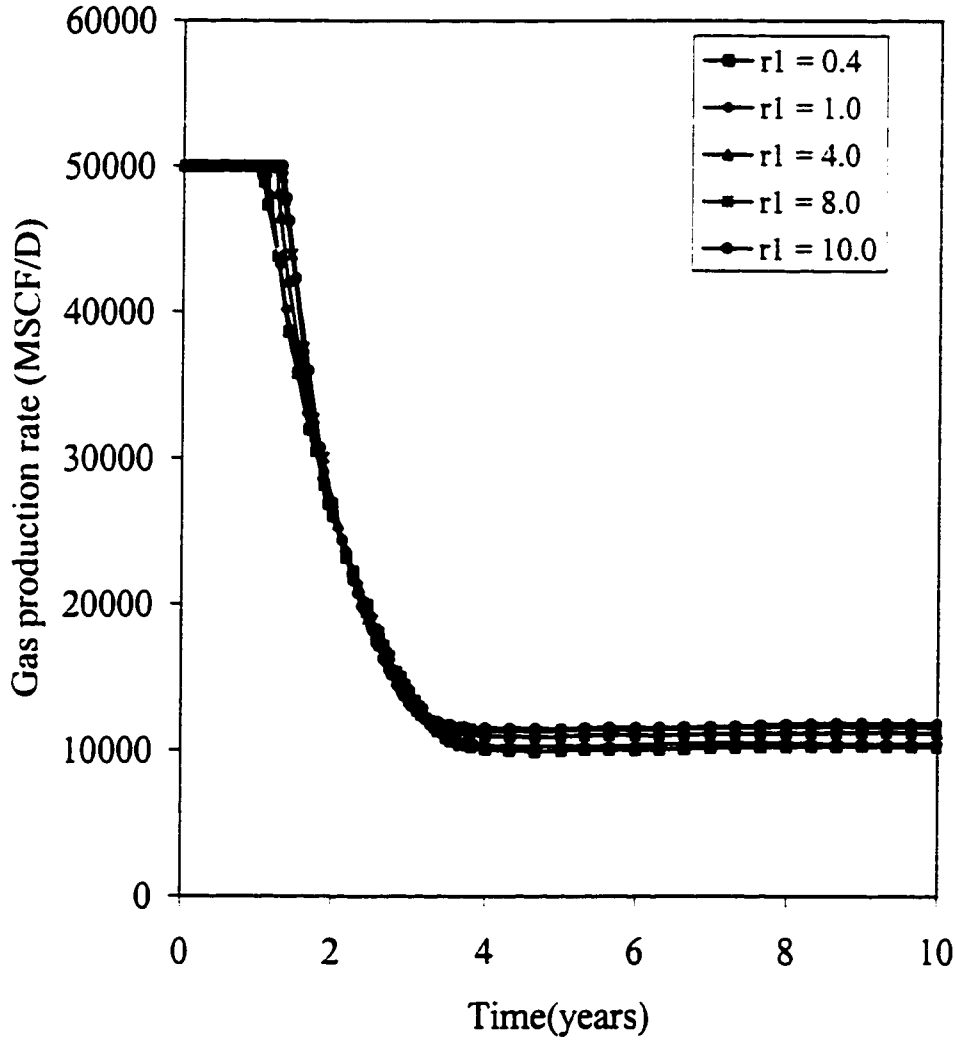

Fig 6.4: Senesitivity of gas condensate well performance to the radius of the first grid cell (r1) when gas production rate is 50MMSCF/D

6.3 MODEL DESCRIPTION

To achieve the study objectives, a single well, compositional, 2 dimensional (r-z coordinate system) with angle of 360^0 simulation model was used. The model consisted of 160 ft of permeable zones but the formation thickness is 230 ft when the shale breaks are included. The drainage radius of the reservoir considered, r_e is equal to 6557.4 ft. The wellbore radius is 0.35 ft, the first cell radius is 0.4 ft and the remaining cells increased geometrically away from the wellbore. Table 6.1 illustrates the cell dimensions used in the simulation study.

Seven-layer reservoir description based on core and petrophysical analysis, initial water saturation and pore size distribution index determined through air displacing water experimental data was used in the single well radial compositional simulation model.

Layers 5, 6 and 7 are very low in permeability so when the depletion run was made, they did not contribute to production. There were no changes in pressure and gas saturation in these layers. It was then decided to remove layers 5, 6 and 7 from the model used in this study.

TABLE 6.1: Dimensions of radial grid cells used in the simulation

BLOCK	INNER (ft)	CENTER (ft)	OUTER (ft)
1	0.35	0.4	0.47
2	0.47	0.56	0.66
3	0.66	0.78	0.92
4	0.92	1.09	1.29
5	1.29	1.53	1.8
6	1.8	2.13	2.52
7	2.52	2.98	3.52
8	3.52	4.16	4.92
9	4.92	5.82	6.88
10	6.88	8.13	9.61
11	9.61	11.36	13.43
12	13.43	15.88	18.77
13	18.77	22.19	26.23
14	26.23	31	36.65
15	36.65	43.32	51.21
16	51.21	60.54	71.57
17	71.57	84.61	100.01
18	100.01	118.23	139.76
19	139.76	165.22	195.31
20	195.31	230.89	272.94
21	272.94	322.65	381.41
22	381.41	450.88	533
23	533	630.08	744.84
24	744.84	880.5	1040.87
25	1040.87	1230.45	1454.56
26	1454.56	1719.48	2032.66
27	2032.66	2402.87	2840.52
28	2840.52	3357.88	3969.46
29	3969.46	4692.43	5547.09
30	5547.09	6557.4	6557.4

6.4 EFFECT OF CRITICAL CONDENSATE SATURATION

Pressure decline below the dew point pressure causes condensation to occur as depletion of reservoir progress with time leading to accumulation of liquid saturation in the vicinity of the wellbore and sometimes the entire reservoir. The liquid saturation will become mobile once the critical condensate saturation has been exceeded. Liquid accumulation acts as a hindrance to well productivity due to reduction in the relative permeability to gas [38,39].

Accurate knowledge of the critical condensate saturation and their relationship to physical properties of the fluids and the petrophysical properties of rocks are essential for an accurate representation of gas condensate flow behavior in reservoirs [35,37]. Connate water has significant influence on the critical condensate saturation. Henderson et al [25] found that gas condensate flow can be extremely affected by the actual distribution and magnitude of connate water. The critical condensate saturation is a key parameter that also affects the relative permeability. Figure 5.1 shows different relative permeability curves generated when critical condensate saturation is 0, 10, 20, 30 and 40 % of pore volume. The initial water saturation was fixed at 33 % for all critical condensate saturation investigated.

It is important to perform a sensitivity study to understand the effect of critical condensate saturation on the performance of a gas condensate well undergoing depletion. Based on this, a sensitivity study on the effect of critical condensate saturation on the gas condenate well performance was carried out. The result presented in figures 6.5 and 6.6 indicate that the higher the critical condensate saturation the lower is the well

productivity and vice versa. When the critical condensate saturation is 0 % as shown in figure 6.5 there exist a decline in the well productivity due to liquid condensation when the dew point is reached.

The sensitivity of gas condensate well performance to critical condensate saturation is also studied. The well performance at a gas production rates of 20 and 50 MMSCF/D for a fixed critical condensate saturation of 0, 10, 20, 30 and 40 % can be seen in figures 6.7 to 6.11. These figures show clearly that at a critical condensate saturation of 0, 10, 20, 30 and 40 % all gas production rates investigated stabilized, after the effect of liquid condensation on well productivity has ceased, to 13500, 1000, 7500, 4000 and 2000 MMSCF/D respectively. The reason for the gas production stabilizing at one rate immaterial of the gas production rate can be linked to the imposed minimum bottom pressure of 500psi. This result show that increasing critical condensate saturation reduces the stabilized gas production rates and this implies reduction in well productivity.

The result of our sensitivity study is in agreement with Barnum et al [2], Affidick et al [44], and Hsu et al [22] but disagree with the conclusion of Fevang and Whitson [11]. It should be noted that for the rest of this study, a fixed residual gas saturation of 10 %, initial water saturation of 33 % and critical condensate saturation of 10% would be used.

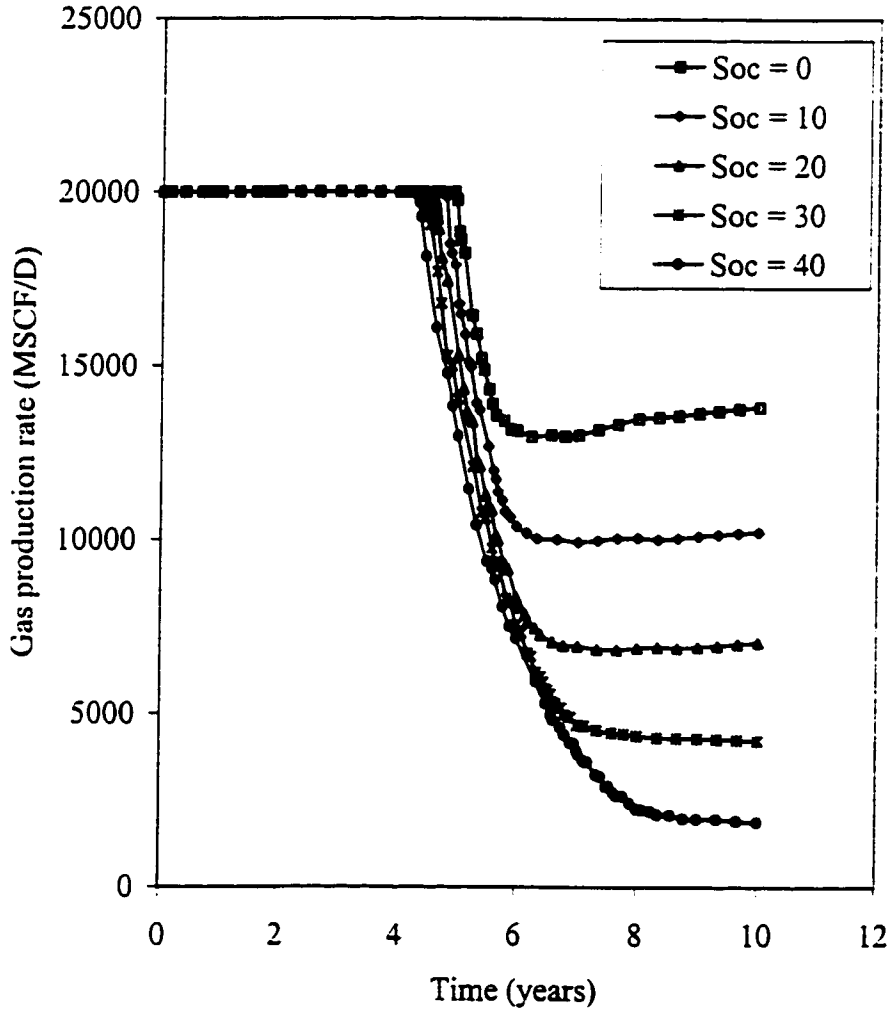

Fig 6.5: Effect of critical condensate saturation on well performance when maximum gas production constraint is 20 MMSCF/D

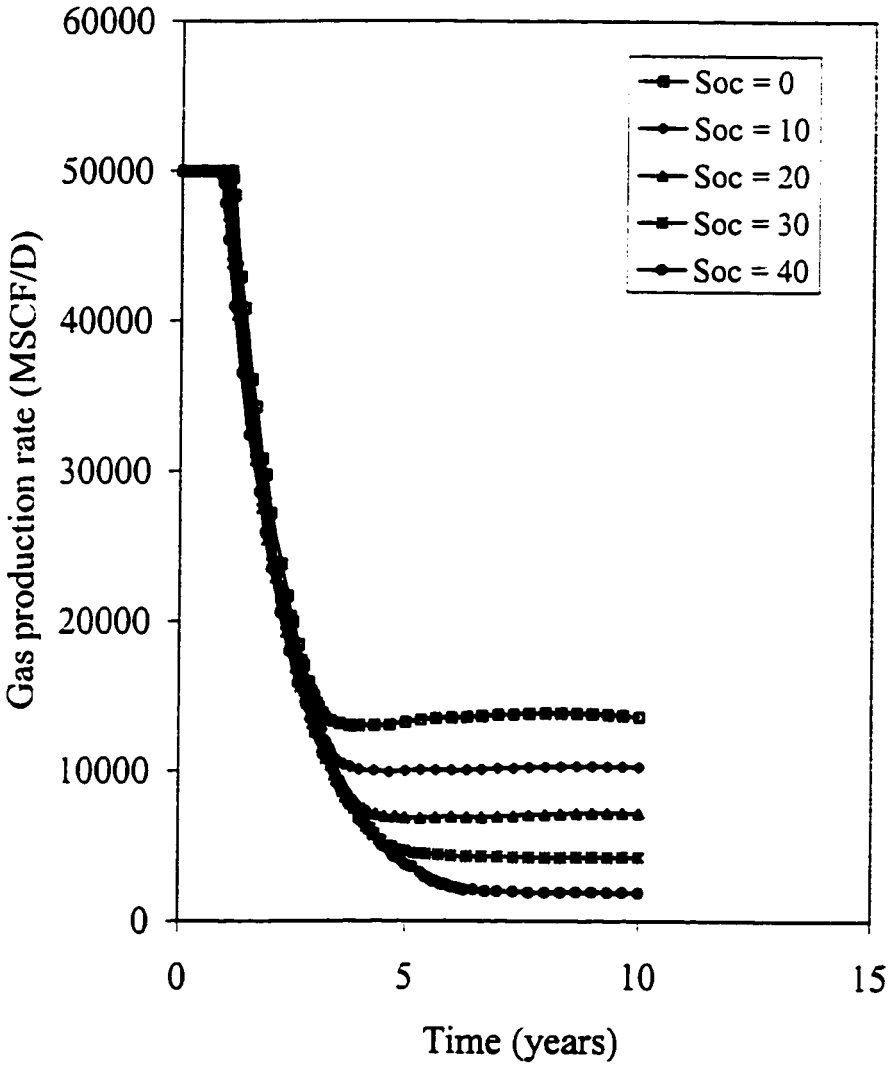

Fig 6.6: Effect of critical condensate saturation on well performance when maximum gas production constraint is 50 MMSCF/D

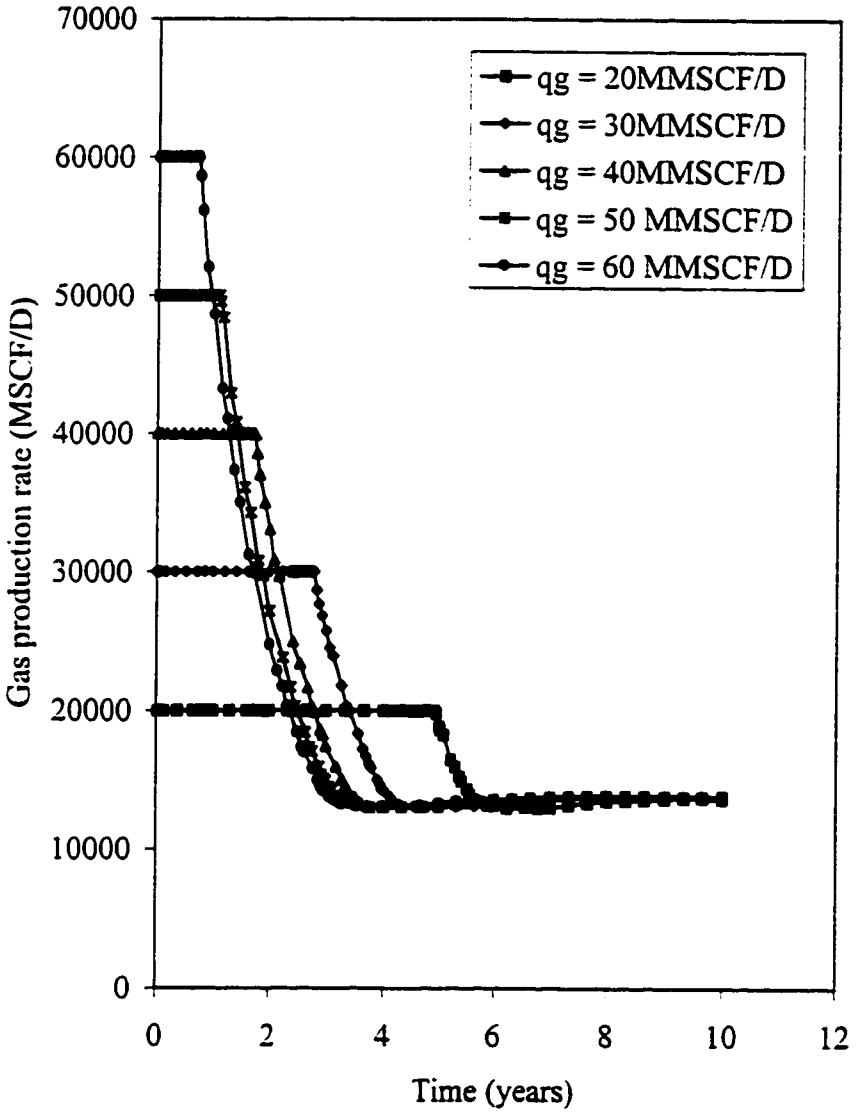

Fig 6.7: Well performance when the critical condensate saturation is 0 %

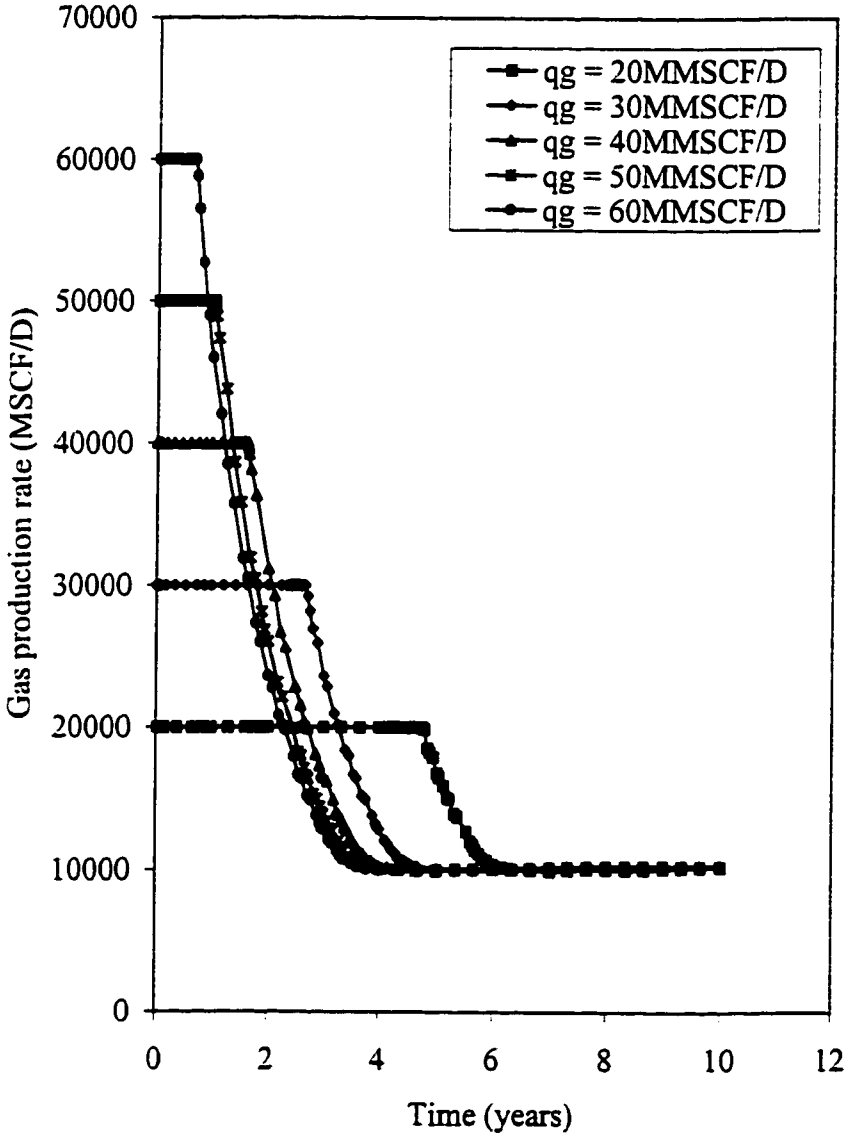

Fig 6.8: Well performance when the critical condensate saturation is 10 %

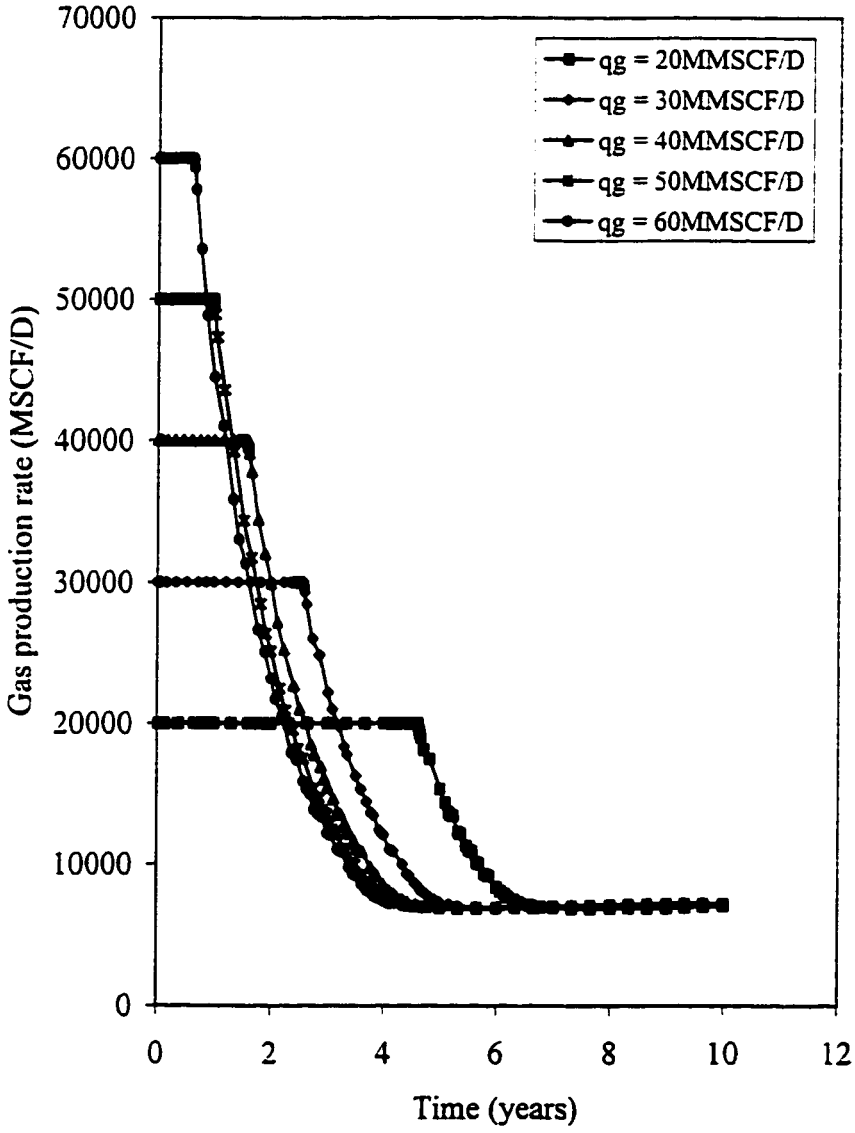

Fig 6.9 : Well Performance when the critical condensate saturation is 20 %

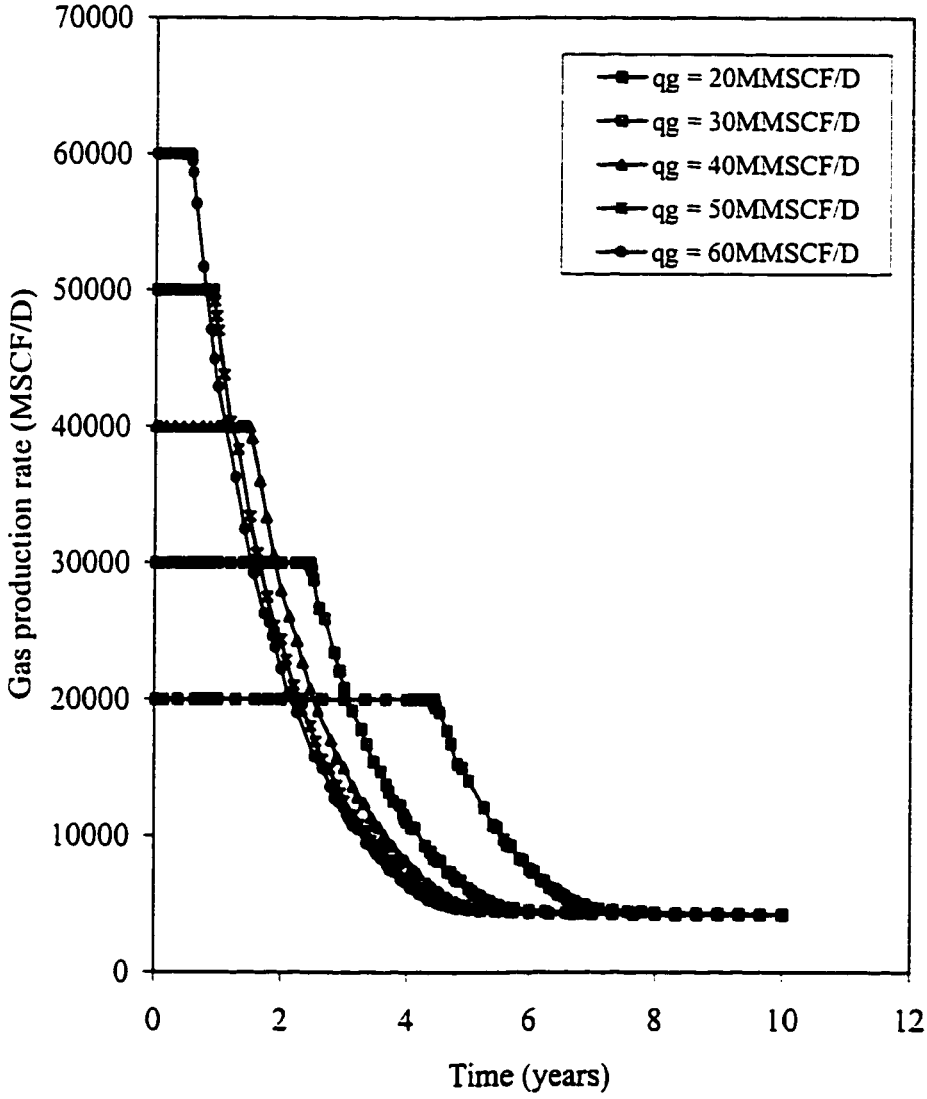

Fig 6.10: Well performance when the critical condensate saturation is 30 %

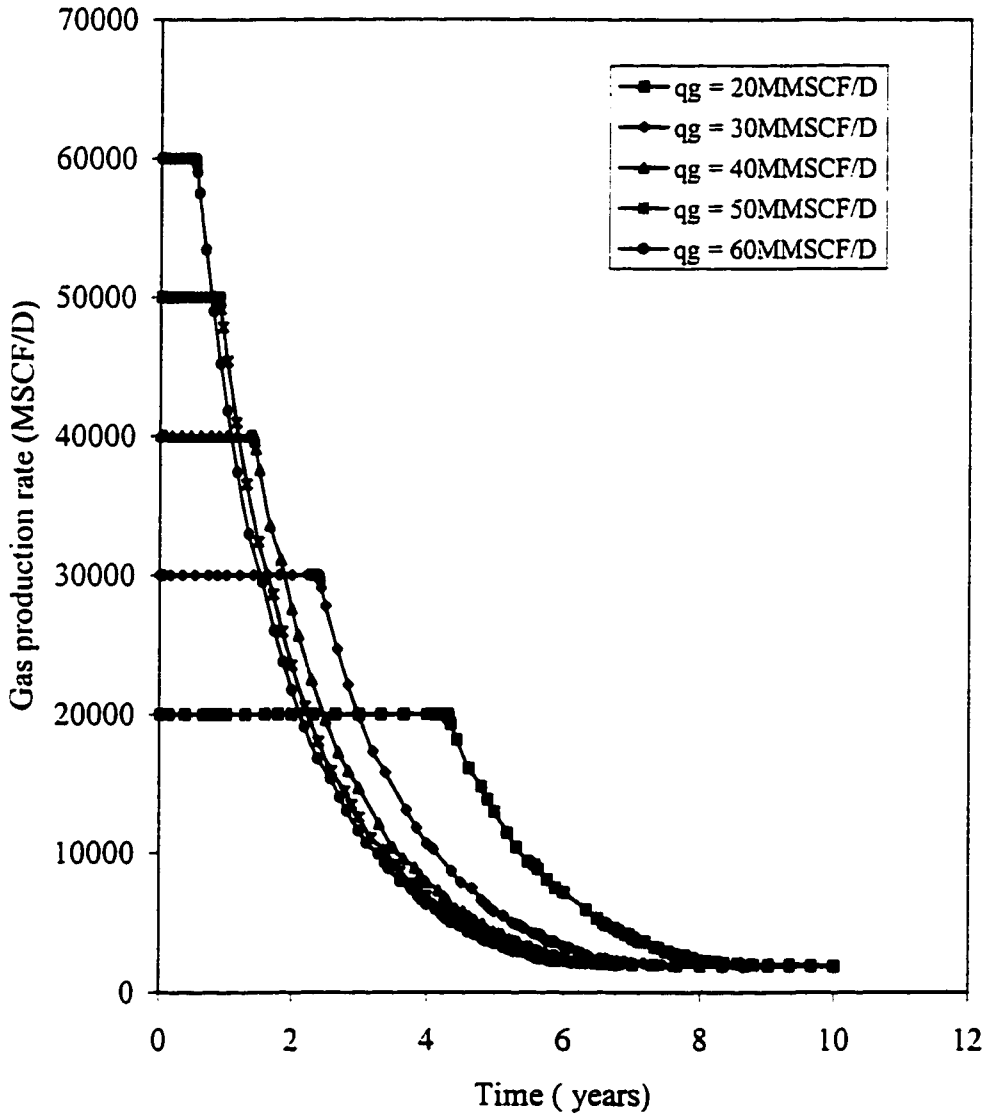

Fig 6.11 : Well performance when the critical condensate saturation is 40 %

6.5 EFFECT OF PRODUCTION RATE

The gas condensate well is made to undergo ten years of depletion with an imposed maximum gas production rates of 20, 30, 40, 50 and 60 MMSCF/D. This investigation will aid in the sensitivity analysis of the well performance to gas production rates. Figures 6.12, 6.13 and 6.14 show the plots of gas production rate, condensate production rate and flowing bottom hole pressure as a function of time.

The gas production rate of 20 MMSCF/D and surface condensate production rate of 3540.9 STB/D were sustained during the first 4.8 years. This is possible as long as the dew point pressure has not been reached. The gas and surface condensate production decrease rapidly during the next 1.2 years. The behavior of the well is similar for higher gas production rates though the length of the plateau is shorter. For the 30 MMSCF/D gas, the well sustained production for 2.7 years while it sustained production for 1.65, 1.03 and 0.66 years respectively when production rate is 40, 50 and 60MMSCF/D. Condensate produced at surface when the gas production rate are 30, 40, 50 and 60MMSCF/D are 5310.29, 7080.39, 8850.48 and 10620.8 STB/D respectively. All gas production rates investigated (i.e. 20, 30, 40, 50 and 60 MMSCF/D) reached stabilized rate of about 10MMSCF/D and 1200 STB/D in the remaining 4, 5.34, 6.22, 6.39 and 6.49 depletion years respectively. All gas production rates stabilized at the same value because of the 500 psia minimum bottom hole flowing pressure imposed on the well. The stabilized rate reached by all rates at 10 MMSCF/D is referred to as pseudosteady state by O'Dell and Miller and Fussel [61]. Figures 6.15 to 6.19 show the evolution of the bottom hole flowing pressure, gas production rate, surface condensate flow rate, average

reservoir pressure and well productivity index when the well is put on a gas rate of 20, 30, 40, 50 and 60 MMSCF/D respectively. The dew point is reached at 4.8, 2.7, 1.65, 1.03 and 0.66 years respectively. Once the flowing bottom hole pressure falls below the dew point, condensate liquid accumulates near the wellbore and throughout the reservoir when the average reservoir pressure falls below the dew point pressure. When this happens, a significant loss in the well productivity index from 22.07 to 2.11, 23.234 to 2.73, 23.16 to 2.79, 22.89 to 2.82 and 22.52 to 2.84 MSCF/D/psia is noticed for 20, 30, 40,50 and 60 MMSCF/D respectively.

Fevang and Whitson [11] observed that reduced gas deliverability due to condensate blockage is only important when the bottom hole flowing pressure reaches a minimum dictated by the surface constraints and the well is forced to go on decline. The significant reduction in the well productivity index shown in figures 6.15 to 6.19 can only be linked to evolution of near wellbore condensate leading to a reduction in the relative permeability to gas.

The average reservoir pressure shown in figures 6.15 to 6.19 did not fall below the dew point pressure (5153 psia) until 13, 5, 4.35, 4.31 and 4 years of depletion when the maximum gas production rates are 20, 30, 40, 50 and 60MMSCF/D respectively. An observation from this is that the higher the production rates the shorter the plateau due to condensate drop out below the dew point whose occurrence is rate dependent.

Several investigators performed sensitivity study on the response of gas condensate well to production rates. Notable among them are Affidick et al [44], Novosad [13], Barnum et al [2], Clark [12], Hsu et al [22], Ali et al [26], Fevang and whitson [11], Bourbiaux [24], Pope et al [6] and Henderson et al [25].

The consensus in the literature is that pressure decline during depletion of a gas condensate reservoir below the dew point pressure causes condensation to occur. An increase in accumulation of hydrocarbon liquid near the wellbore and in the entire reservoir follows if the average reservoir pressure falls below the dew point pressure. The accumulation of condensed liquid reduces liquid recovery, gas productivity and bottom hole flowing pressure. This conclusion is in agreement with the findings presented above on the sensitivity of gas condensate well performance to production rates.

Figures 6.20 and 6.21 present cumulative gas and condensate produced respectively as a function of time for gas production rates of 10, 20, 30, 40, 50 and 60 MMSCF/D. It can be seen from these figures that there is no significant improvement in gas production if the well is produced at a rate higher than 40 MMSCF/D. This observation is more clear in figures 6.22 and 6.23. Figure 6.12 is a plot showing the effect of gas production rate on the performance of gas condensate well. The figure shows that the well can sustain production at 20, 30, and 40 MMSCF/D for 4.77, 2.7, and 1.65 years while 10MMSCF/D will be sustained throughout the 10 years depletion time.

Based on the above result it can be concluded that the well should be put on a minimum gas production rate of about 40MMSCF/D to obtain maximum recovery.

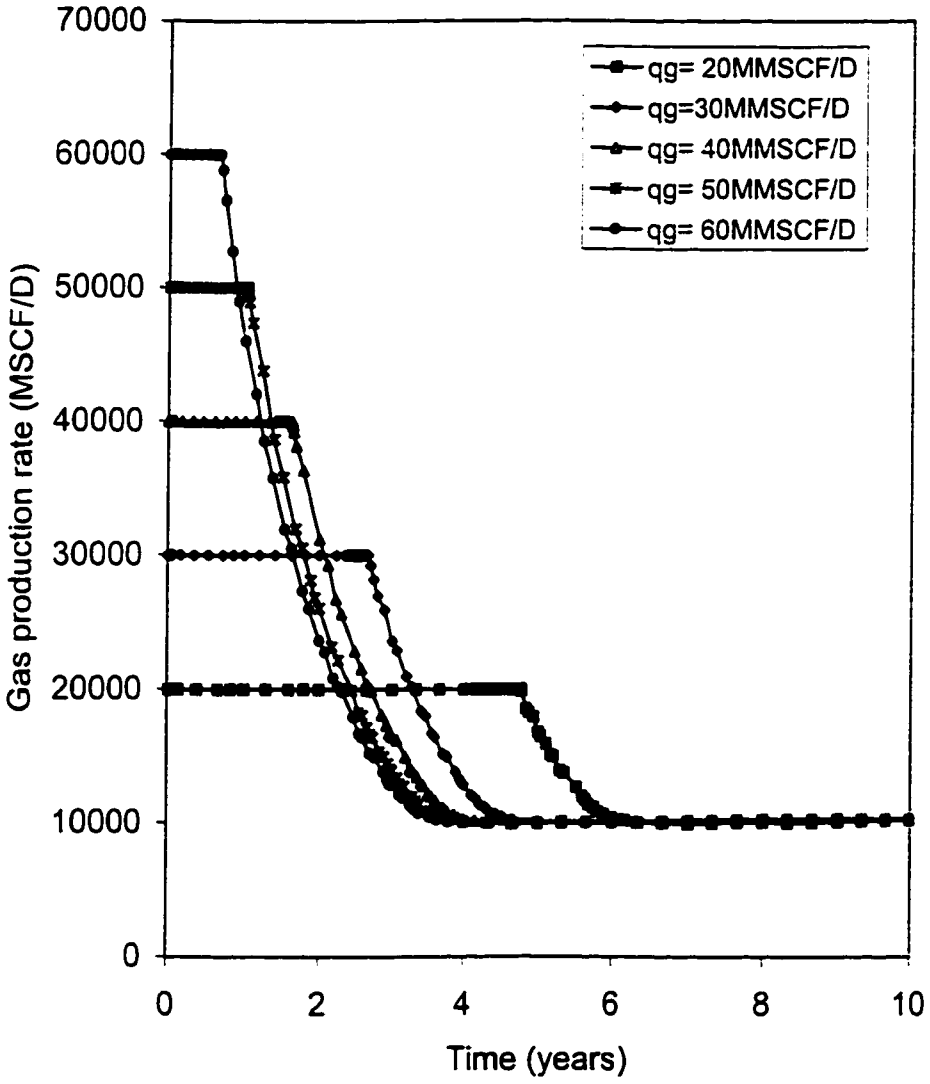

Fig 6.12: Effect of gas production rate on the performance of a gas condensate well

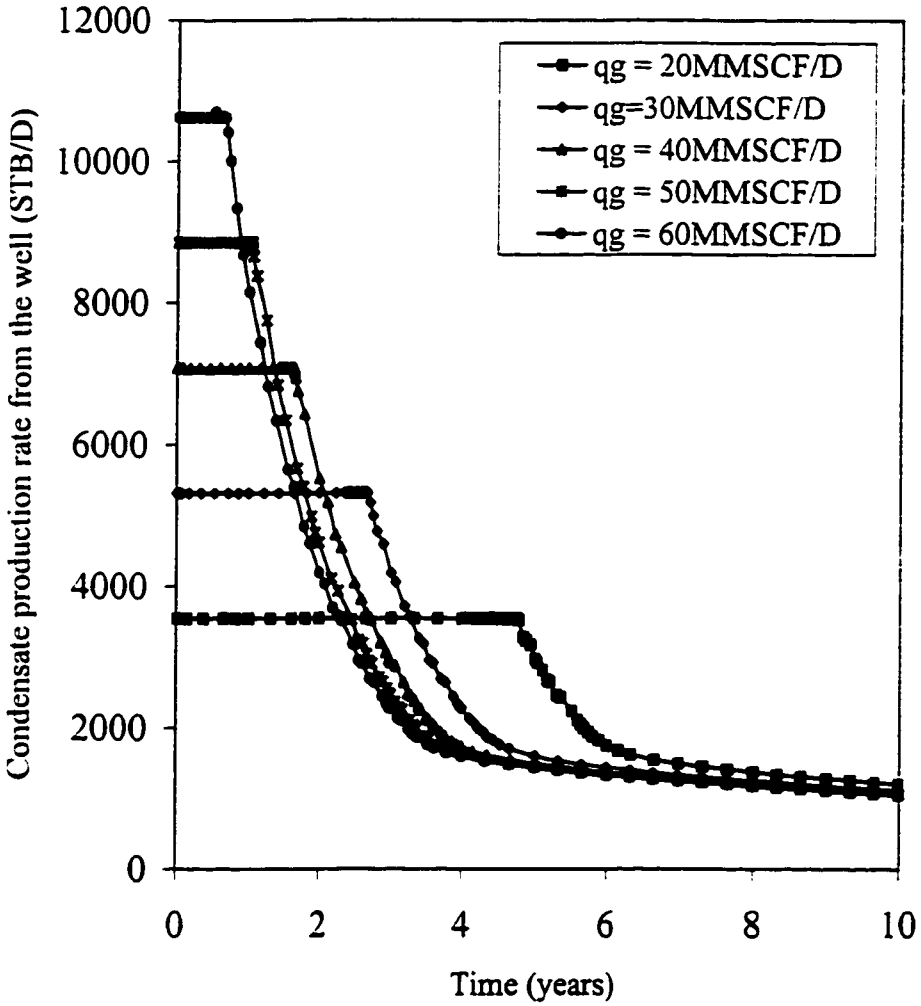

Fig 6.13 : Effect of gas production rate on condensate production from the well

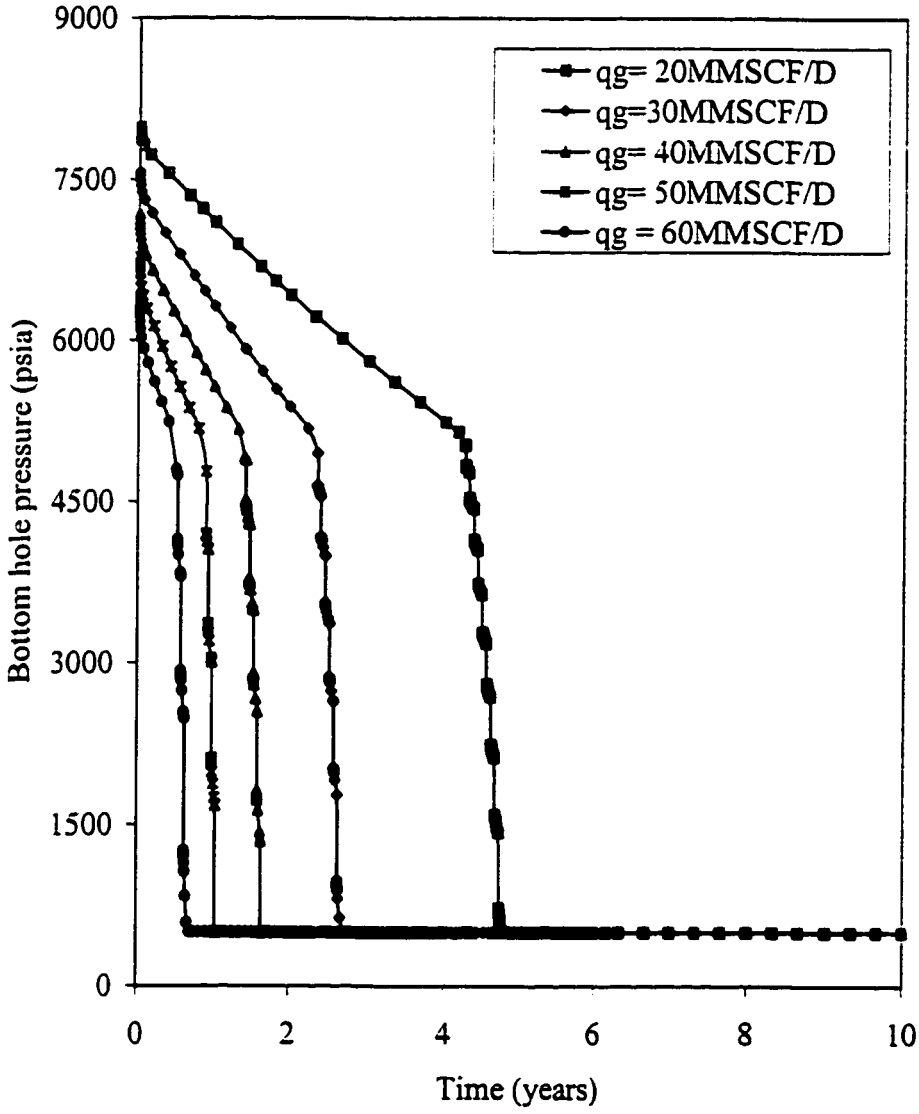

Fig 6.14: Bottom hole flowing pressure versus time for different gas production rate when the dewpoint pressure is 5153 psia and the minimum BHFP is 500 psia

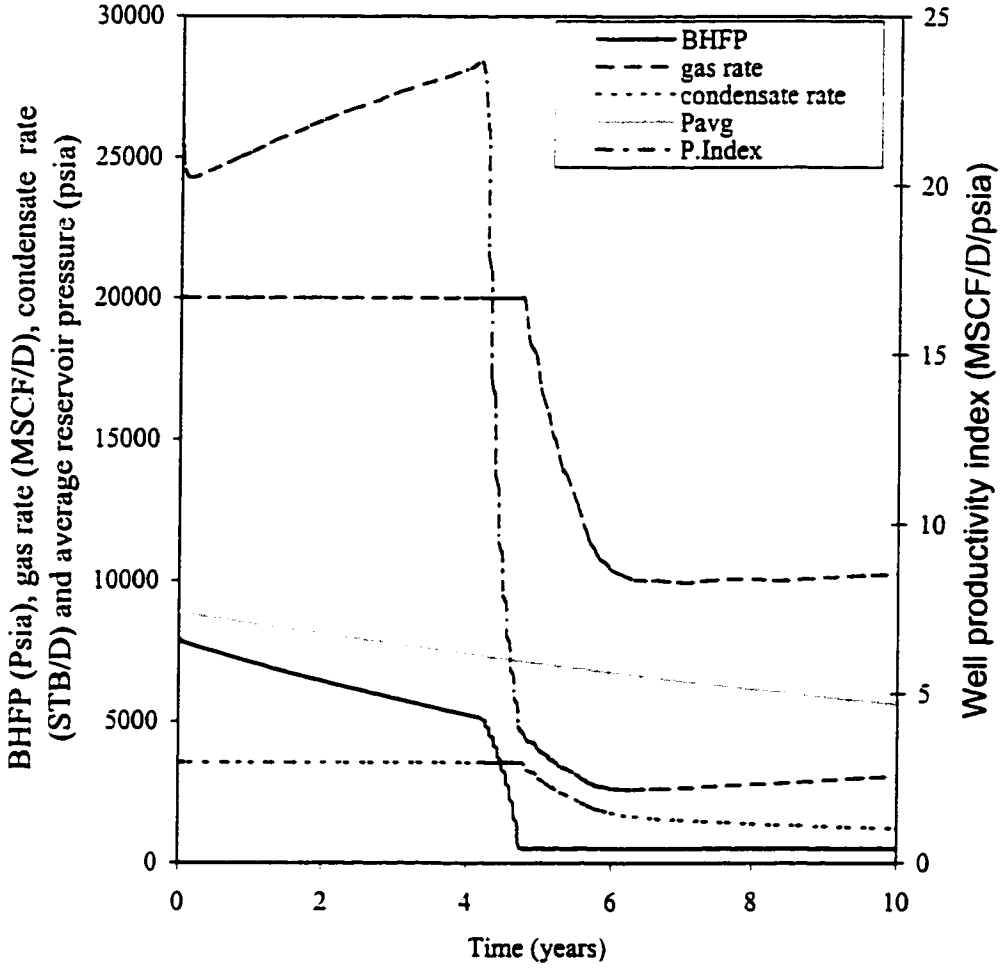

Fig 6.15 : Simulated depletion for a gas condensate reservoir when the maximum gas production constraint is 20 MMSCF/D

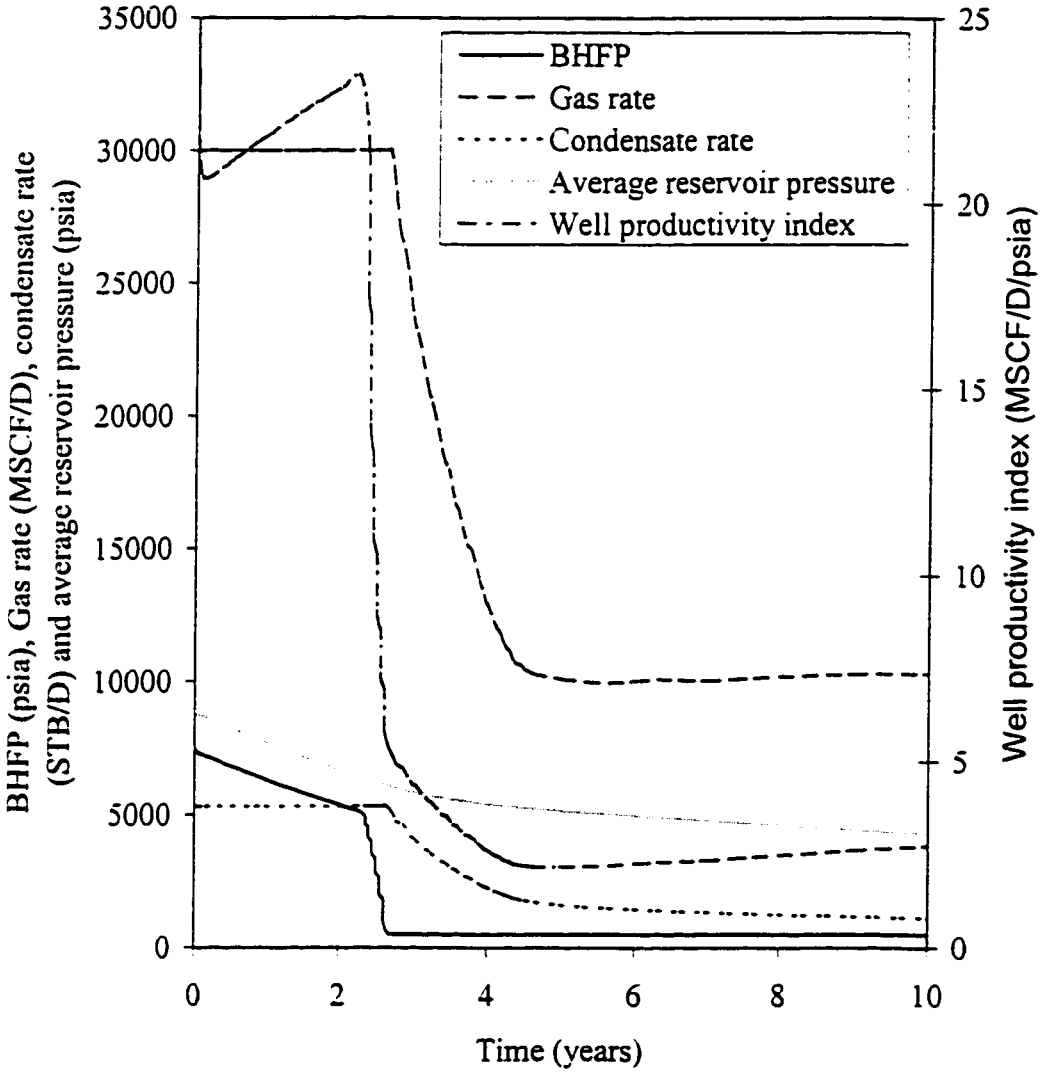

Fig 6.16: Simulated depletion for a gas condensate reservoir when the maximum gas production constraint is 30 MMSCF/D

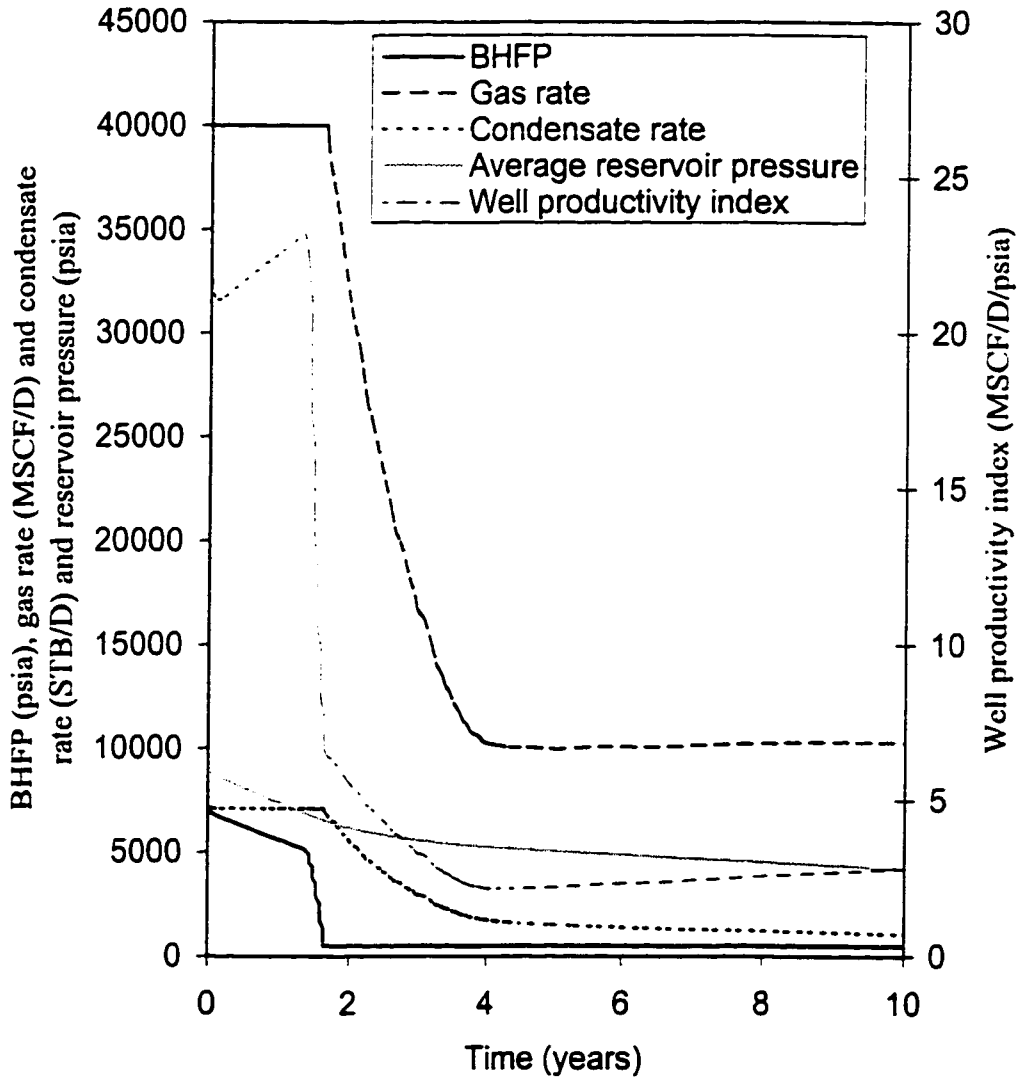

Fig 6.17 : Simulated depletion for a gas condensate reservoir when the maximum gas production constraint is 40 MMSCF/D

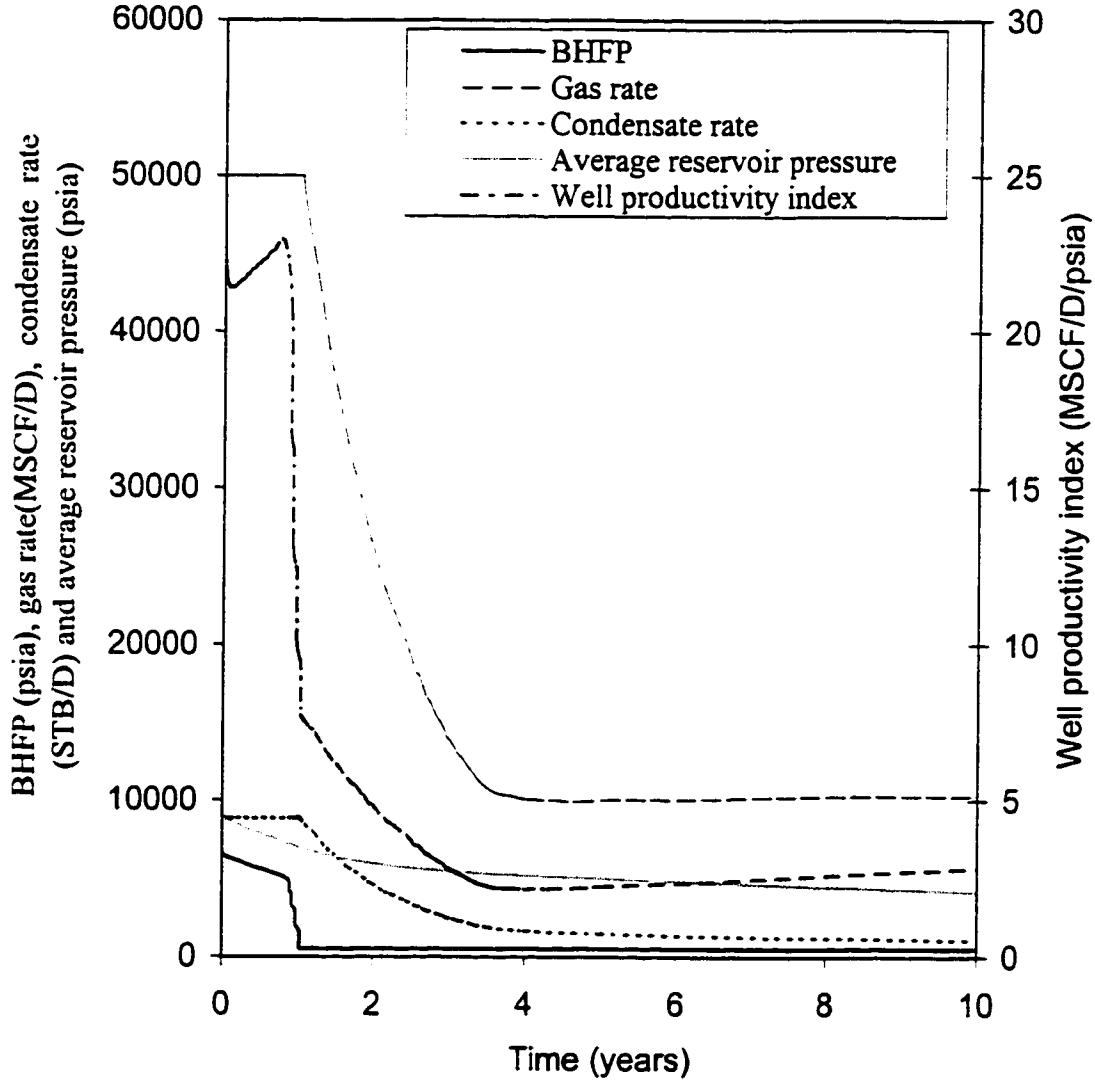

Fig 6.18: Simulated depletion for a gas condensate reservoir when the maximum gas production constraint is 50MMSCF/D

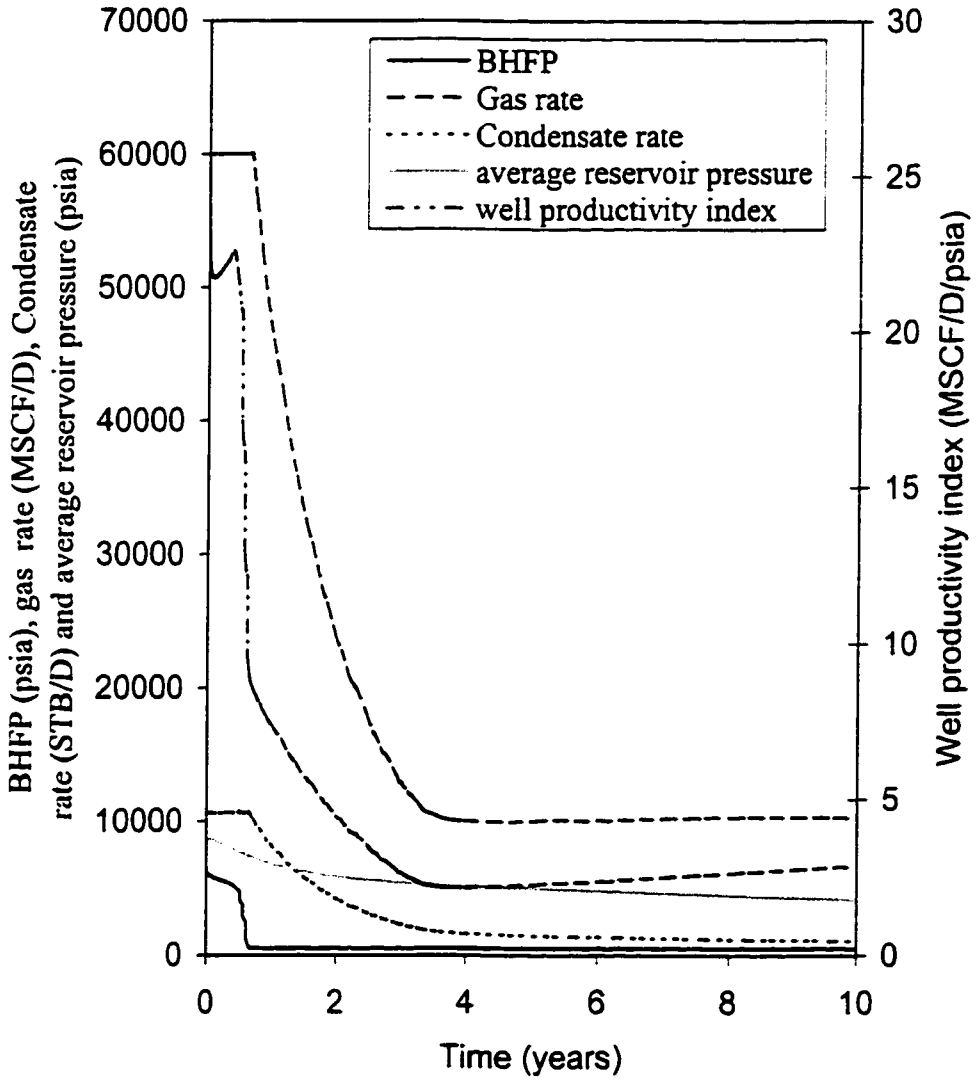

Fig 6.19: Simulated depletion for a gas condensate reservoir when the maximum gas production constraint is 60 MMSCF/D

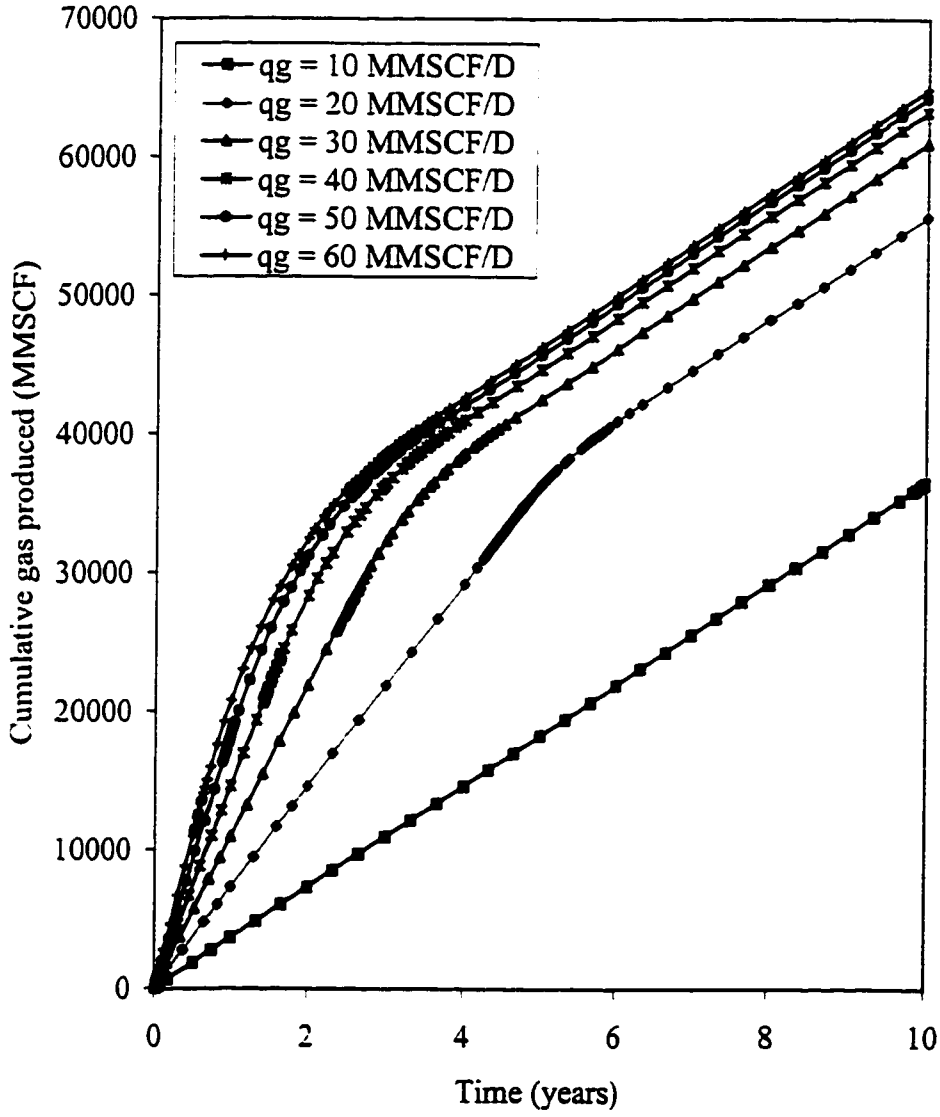

Fig 6.20: Cumulative gas produced versus time

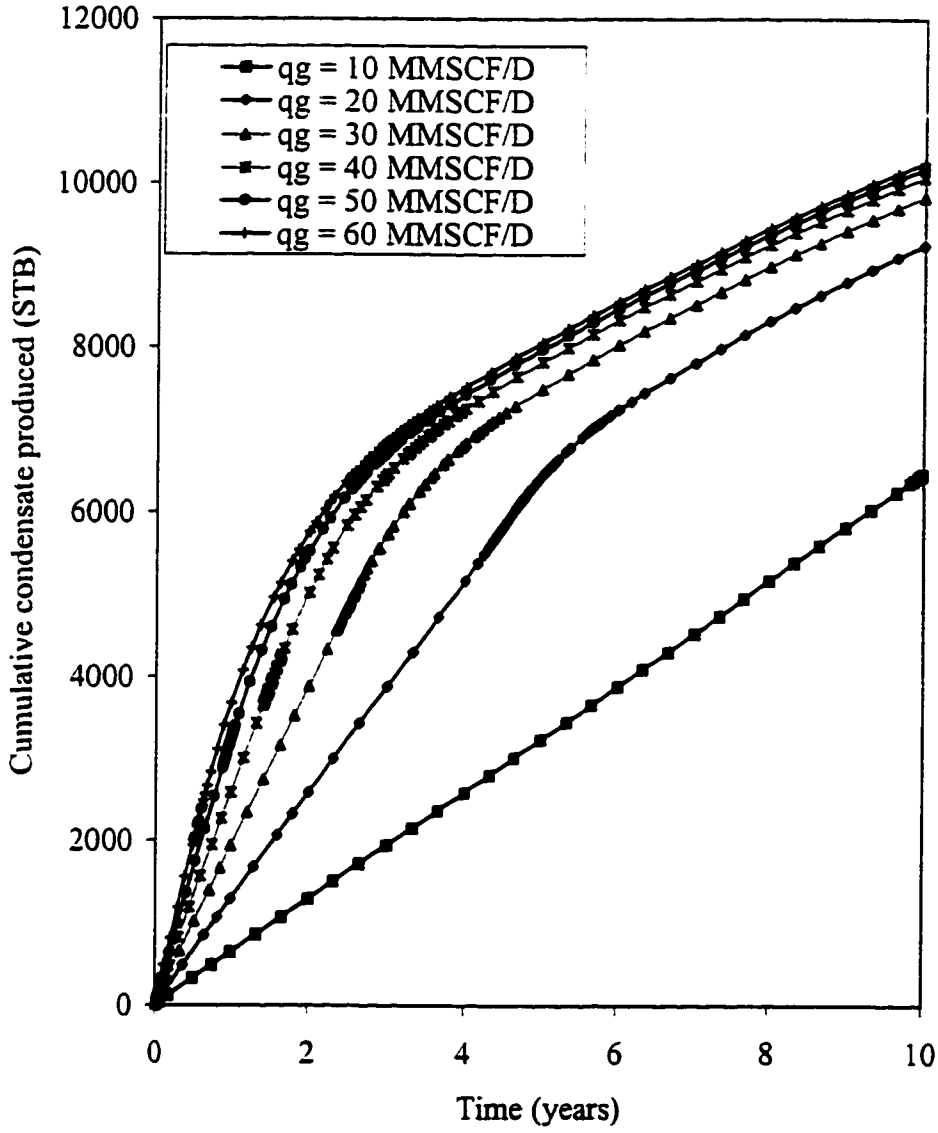

Fig 6.21: Cumumlative condensate produced with time

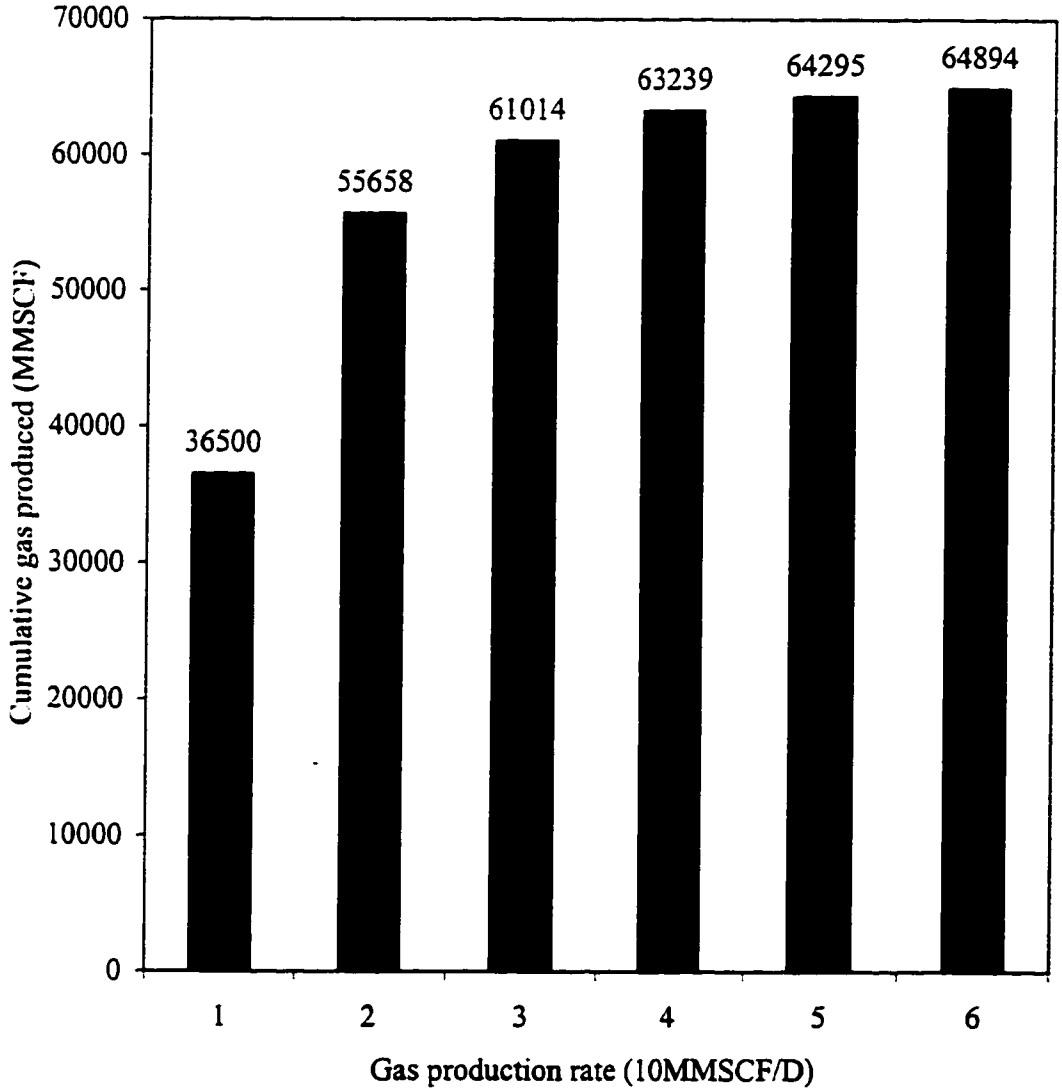

Fig 6.22: Cumulative gas production versus gas production rate at 10 years

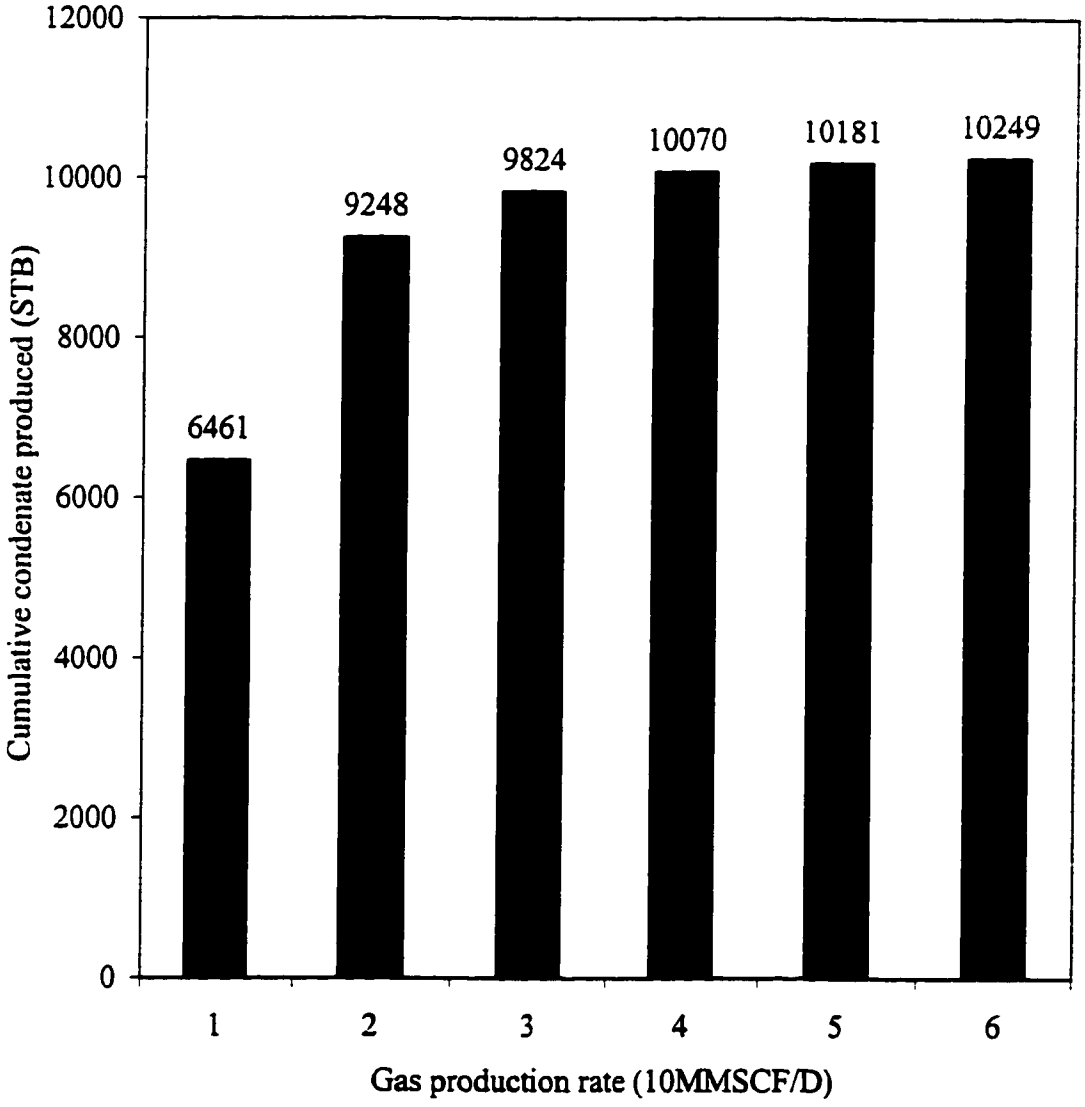

Fig 6.23: Cumulative condensate produced versus gas production rate at 10 years

6.6 GAS FLOW PRODUCTIVITY INDEX

Gas condensate reservoir productivity declines immediately when the pressure drops below the dew point pressure. The conventional approach used to calculate productivity index of a well is to use equation (6-1) but it is valid for a single-phase flow, single layer reservoir and a steady (or pseudosteady) state condition [45].

$$PI = \frac{Q_g}{P_e - P_{wf}} \tag{6-1}$$

Equation (6-1) cannot be used to calculate the productivity index for the multilayer reservoirs described in the geological model of section 3.3. This is because the pressure on the outside radius (P_e) varies in different layers due to uneven depletion and the time to reach steady (or pseudo steady) state in different layers is different. Based on the difficulty in applying equation (6-1) to calculate the gas flow productivity index, Settari et al [45] modified equation (6-1) by proposing equation (6-2) which they called instantaneous productivity index.

$$PI(t) = \frac{Q_g}{P_{avg}(t) - P_{wf}(t)} \tag{6-2}$$

Where P_{avg} (t) is the average reservoir pressure for the entire model at time t. Settari et al [45] observed that early values of productivity indices calculated by using equation (6-2) are high reflecting the inaccuracy of using a pseudosteady state formula during a transient flow period.

In this study the productivity index is calculated using equation (6-2). The result obtained is presented in figure 6.24 which shows a plot of the gas flow productivity index with time for different production rates while figures 6.25 and 6.26 are plots of gas flow productivity index and the normalized productivity index with average reservoir pressure.

It can be seen from these figures that for all production rates of 20, 30, 40, 50 and 60MMSCF/D, the gas condensate well undergoing depletion reached the dew point pressure at 4.8, 2.7, 1.65, 1.03, and 0.66 years respectively. The productivity index started to decline at 4.2, 2.23, 1.32, 0.786, 0.4018 years just before the dew-point pressure is reached as shown in figure 6.25 and also in figures 6.16 to 6.20. The productivity index drops from 23.58, 23.38, 23.16, 22.893MSCF/D/psia, to 2.1MSCF/D/psia for production rates of 30, 40, 50, and 60 MMSCF/D respectively.

It should be noted that there is an abrupt drop in productivity index followed by a moderate drop to 2.1 for all rates. Stabilized productivity index exists from 4.5 years to the end of depletion at 10 years. This confirms that the system has reached a pseudo-steady state at 4.35 years when the productivity index is 2.1MSCF/D/psia for all rates as can be seen in figure 6.24. The plot of average pressure versus productivity index and normalized productivity index in figure 6.25 and 6.26 shows that the gas flow productivity index has dropped and stabilized at the same final value when the average reservoir pressure falls below the dewpoint pressure.

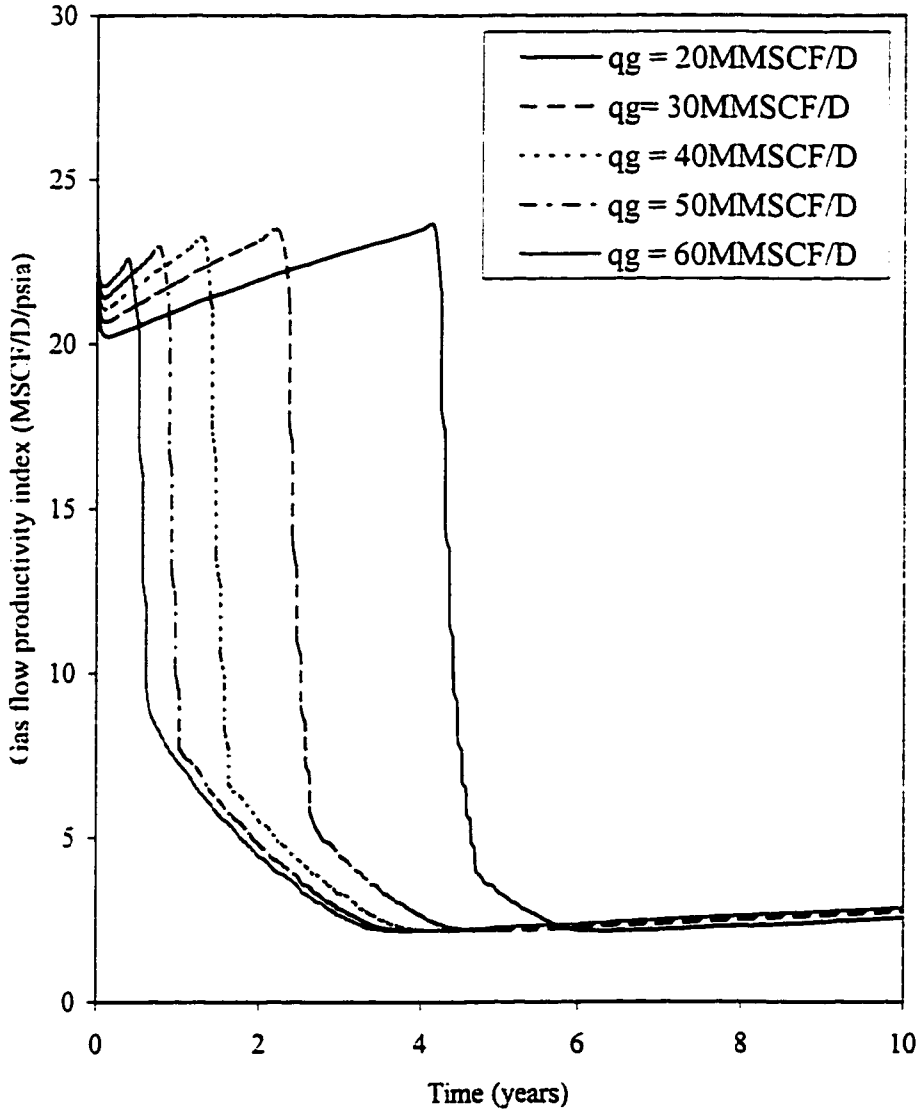

Fig 6.24: Effect of gas production rates on gas flow productivity index

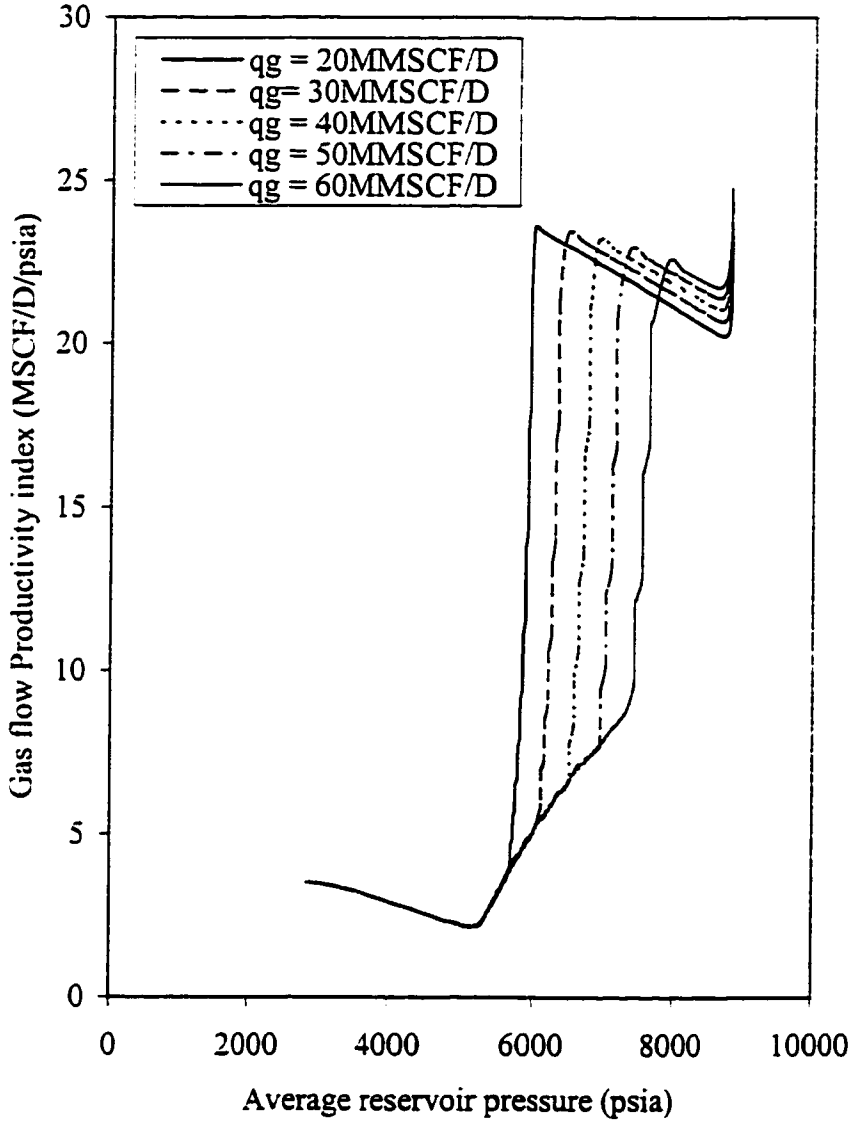

Fig 6.25 : Effect of gas production rates on gas flow productivity index

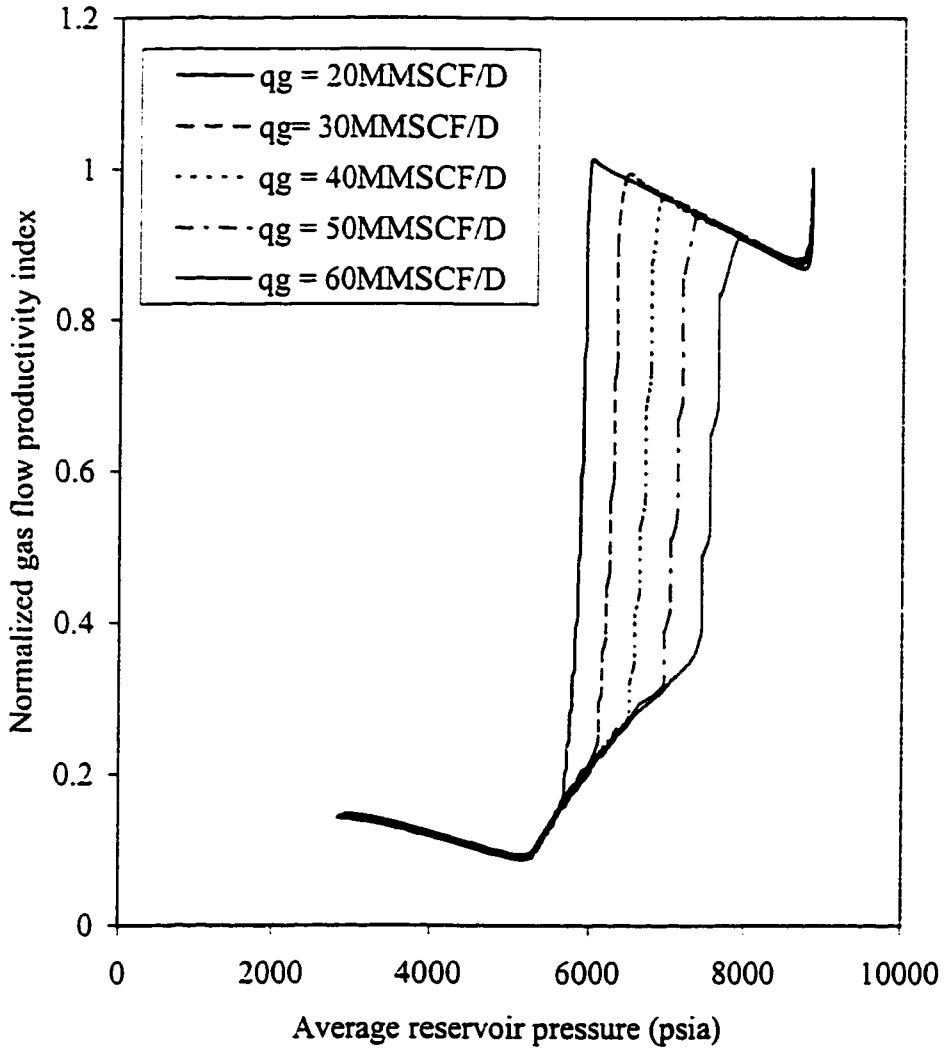

Fig 6.26: Plot of normalized gas flow productivity index versus average reservoir pressure.

6.7 CONDENSATE SATURATION DISTRIBUTION AS A FUCTION OF DISTANCE FROM THE WELLBORE

For the five production rates studied, the dew point pressure was reached at different times during depletion. The dew point pressure of 5153 psia was reached at 4.8, 2.704, 1.639, 1.038, 0.66 years when gas production rate is 20, 30, 40, 50 and 60MMSCF/D respectively. Figure 6.10 shows clearly the time liquid condensation begins and the time pseudo steady state has been reached in the system.

In order to have a better grasp of the condensate saturation distribution away from the wellbore at the different gas production rates considered, simulator results from the time condensate liquid drops out of the gas to the end of depletion was considered. In this section, condensate saturation distribution is discussed for production rates of 20, 30, 40, 50 and 60 MMSCF/D.

For a gas production rate of 20MMSCF/D, figures 6.27 to 6.31 show the plot of condensate saturation distribution away from the wellbore in the four layers at 5, 5.5, 6, 8 and 10 years. At 5 years, the pressure has just fallen below the dew point pressure with 44% liquid saturation near the wellbore. Liquid saturation decreases with distance away from the wellbore until it becomes 0 % from 20 ft to 6557.4 ft. In the 4 layers, the same amount of liquid condensed from the gas with some little variation from 10 to 20 ft away from the wellbore. Meanwhile, the condensation and accumulation of condensed phase reached 100ft at 5.5 years. Liquid saturation and accumulation of condensed phase reached 100ft at 5.5 years. Liquid condensation is a little higher in layers 3 and 4 than in

layer 1 until 100ft is reached after which a single gas phase is flowing. Liquid condensation continued to extend far away from the wellbore reaching 1000ft, 6557.4 ft and 6557.4 ft at 6, 8 and 10 years respectively. At 8 and 10 years, the average reservoir pressure in the entire reservoir has fallen below the dew point pressure with the 25^{th} to 30^{th} cells having condensate accumulation reaching the critical condensate saturation of 10%. Figures 6.27 to 6.31 show that layer 1 and layer 2 have almost the same amount of percent liquid condensation (43%) near the wellbore though it differs with distance away from the wellbore. Similar trends were observed for layers 3 and 4 but from 6 years layer 3 (k= 115.6 md) has lower amount of percent liquid condensed near the wellbore than layer 2 (k = 21.68 md). Farther into the reservoir, percent liquid condensation is higher in layer 3 than layer 2. The explanation that can be given for this behavior in layer 3 is that liquid evaporation has taken place at lower reservoir pressure. Similar results were observed when the gas production rate is 40 MMSCF/D as can be seen in figures 6.32 to 6.37.

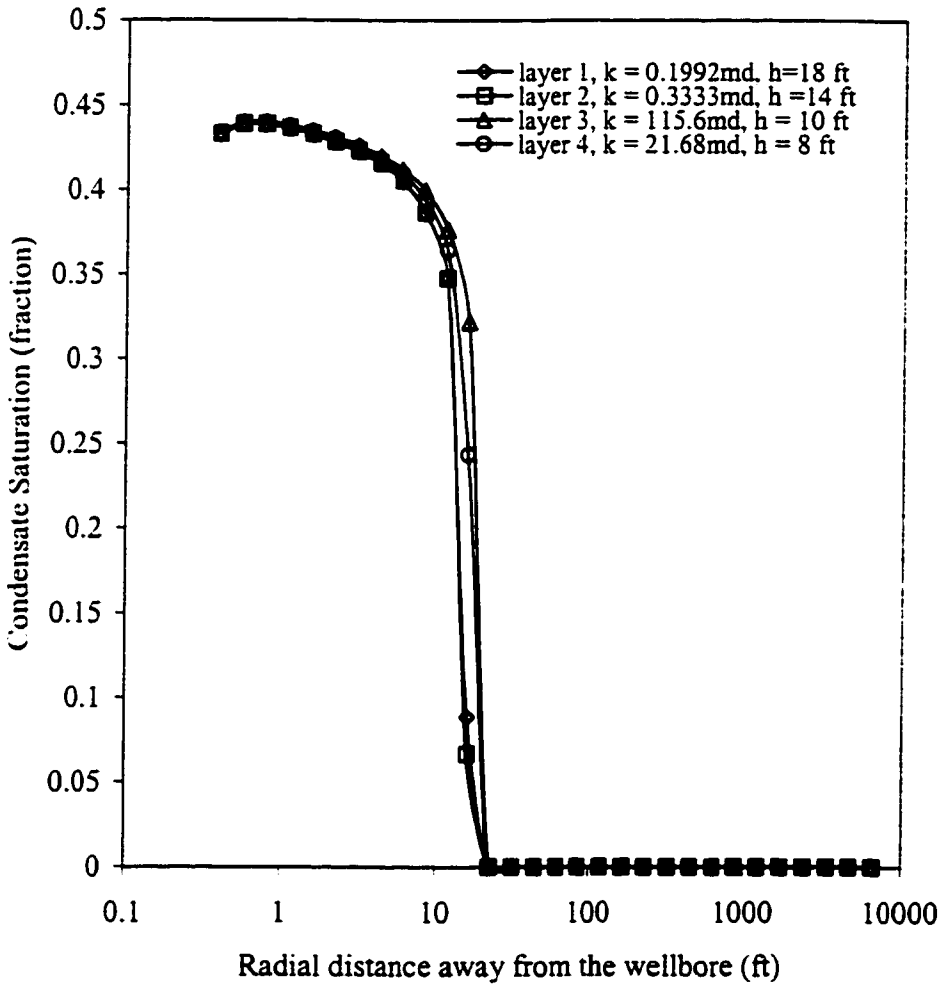

Fig 6.27: Condensate saturation distribution at 5 years when the maximum gas production constraint is 20 MMSCF/D

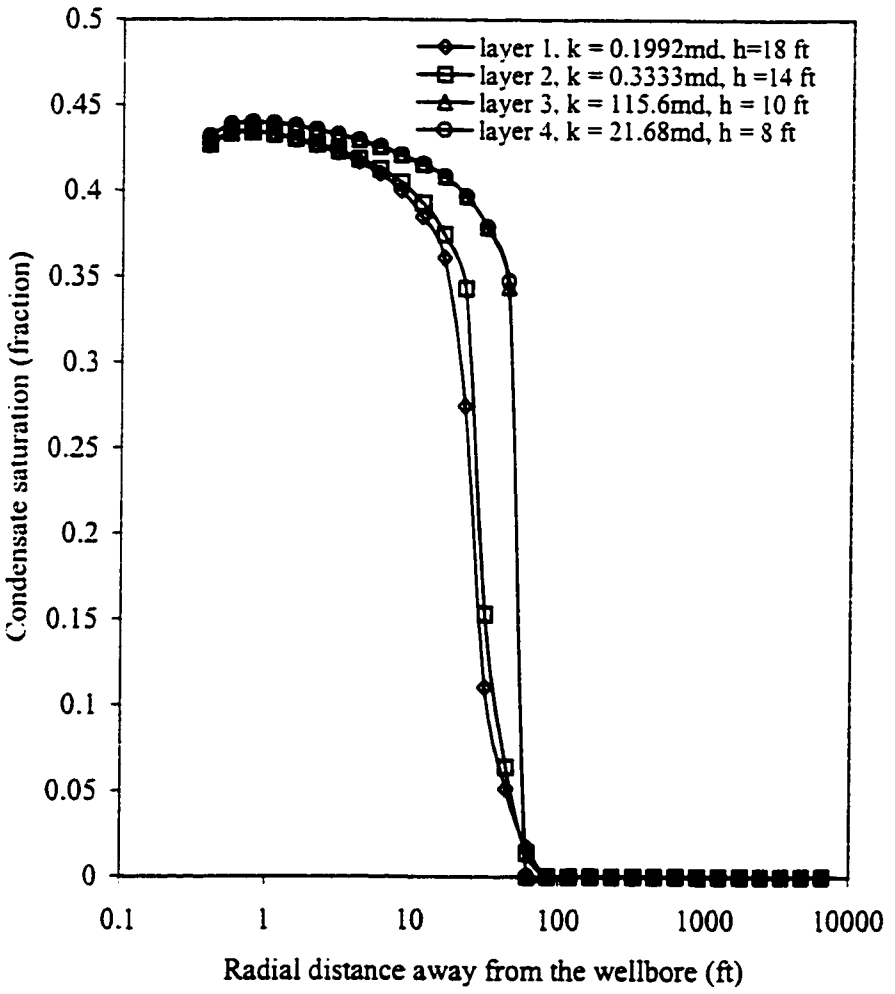

Fig 6.28: Condensate saturation distribution at 5.5 years when the maximum gas production constraint is 20 MMSCF/D

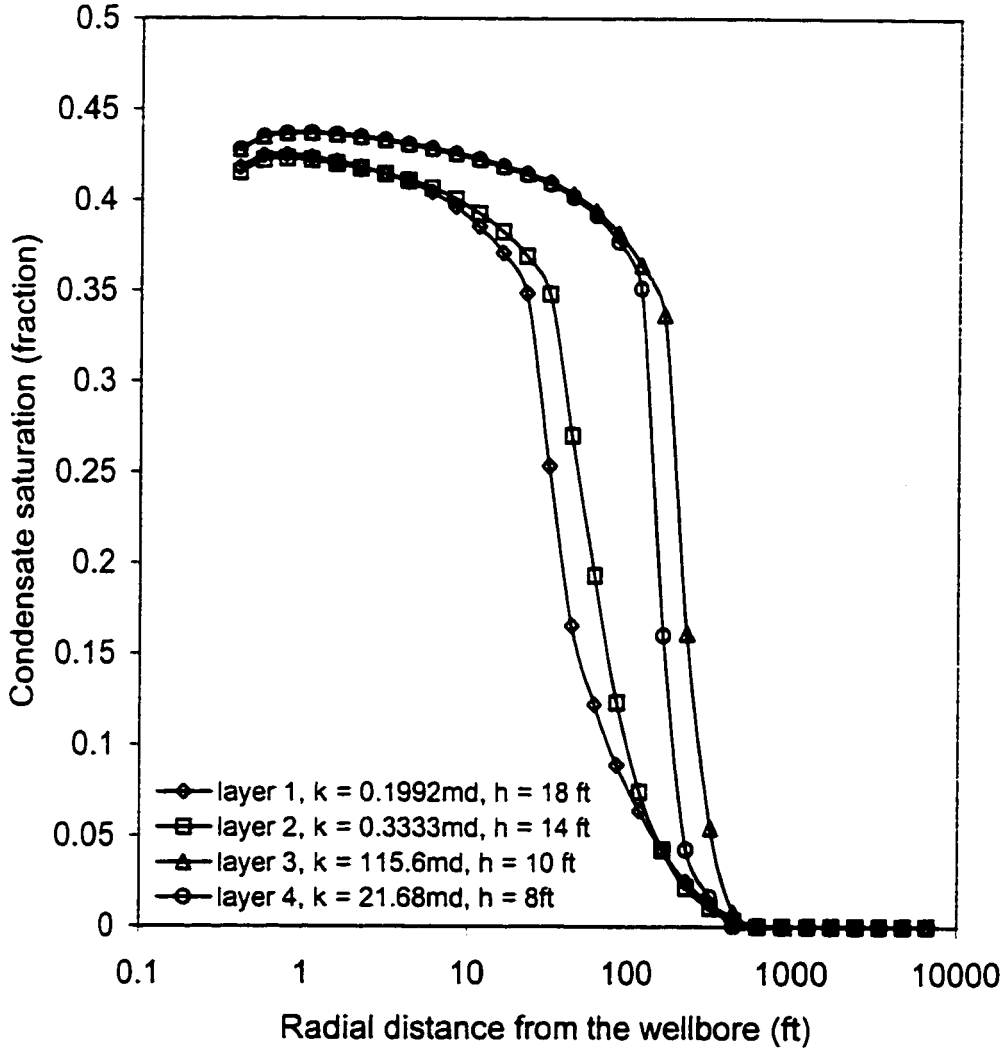

Fig 6.29: Condensate saturation distribution at 6 years when maximum gas production constraint is 20 MMSCF/D

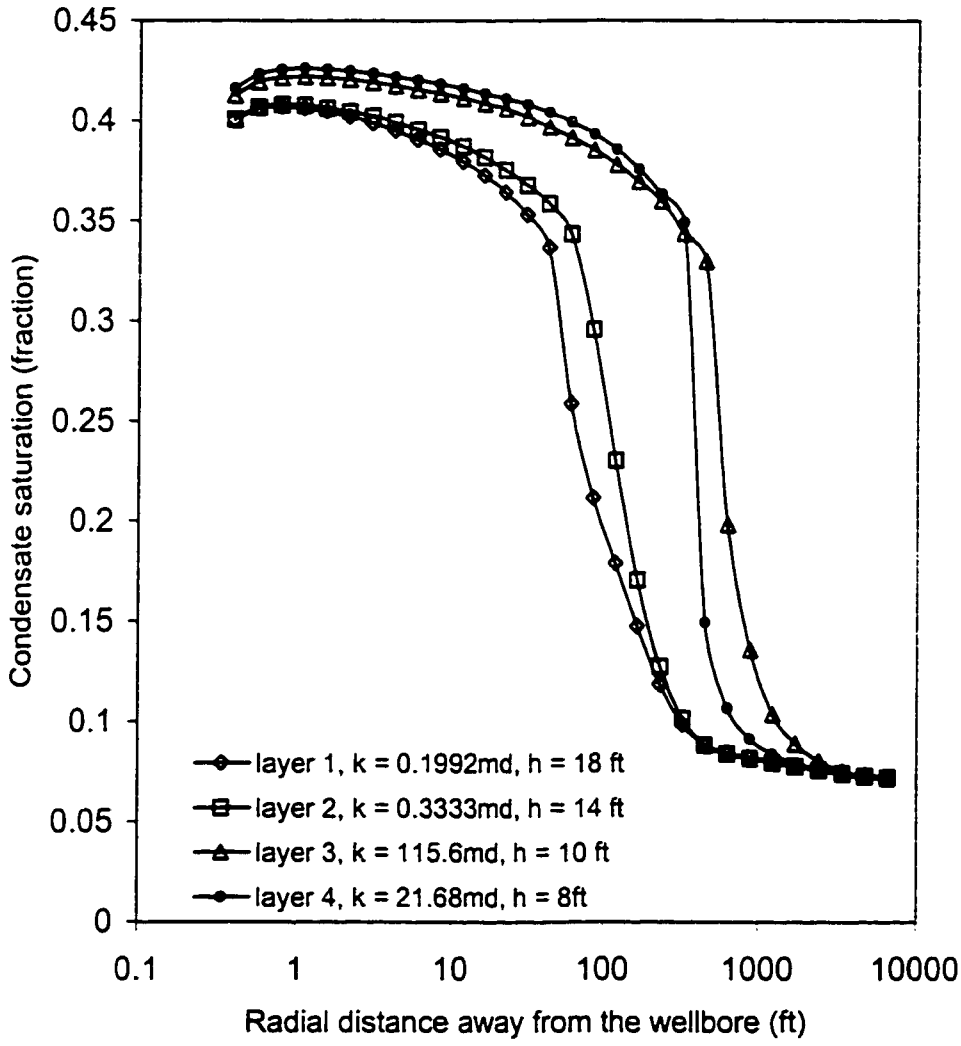

Fig 6.30: Condensate saturation distribution at 8 years when maximum gas production constraint is 20 MMSCF/D

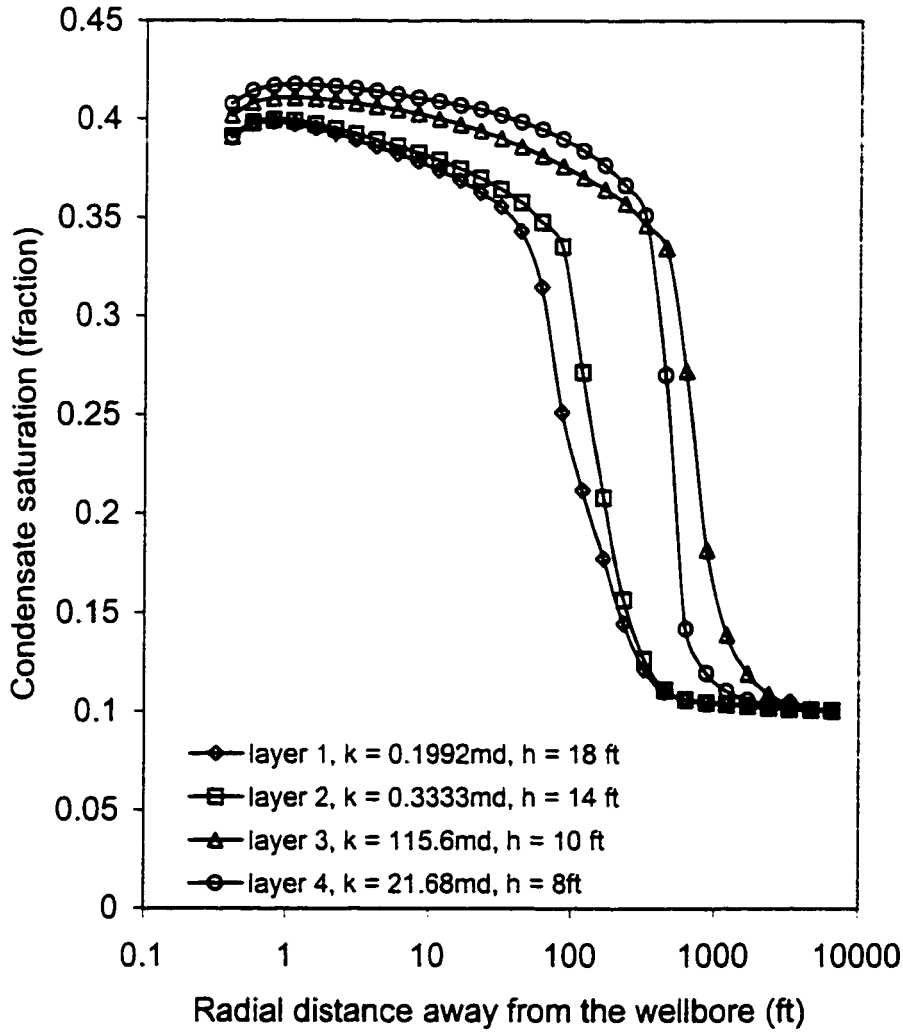

Fig 6.31: Condensate saturation distribution at10 years when maximum gas production constraint is 20 MMSCF/D

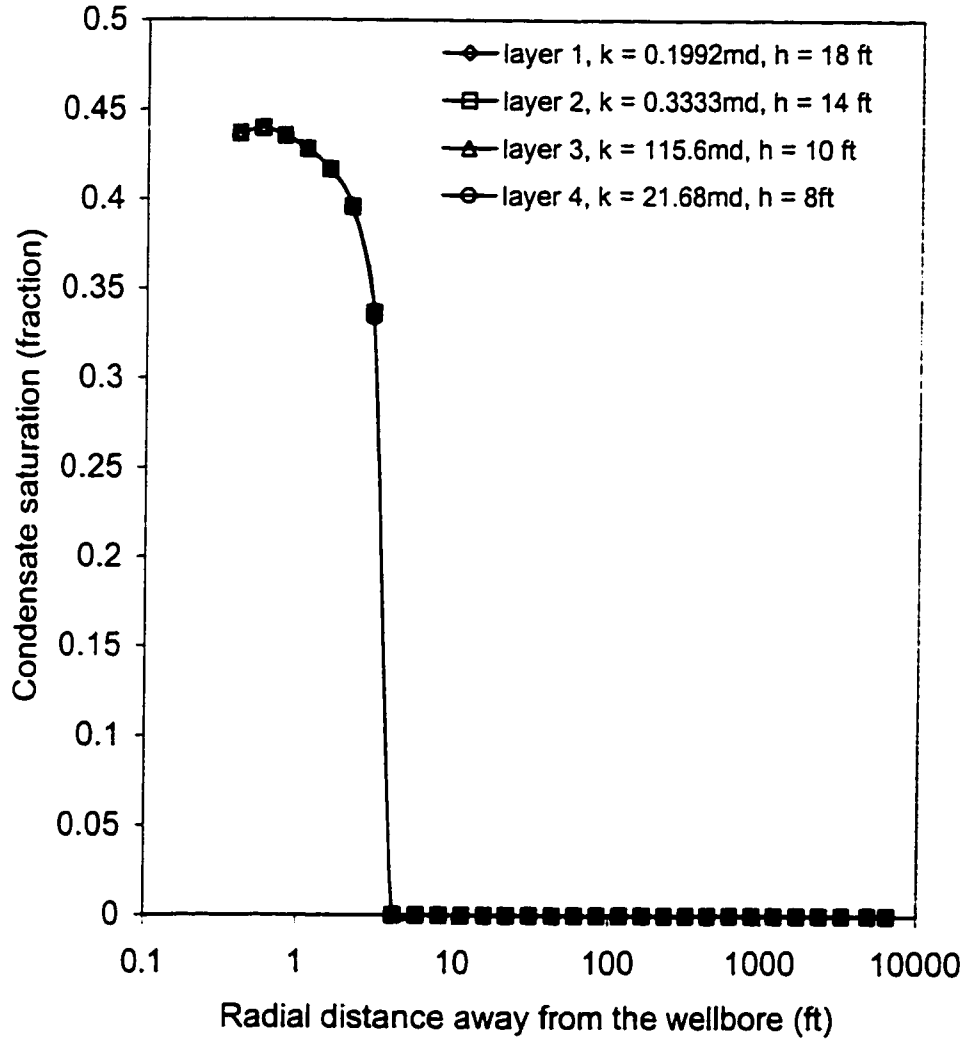

Fig 6.32 : Condensate saturation distribution at 2 years when maximum gas production constraint is 40 MMSCF/D

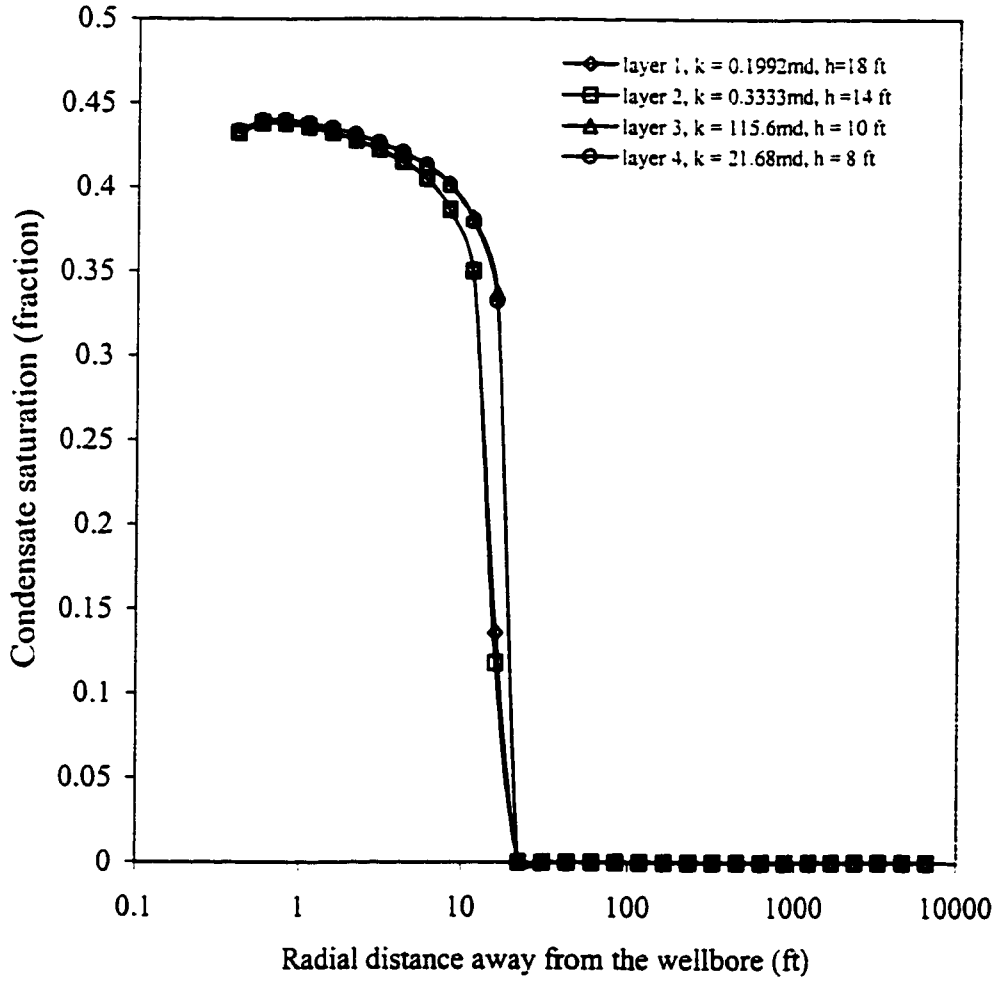

Fig 6.33: Condensate saturation distribution at 3 years when the maximum gas production constraint is 40 MMSCF/D

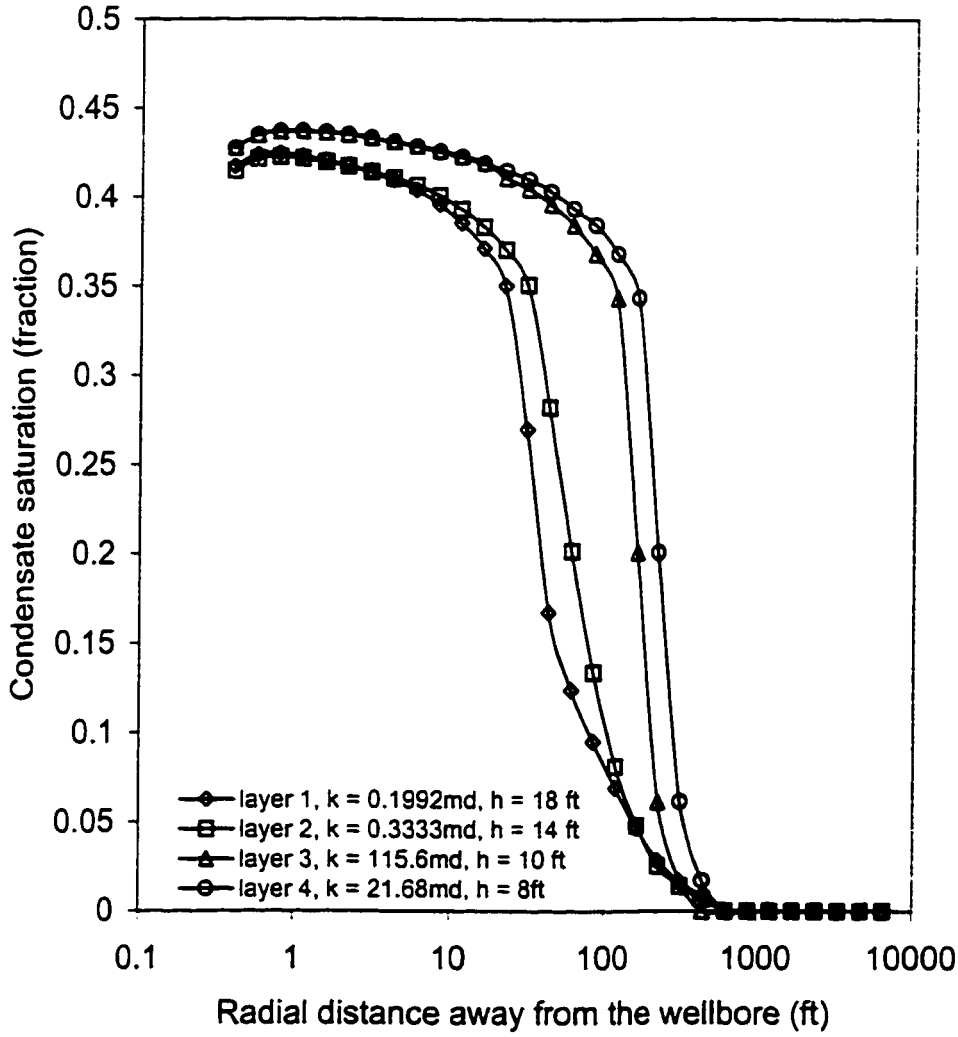

Fig 6.34: Condensate saturation distribution at 4 years when the maximum gas production constraint is 40 MMSCF/D

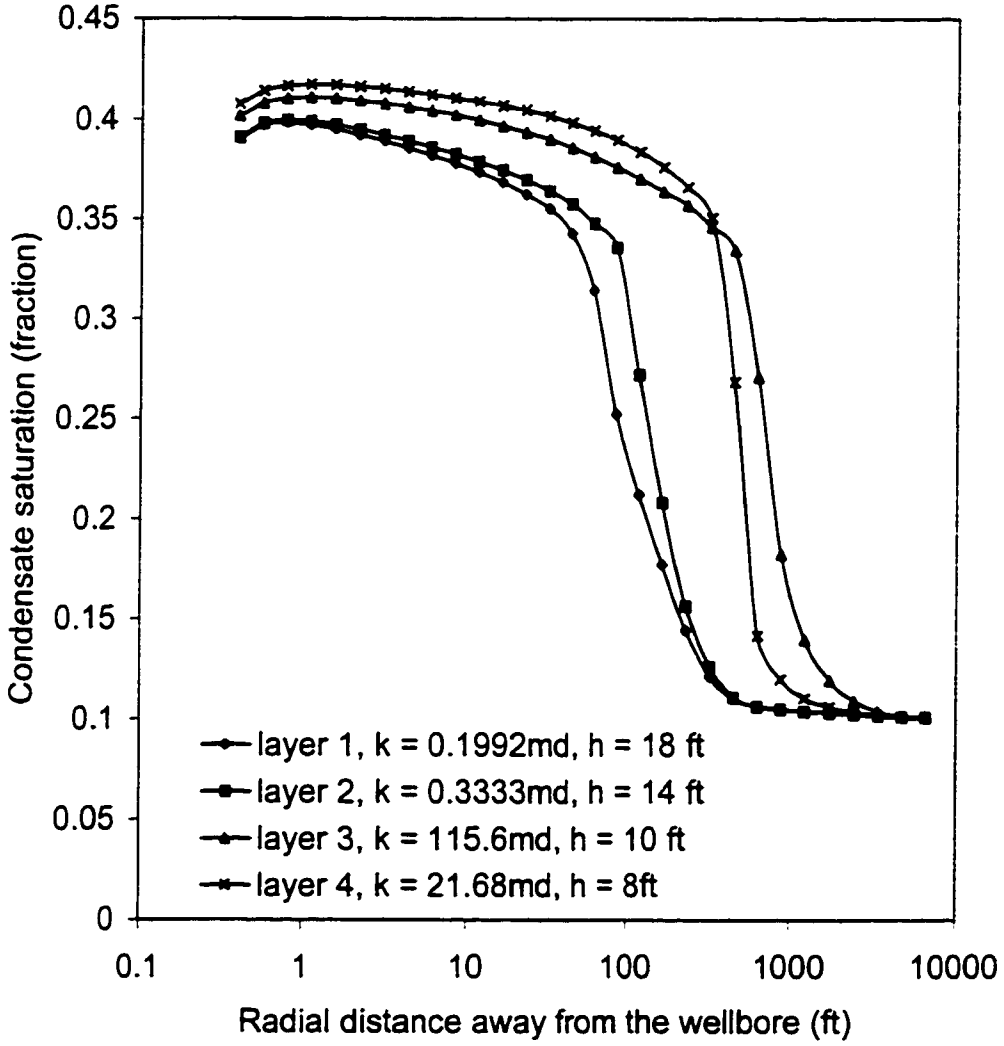

Fig 6.35 : Condensate saturation distribution at 6 years when the maximum gas production constraint is 40MMSCF/D

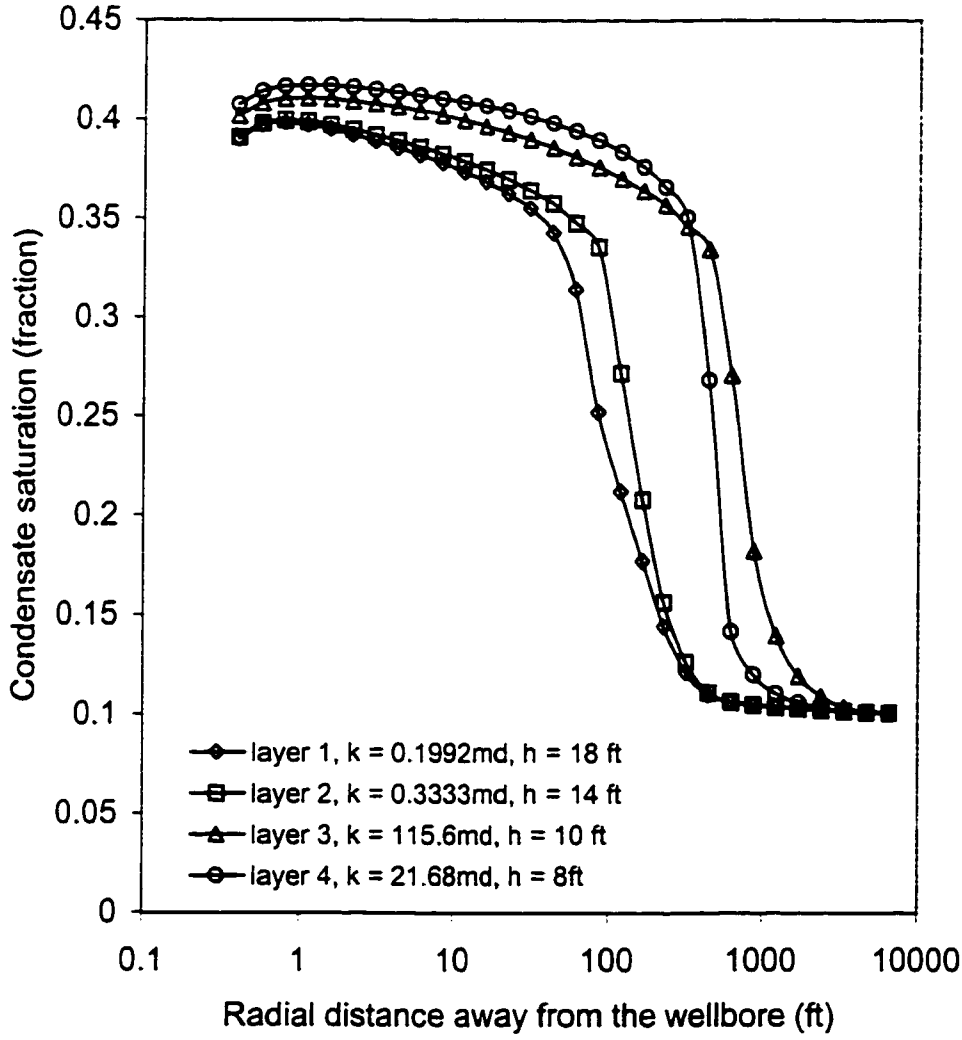

Fig 6.36: Condensate saturation distribution at 8 years when the maximum gas production constraint is 40 MMSCF/D

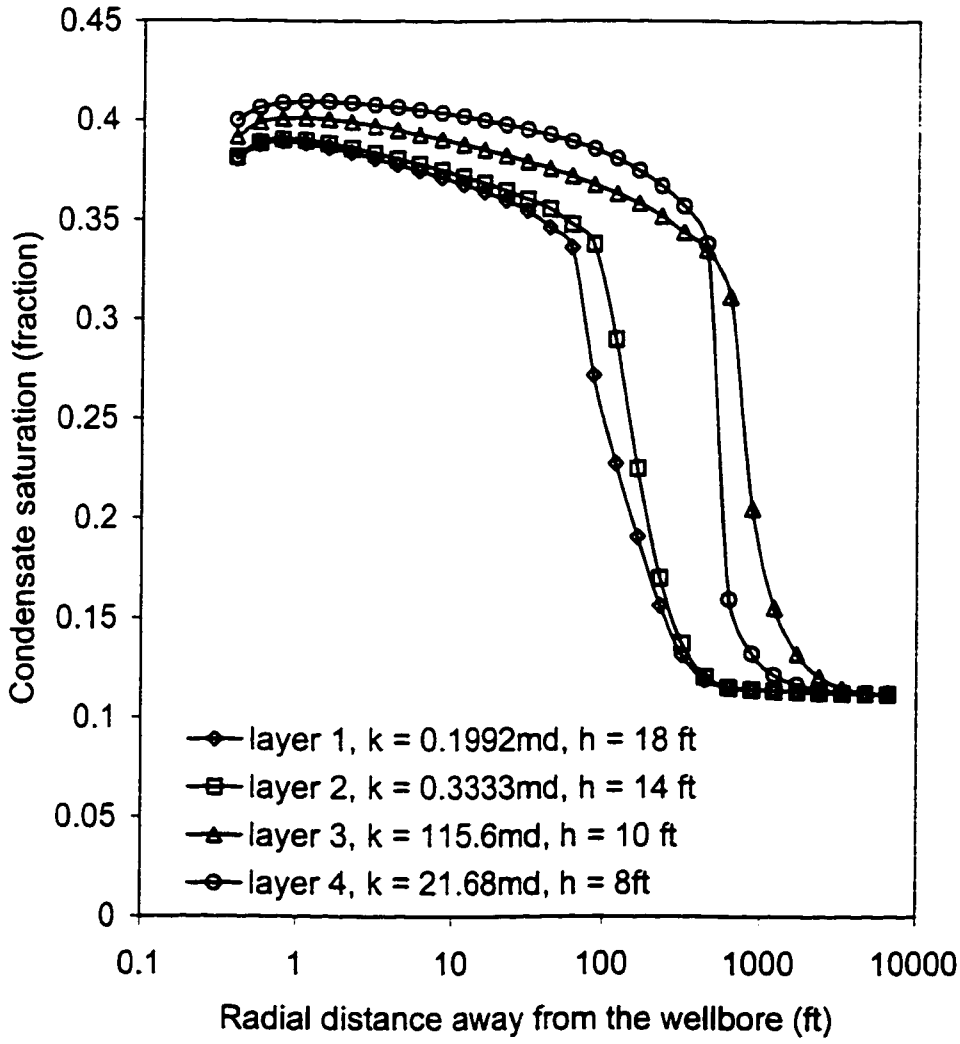

Fig 6.37 : Condensate saturation distribution at 10 years when the maximum gas production constraint is 40 MMSCF/D

6.8 CONDENSATE SATURATION DISTRIBUTION IN THE LAYERS AS A FUNCTION OF TIME

Figures 6.38 to 6.41 present plots of variation of condensate saturation distribution with time in layers 1 to 4 for the case of 40MMSCF/D.

In layer 1, the percent liquid saturation at 2 years is about 44% within 1ft away from the wellbore and declines sharply to 0% at about 8ft from the wellbore. Farther than 8 ft away from the wellbore there is no liquid condensation. At 3 years, liquid saturation is about 44 % within 1 ft but declines with distance away from the wellbore. At a distance of about 20 ft or more from the wellbore, liquid condensation from the gas is yet to occur. In 4 years, percent liquid accumulation near the wellbore has started decreasing and this is probably due to vaporization of the condensed phase but farther into the reservoir, condensation has taken place with the liquid saturation reaching about 12% at about 1000ft to 6557.4 ft away from the wellbore.

In layer 2, the percent liquid saturation near the wellbore declines from 44 % to about 37 % as depletion time increases from 2 to 10 years. Meanwhile, condensate accumulation is increasing with time farther from the wellbore region. At 2, 3 or 4 years, liquid saturation declines from 44, 44 and 42 % within 1ft from the wellbore until it reaches 0% at about 8, 20 and 1000ft, respectively, from the wellbore. At distances more than this, there exist no liquid condensation from the gas. When time is 6, 8 or 10 years, the percent liquid saturation near the wellbore are 40, 39 and 38 %. The decline in liquid saturation with distance away from the wellbore is not sharp but rather gradual with 35

percent liquid saturation at about 90 ft from wellbore. Liquid saturation has reached about 7, 10 and 12% at distances of 1000 to 6557.4 ft in 6, 8 and 10 years respectively.

For layer 3, the percent liquid saturation near the wellbore is 44 % at 2 years but decline to 37.5% at 10 years due to revaporization of the condensate phase. The percent liquid declines gradually to 35% at a distance of 1000 ft away from the wellbore for all times considered. At 2 years, 44% condensate liquid accumulation occurs near the wellbore and declines to zero at a distance of about 8 ft or more but at 3 and 4 years, liquid condensation has reached about 1000 ft away from the wellbore. At 6, 8 and 10 years, the pressure in the layer is now below the dew point pressure so liquid saturation as high as 7, 10 and 12 % has condensed out of the gas at a distance more than 1000 ft away from the wellbore.

Figure 6.41 shows the variation of condensate saturation distribution with time in Layer 4. Near the wellbore, at a distance less that 1ft, the liquid saturation is 44 percent in layers 4 at 2, 3,and 4 years. The 44 percent liquid saturation decline to 0 % at distance of about 8 ft, 20 ft and 1000 ft at 2, 3, 4 and 6 years respectively. The liquid condensate has re-vaporized reducing condensate saturation from 44 % at 2 or 3 years to 43, 41 and 40 % at 6, 8 and 10 years near the wellbore. The accumulation of liquid phase away from the well is gradual at 4, 6, 8, and 10. Liquid saturation is as high as 36 percent at a distance of 1000 ft away from the wellbore. The liquid saturation even reached 7, 10 and 12% respectively in the last radial grid cells.

We set the minimum bottom hole pressure to 500 psia to observe if there will be liquid revaporization at lower pressure. This expectation was confirmed by the observed liquid re-vaporization noticed near the wellbore (at a distance less than 1ft) in the four layers.

It should be noted that the pressure at a distance less than 1 ft is about 1000 psia at 2 years and 500 psia at 4, 6, 8 and 10 years as can be seen from figures 6.42 to 6.45. All re-vaporization observed took place from 4 to 10 years linking this behavior to the low pressure near the wellbore. The conclusion from this study is that liquid accumulation is significant near the wellbore immediately when the bottom hole flowing pressure falls below the dew point pressure even though the average reservoir pressure is still above the dew point. This accumulation of the liquid condensate reduced the pressure near the wellbore very significantly to 500 psia in 4 years. As depletion of the reservoir progresses with time, liquid condensation occurs all over the reservoir with the average reservoir pressure now below the dew point pressure.

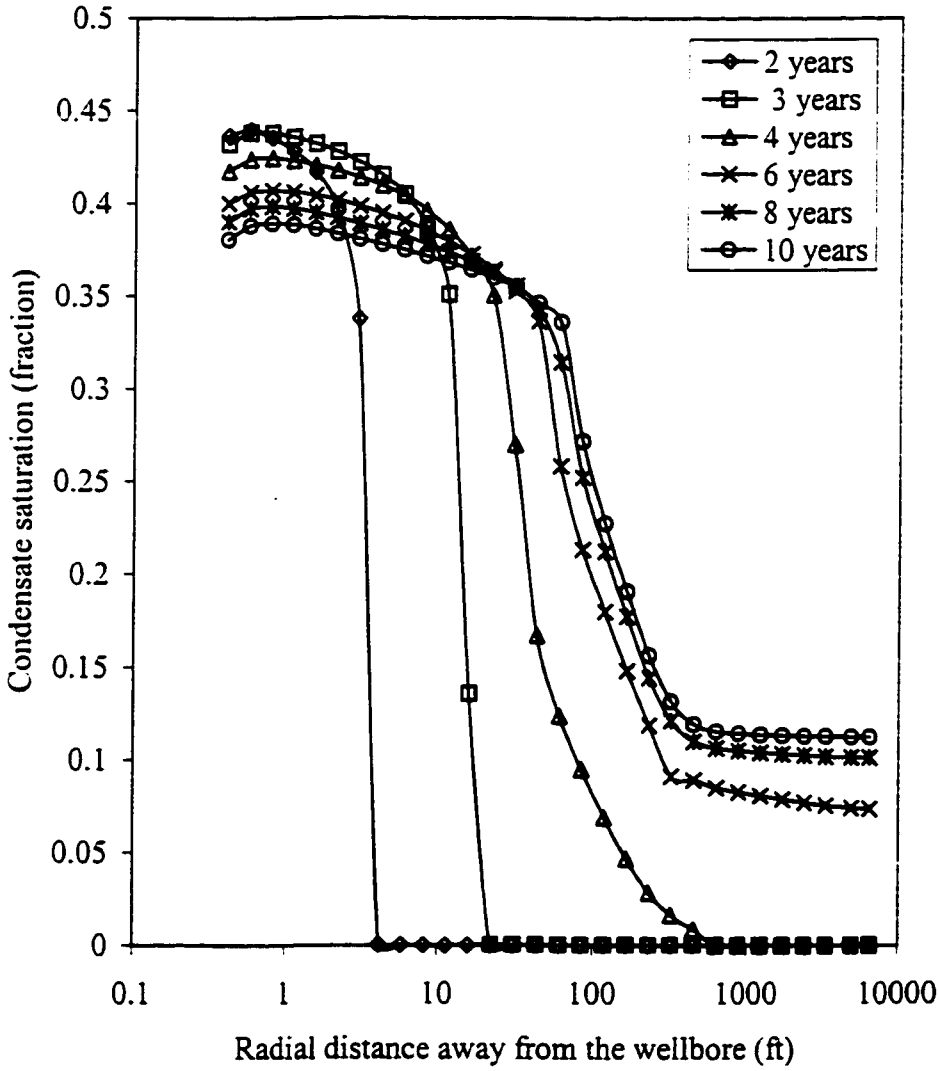

Fig 6.38:Variation of condensate saturation distribution with time in layer 1 when the maximum gas production constraint is 40 MMSCF/D

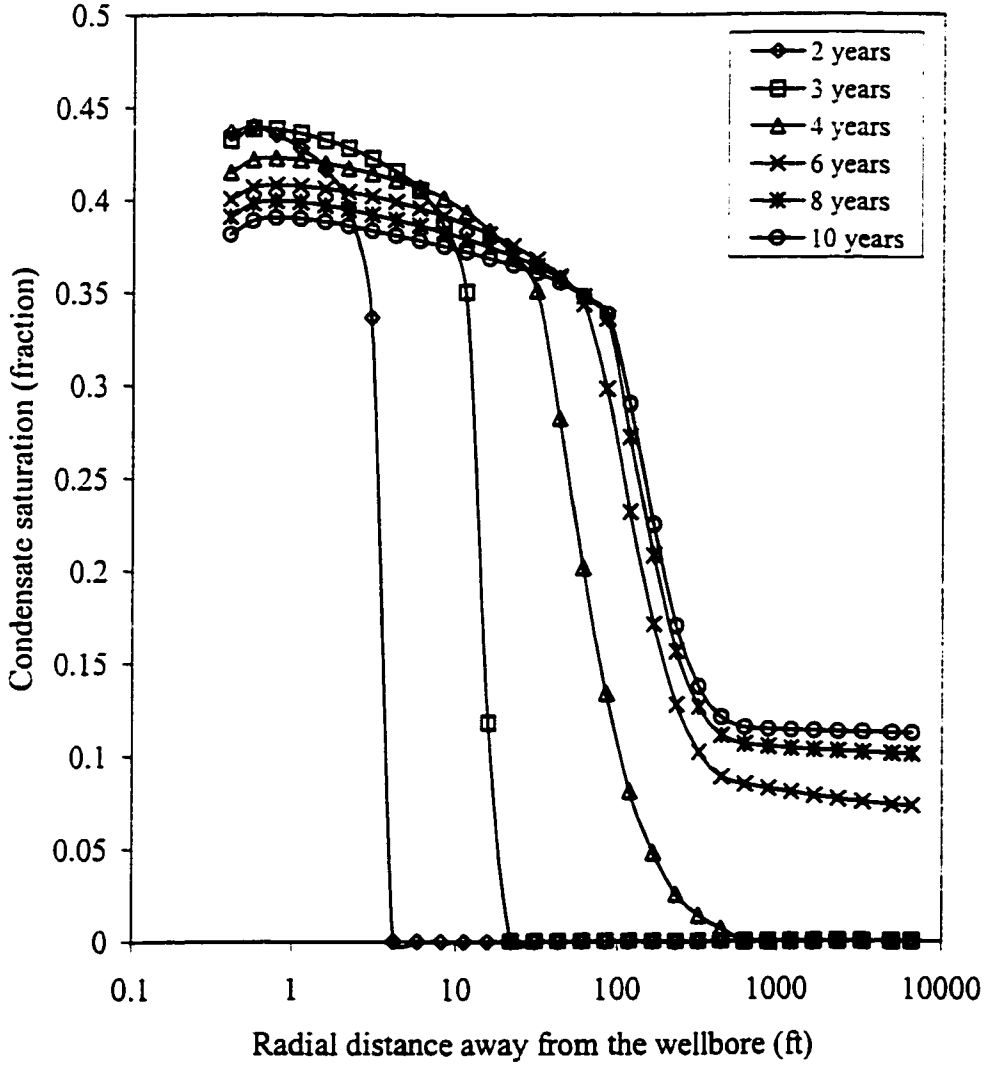

Fig 6.39: Variation of condensate saturation distribution with time in layer 2 when the maximum gas production constraint is 40 MMSCF/D

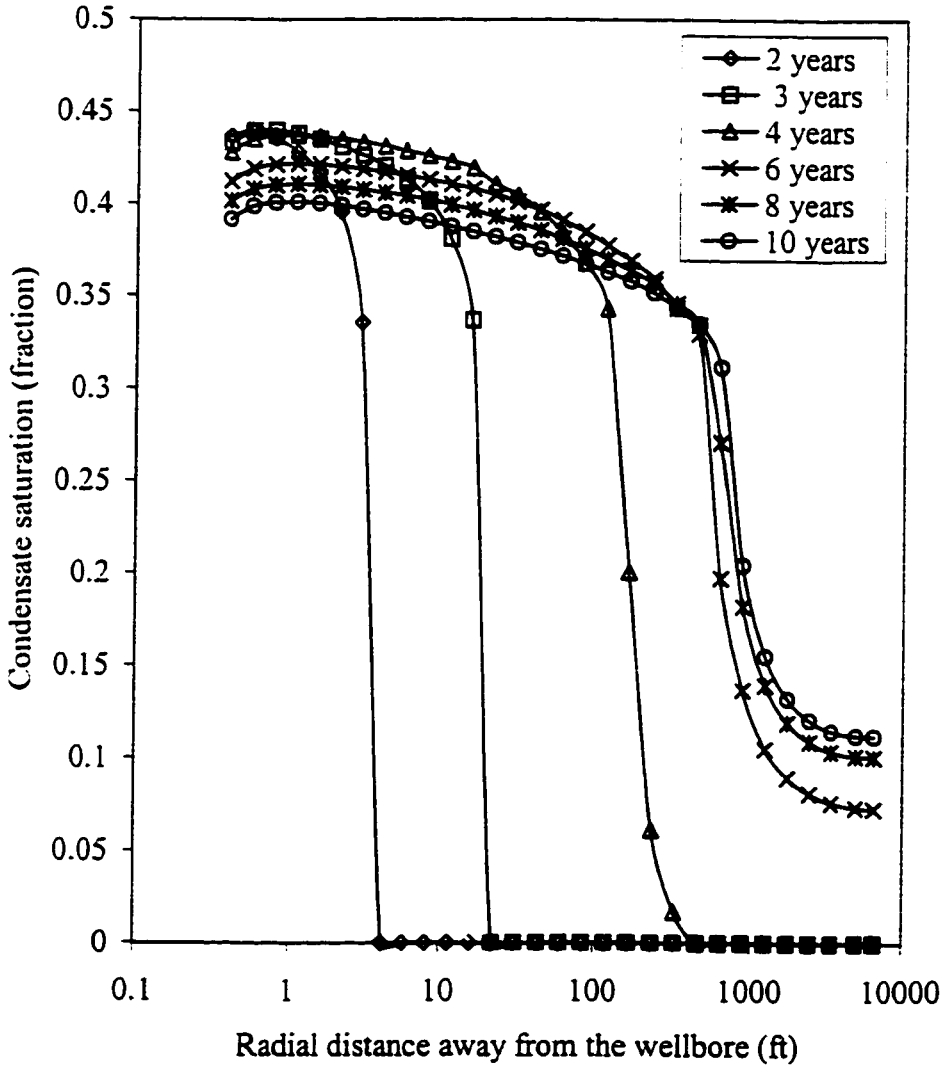

Fig 6.40: Variation of condensate saturation distribution with time in layer 3 when the maximum gas production constraint is 40 MMSCF/D

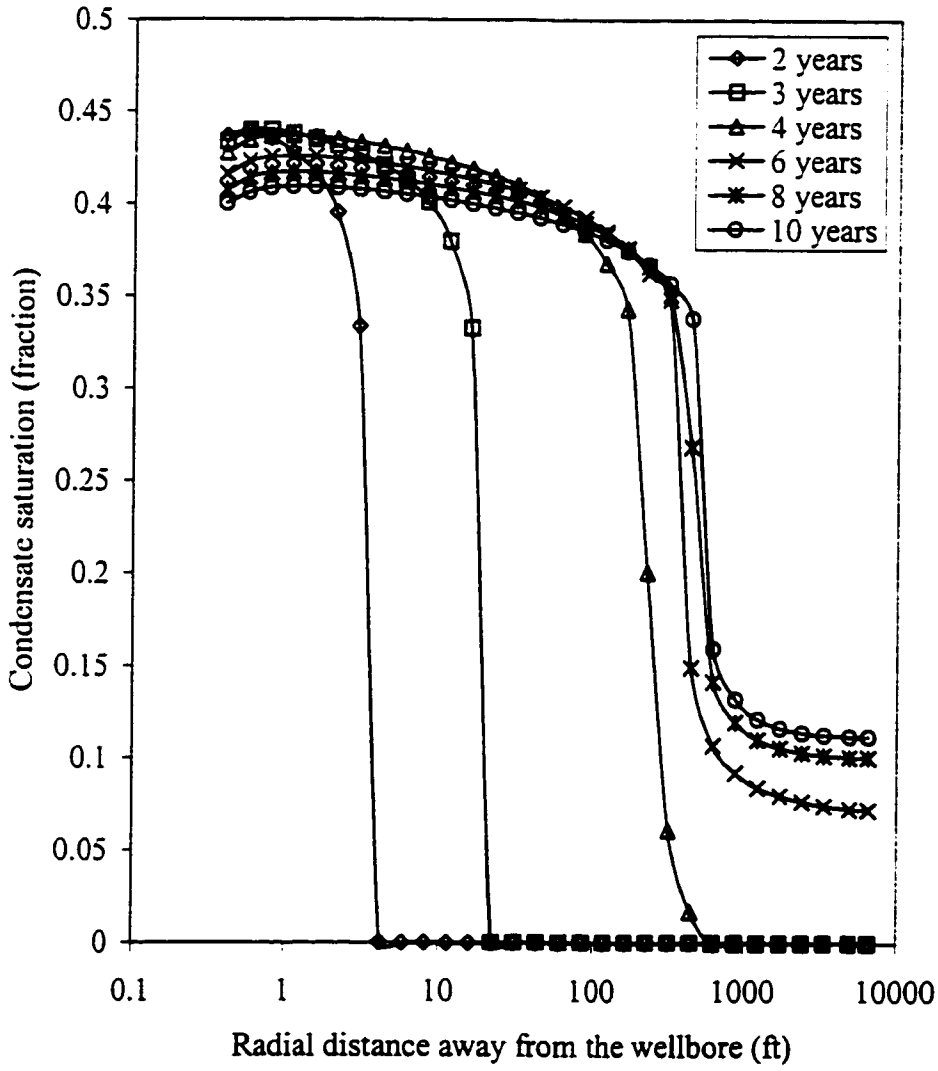

Fig 6.41: Variation of condensate saturation distribution with time in layer 4 when the maximum gas production constraint is 40 MMSCF/D

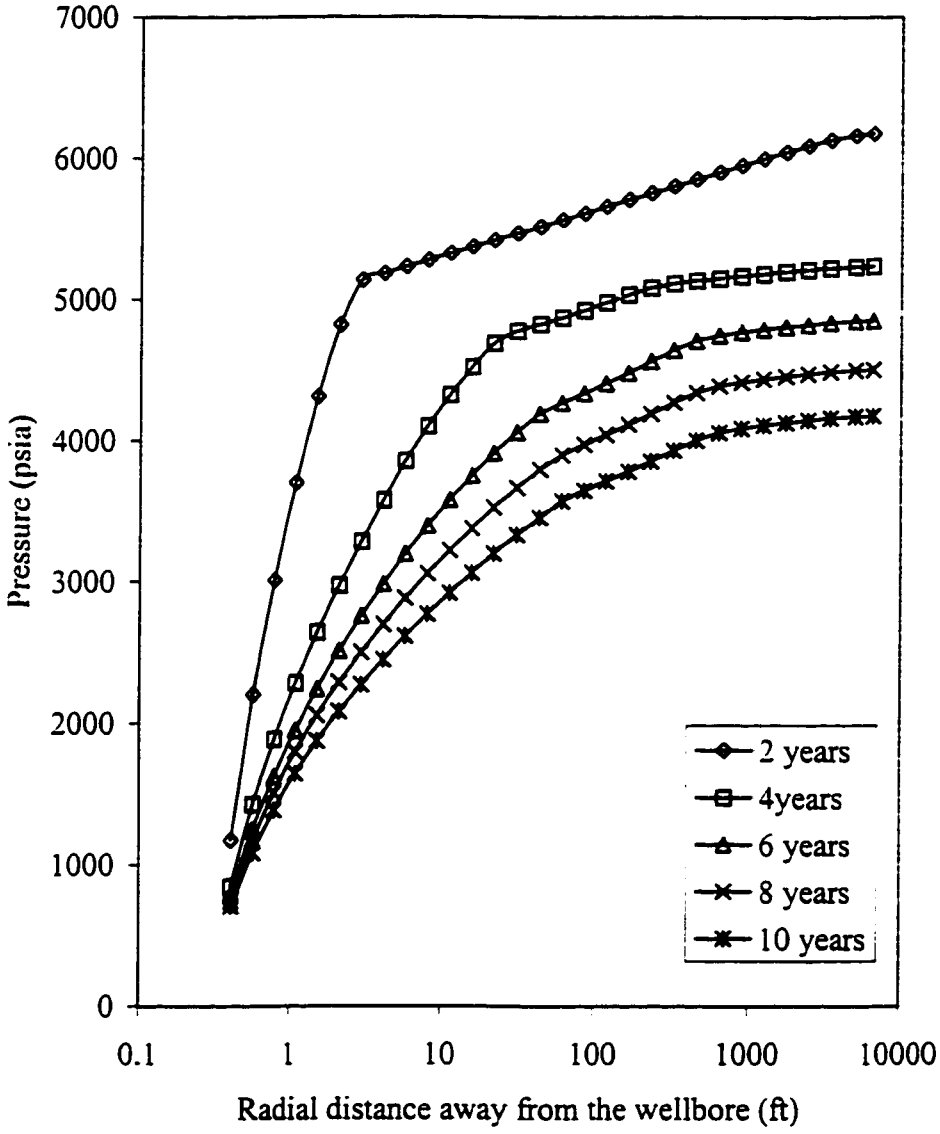

Fig 6.42: Pressure distribution in layer 1 (k = 0.1992md and h = 18 ft)

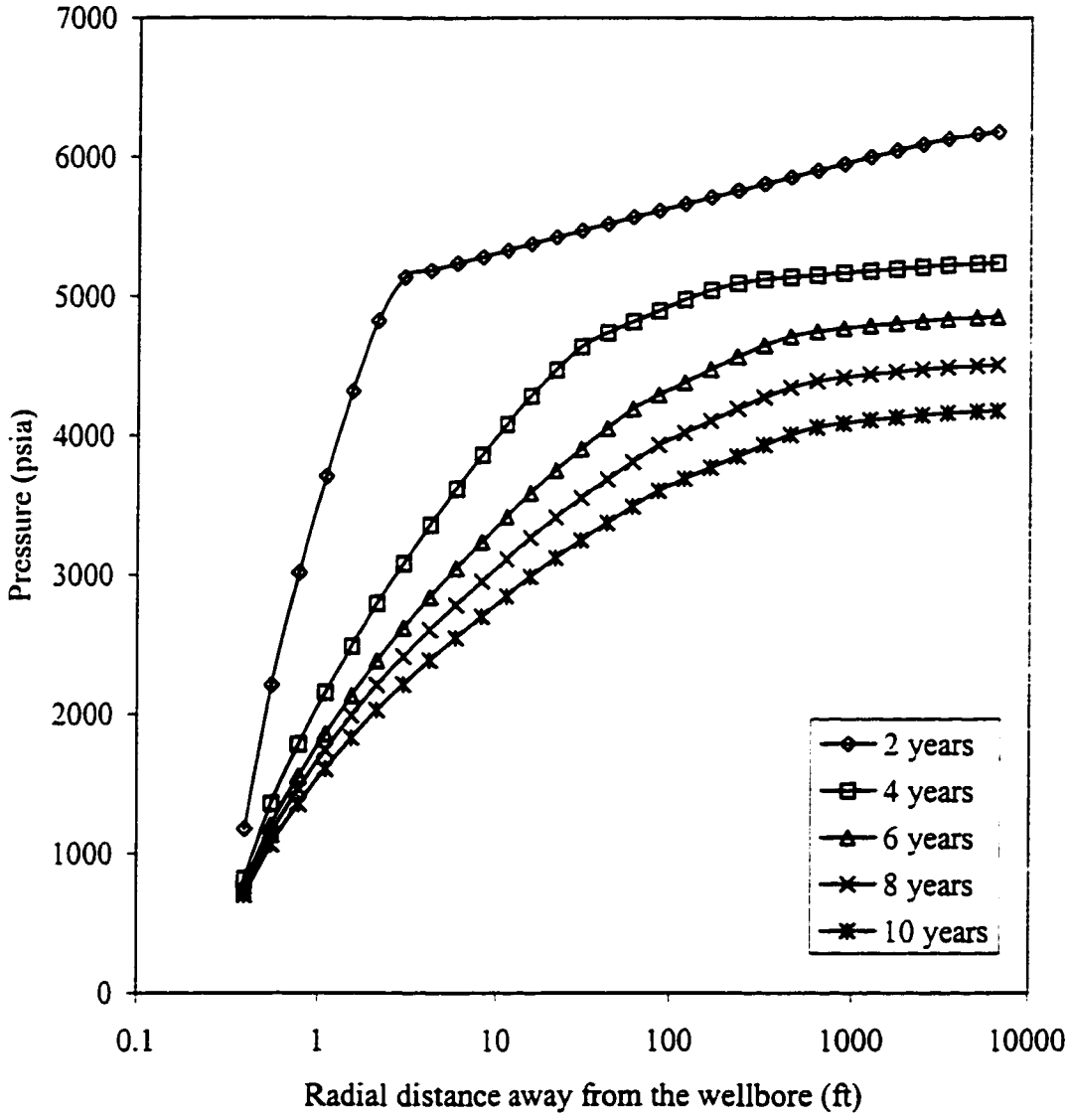

Fig 6.43: Pressure distribution in layer 2 (k = 0.3333md and h = 14 ft)

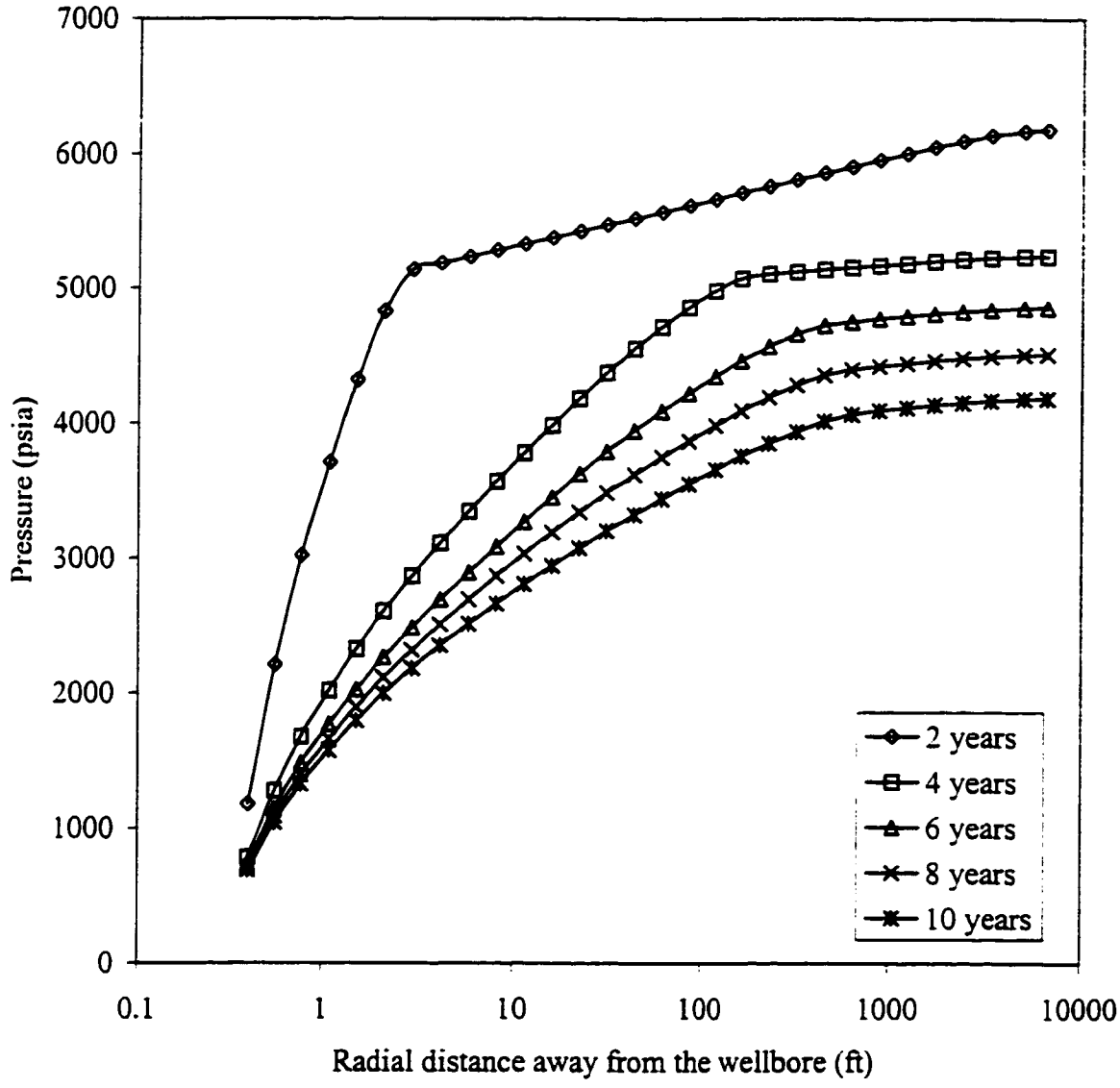

Fig 6.44: Pressure distribution in layer 3 (k = 115.6 md, h = 10 ft)

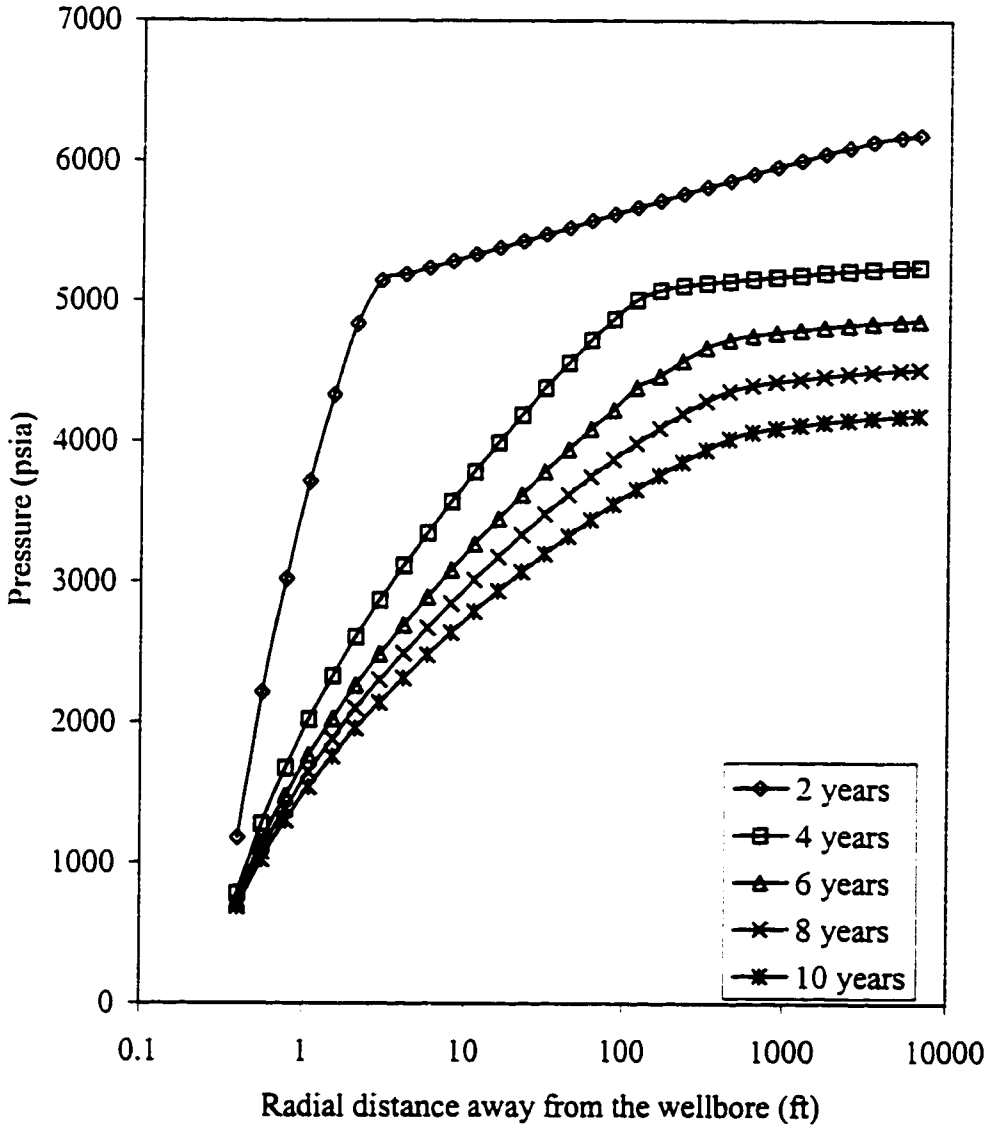

Fig 6.45 : Pressure distribution in layer 4 (k = 21.68 md and h = 8 ft)

6.9 EFFECT OF GAS PRODUCTION RATE ON CONDENSATE SATURATION DISTRIBUTION IN LAYERS 1 TO 4

Figures 6.46 to 6.50 show the sensitivity of condensate saturation distribution away from the wellbore to production rate in layer 1 at 2, 4, 6, 8 and 10 years. At 2 years the dew point pressure has not been reached when the production rate is 20 and 30 MMSCF/D but there is 45 % liquid condensate saturation near the wellbore for gas production rate of 40, 50 or 60 MMSCF/D. There is no liquid condensation from 10 ft away from the wellbore. However at 4 years, the percent liquid saturation is 44, 43,42 and 42 % near the wellbore when the gas production rate is 30, 40, 50 or 60 MMSCF/D but drops to 0% at 100ft, 1000ft and 6000ft and 6557.4ft respectively. The 20MMSCF/D gas production rate is yet to reach the dew point pressure at 4 years. At 6 years the liquid saturation has reached 1000 ft when the production rate is 20 MMSCF/D while whole reservoir is below the dew point pressure at higher rates. At 8 years, we observed that the percent liquid saturation in all the cells in layer 1 ranges from 45 % to 5% depending on the rate but the percent liquid saturation is the same when gas rate is 40, 50 or 60 MMSCF/D.

At 10 years, almost the same amount of percent liquid condensation can be observed for all gas production rates except the 20MMSCF/D gas production which has about 1% more liquid saturation near the wellbore. The liquid saturation when rate is 20 MMSCF/D is less than liquid saturation when gas rate is 30, 40, 50 or 60 MMSCF/D by about 1%. The trend in layers 2, 3 and 4 is similar to what is observed in layer 1 discussed above as can be seen in figures A-1 to A-15 in appendix-A.

The conclusion that can be made from our observation and discussion of the results obtained in this study of effect of gas production rate on condensate saturation distribution is that liquid condensation occurs throughout the reservoir when production rate is 40, 50 or 60MMSCF/D from 4 to 10 years. In addition, one can see clearly that the condensed phase is almost the same at 8 or 10 years for all gas production rates considered. Therefore, the effect of rate becomes negligible on condensate saturation distribution away from the wellbore at 10 years confirming that the system has reached pseudo-steady state.

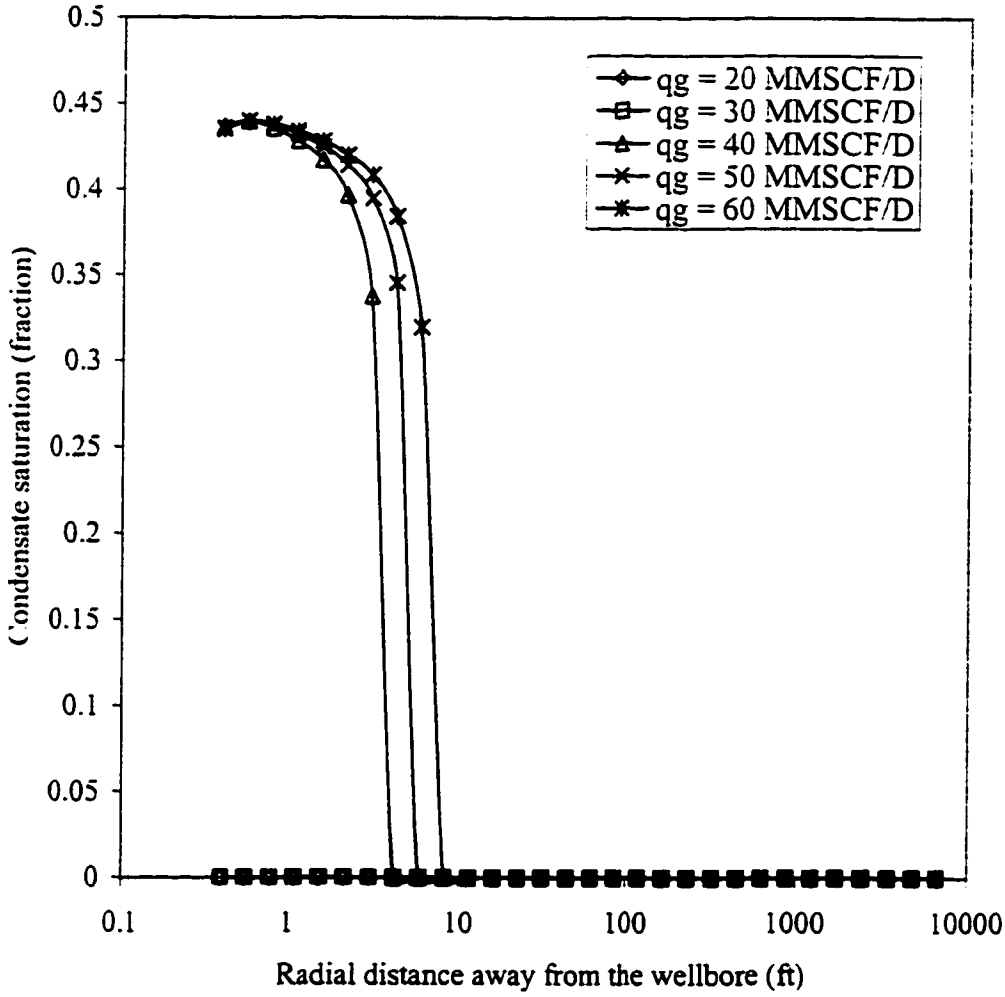

Fig: 6.46 Effect of gas production rate on condensate saturation distribution in layer 1 at 2 years

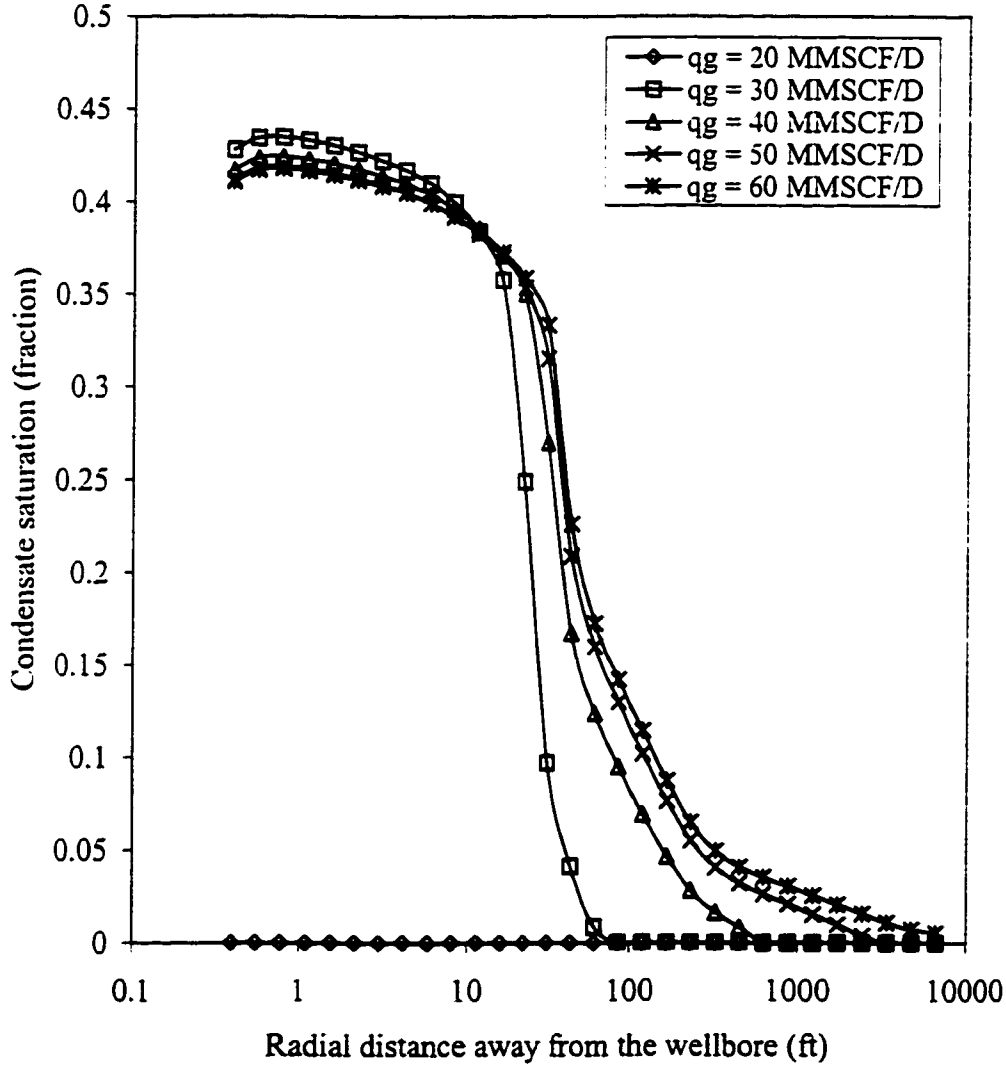

Fig 6.47: Effect of gas production rate on condensate saturation distribution in layer 1 at 4 years

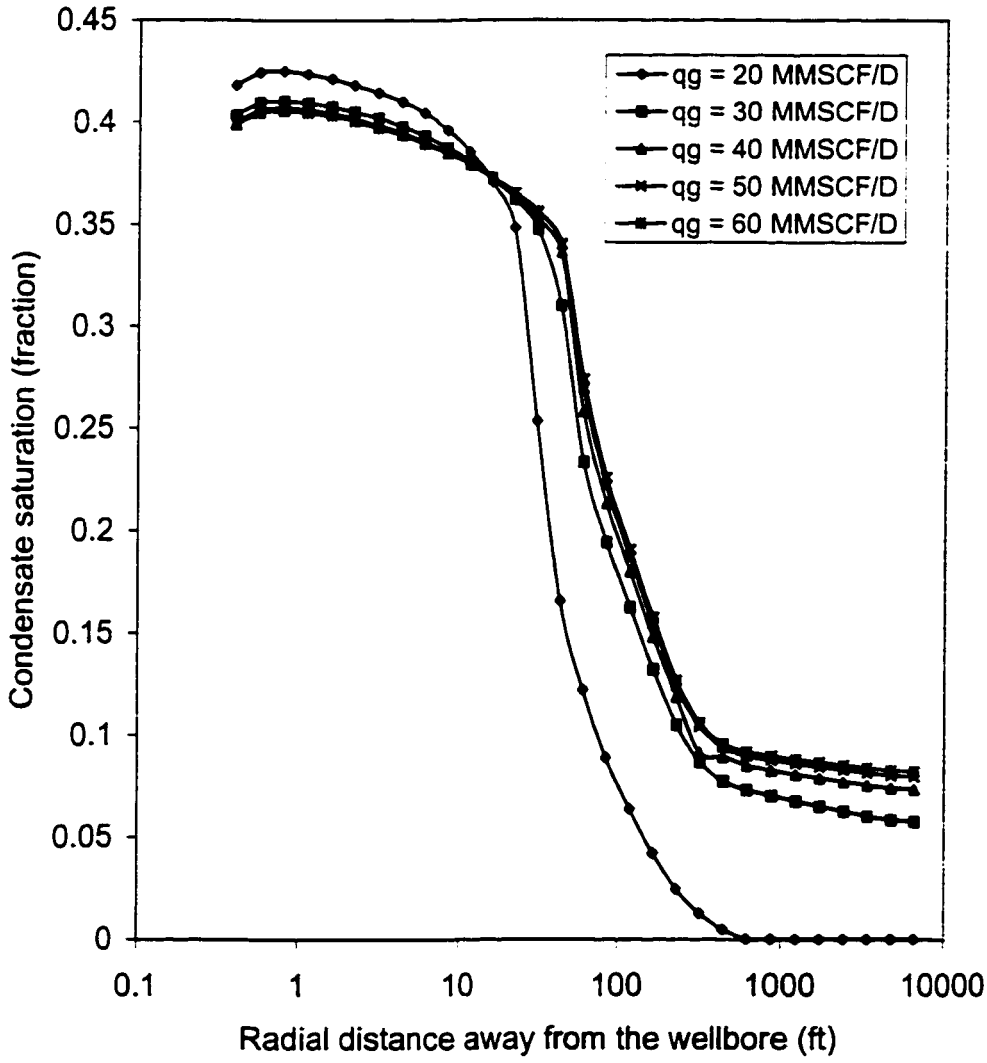

Fig 6.48 : Effect of gas production rate on condensate saturation distribution in layer 1 at 6 years.

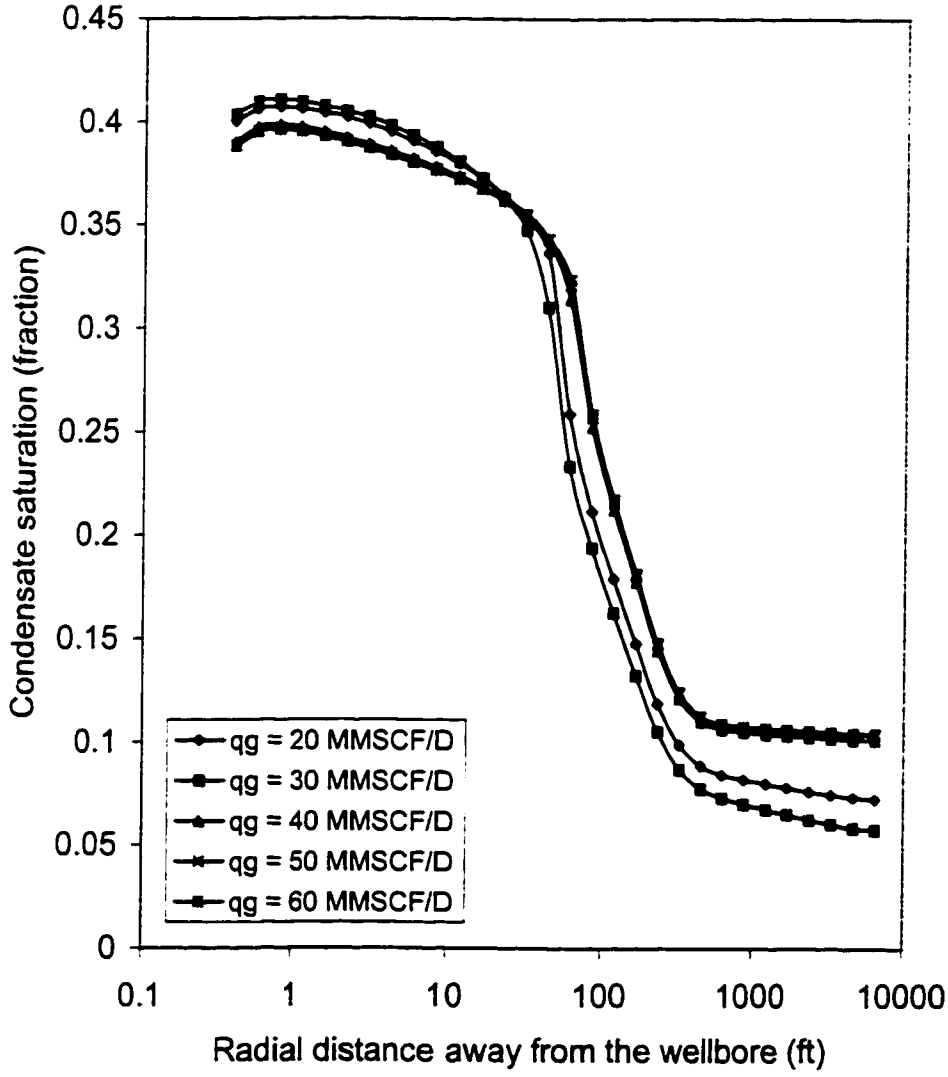

Fig 6.49: Effect of gas production rate on condensate saturation distribution in layer 1 at 8 years

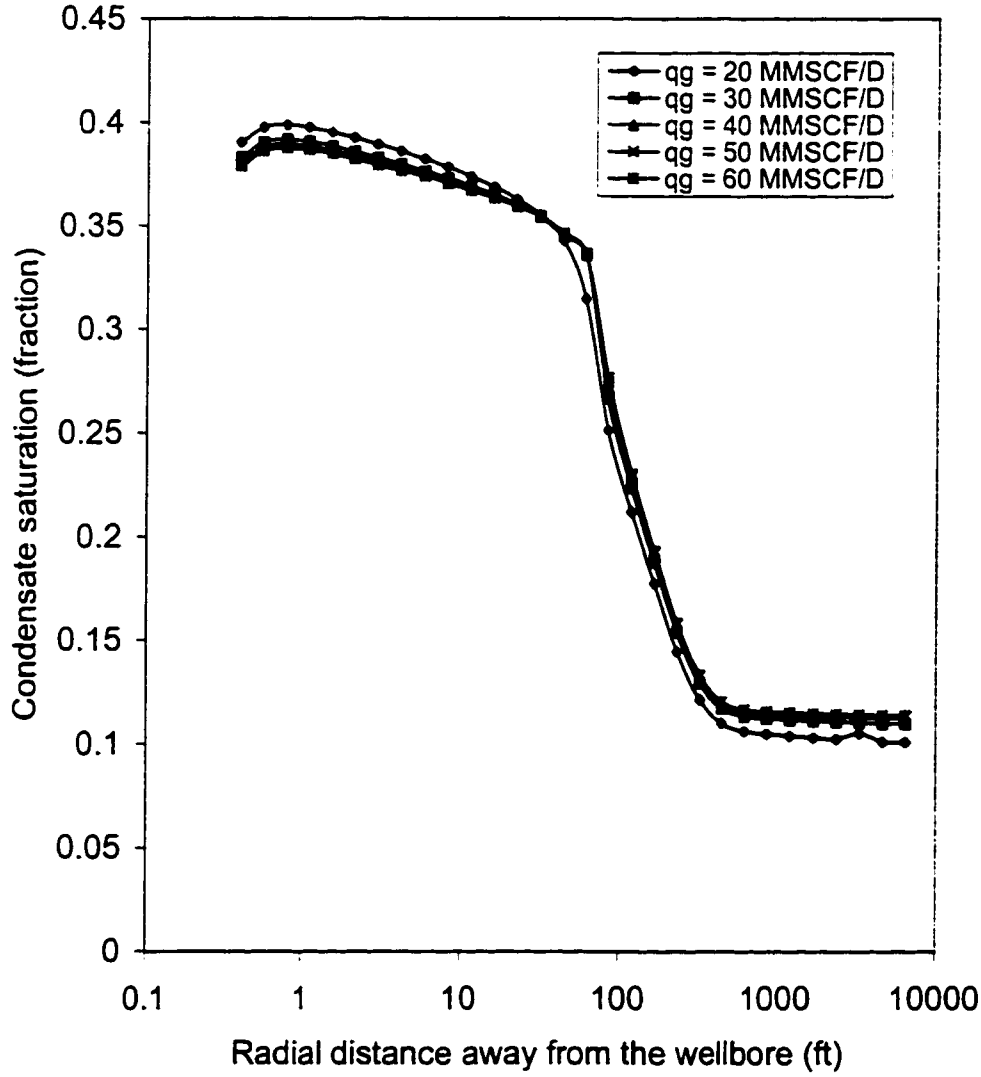

Fig 6.50: Effect of gas production rate on condensate saturation distribution in layer 1 at 10 years

6.10 PRESSURE DISTRIBUTION IN THE RESERVOIR

The pressure distribution for each layer at five different gas production rates investigated gave us an insight into what is going on in the reservoir. For gas production rate of 20MMSCF/D, the same pressure response is observed in all layers at 2 and 4 years. Single phase gas is flowing at this times but at 6, 8 and 10 years, there is exist significant drop in the pressure in all layers to the minimum bottom hole flowing pressure of 500 psia specified at around 1 ft away from the wellbore. At 100 ft from the wellbore the pressure drop is more in the high permeability layers than the low permeability layers but layers 3 and 4 pressure distribution are exactly the same. Figures 6.51 to 6.60 show this clearly.

At a gas production rate of 40MMSCF/D, the pressure response in all layers is the same at 2 years. When the depletion time is 2 years, only gas was flowing so the pressure distribution in all layers is the same. After 2 years, we observed that there are differences in the pressure distribution up to 100 ft away from the wellbore. At a distance more than 100 ft away from the wellbore, the pressure distribution is the same in all layers. This behavior is presented in figures 6.52 to 6.56.

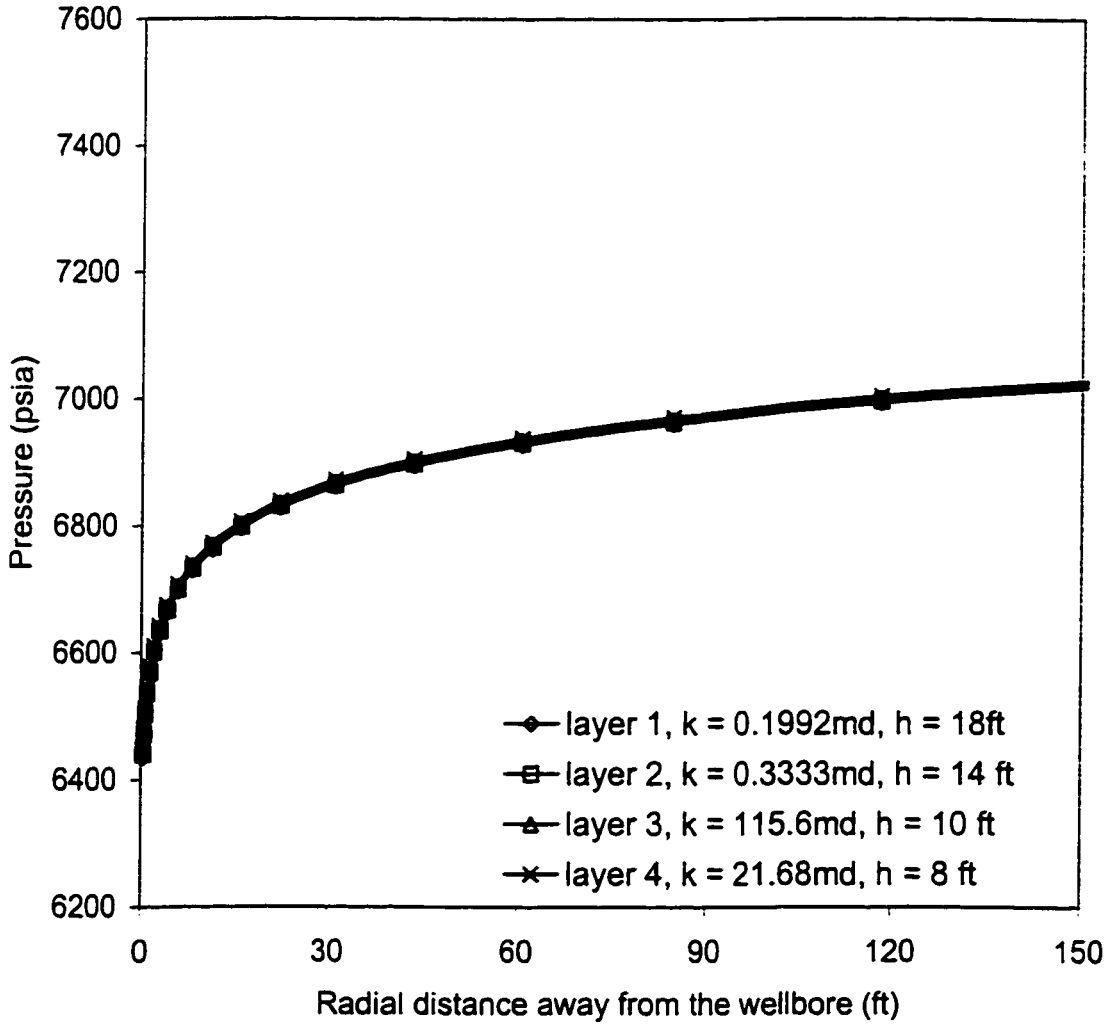

Fig 6.51: Pressure distribution away from the wellbore at 2 years when the maximum gas production constraint is 20 MMSCF/D

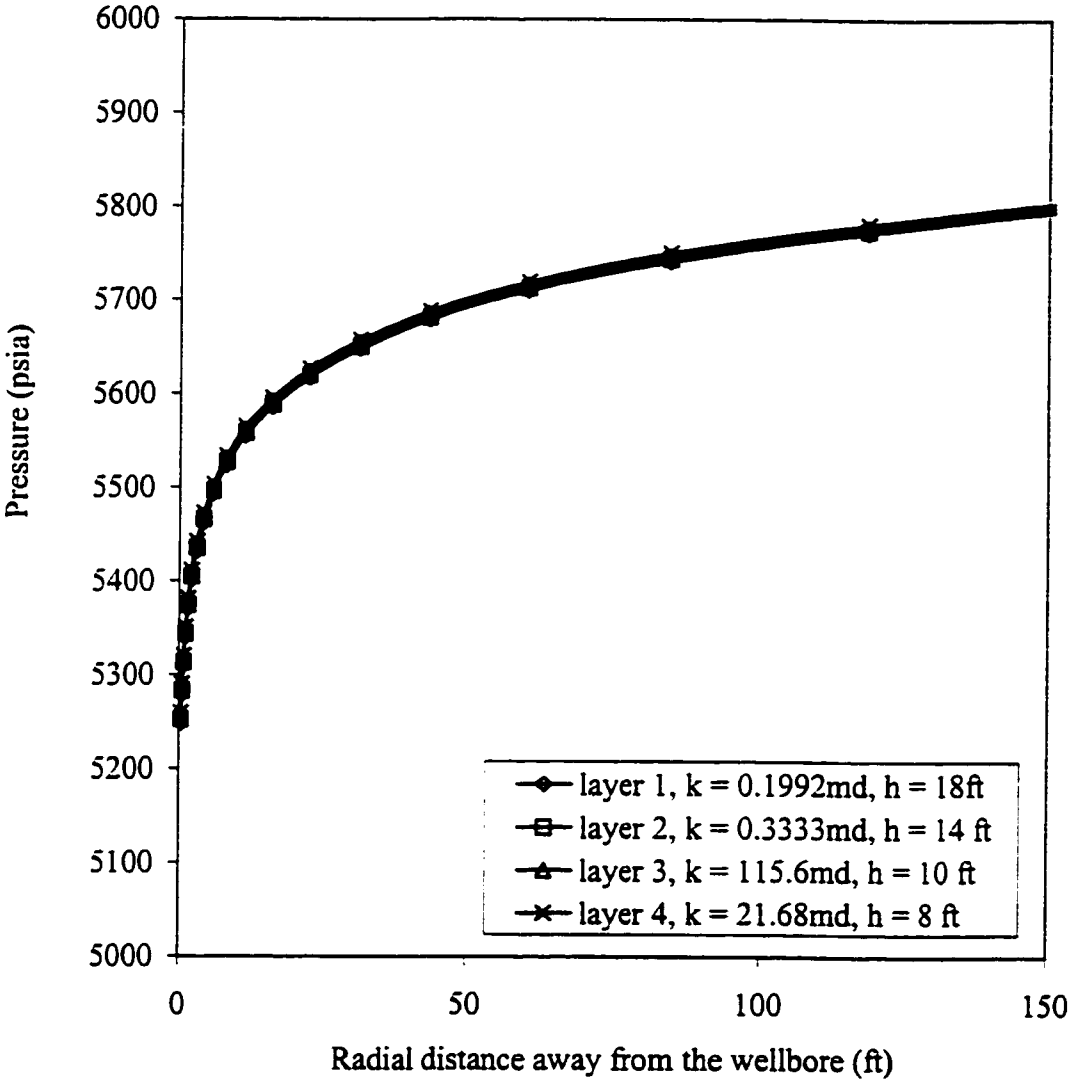

Fig 6.52: Pressure distribution away from the wellbore at 4 years when the maximum gas production constraint is 20 MMSCF/D

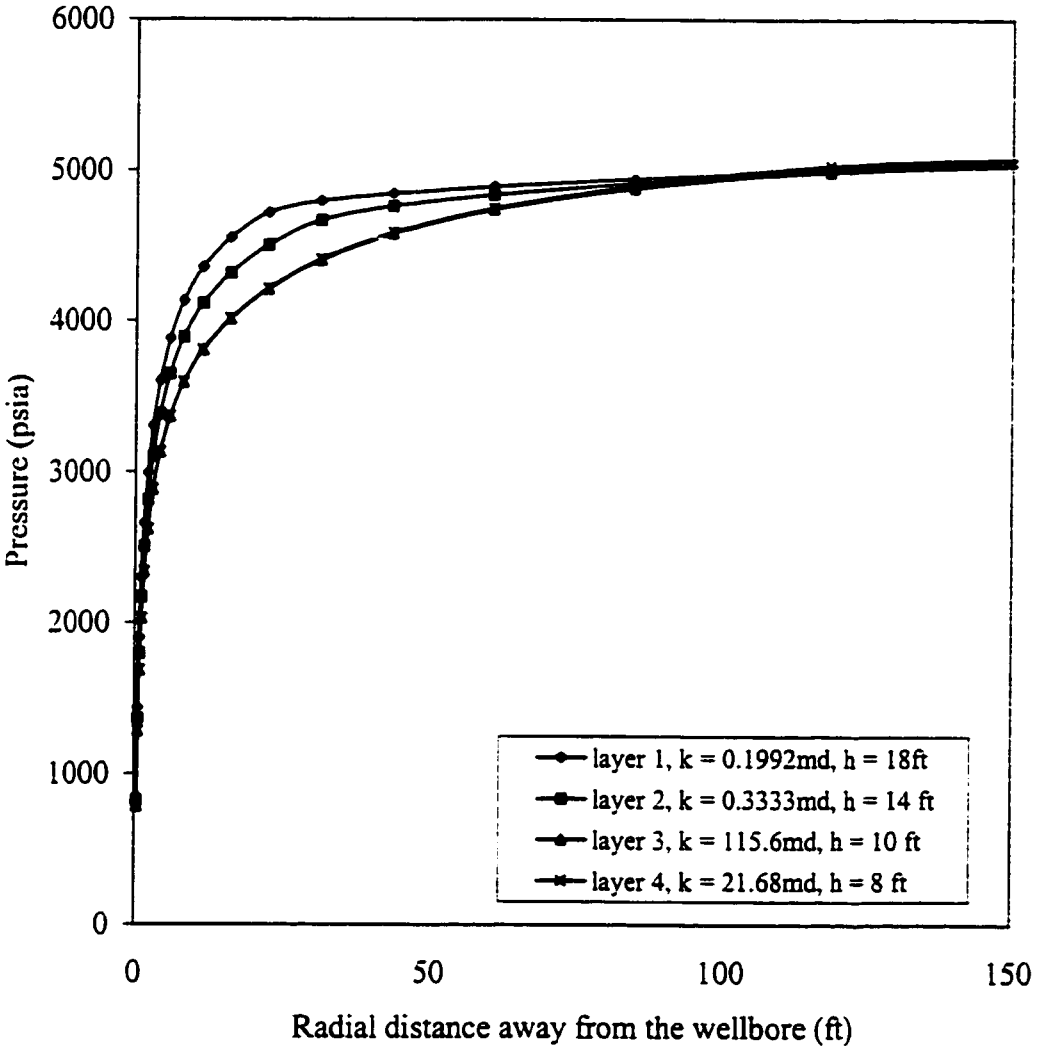

Fig 6.53: Pressure distribution away from the wellbore at 6 years when the maximum gas production constraint is 20 MMSCF/D

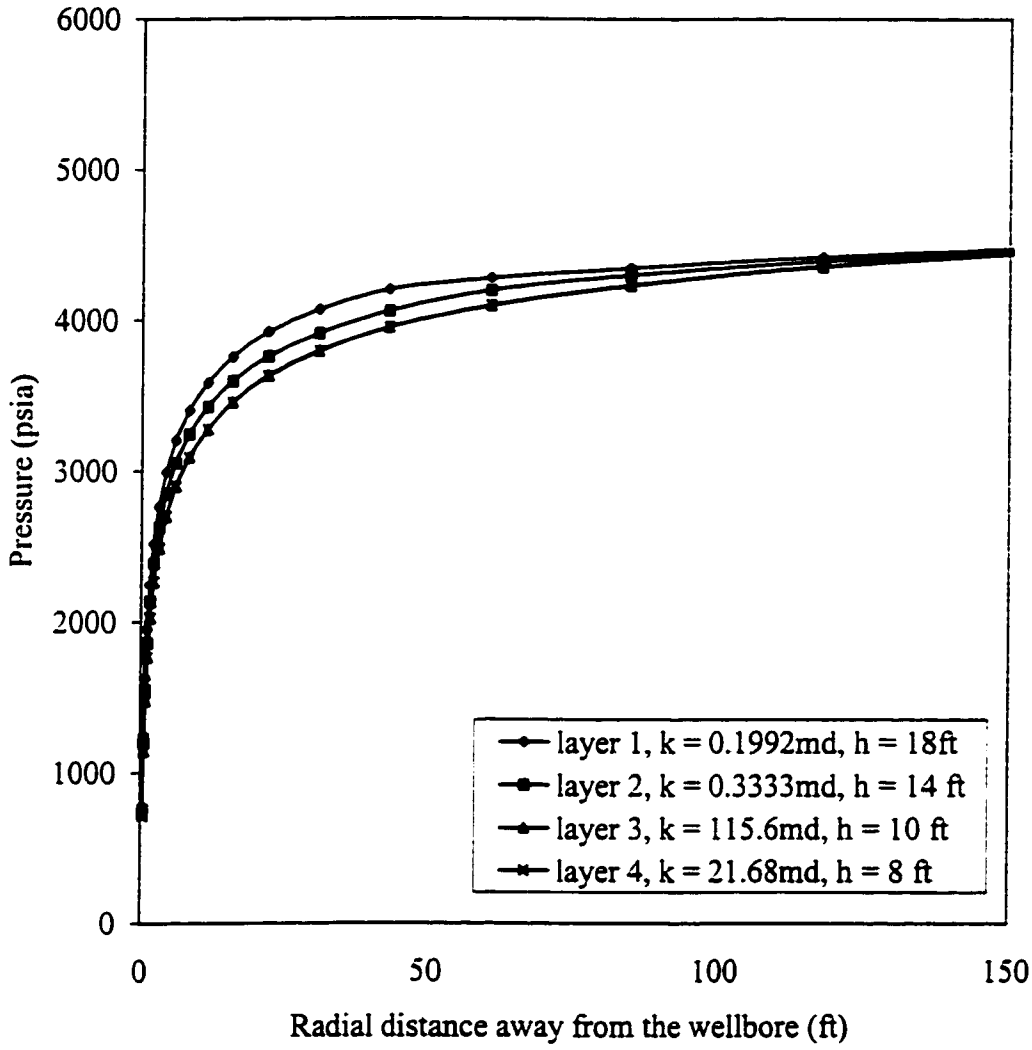

Fig 6.54: Pressure distribution away from the wellbore at 8 years when the maximum gas production constraint is 20 MMSCF/D

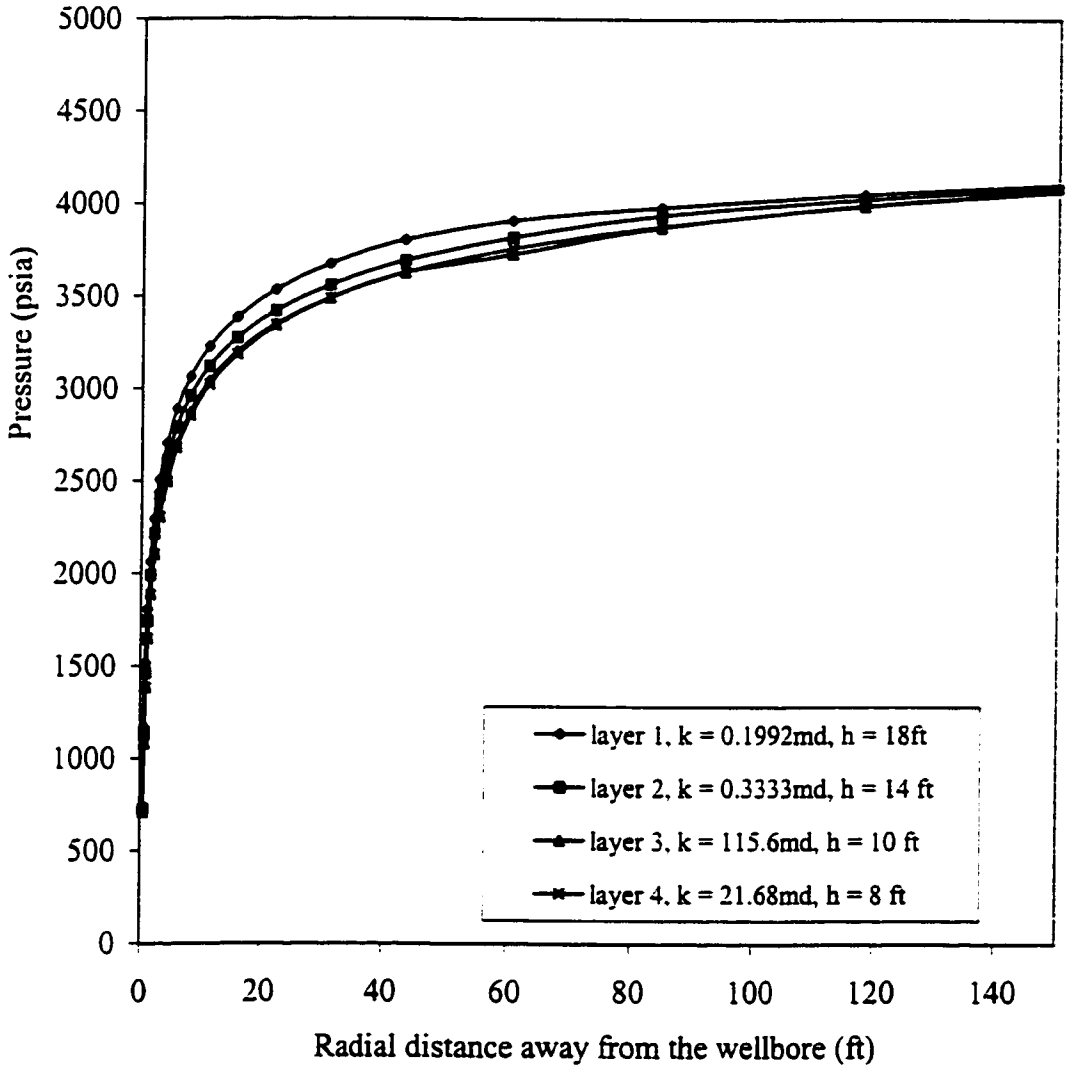

Fig 6.55 : Pressure distribution away from the wellbore at 10 years when the maximum gas production constraint is 20 MMSCF/D

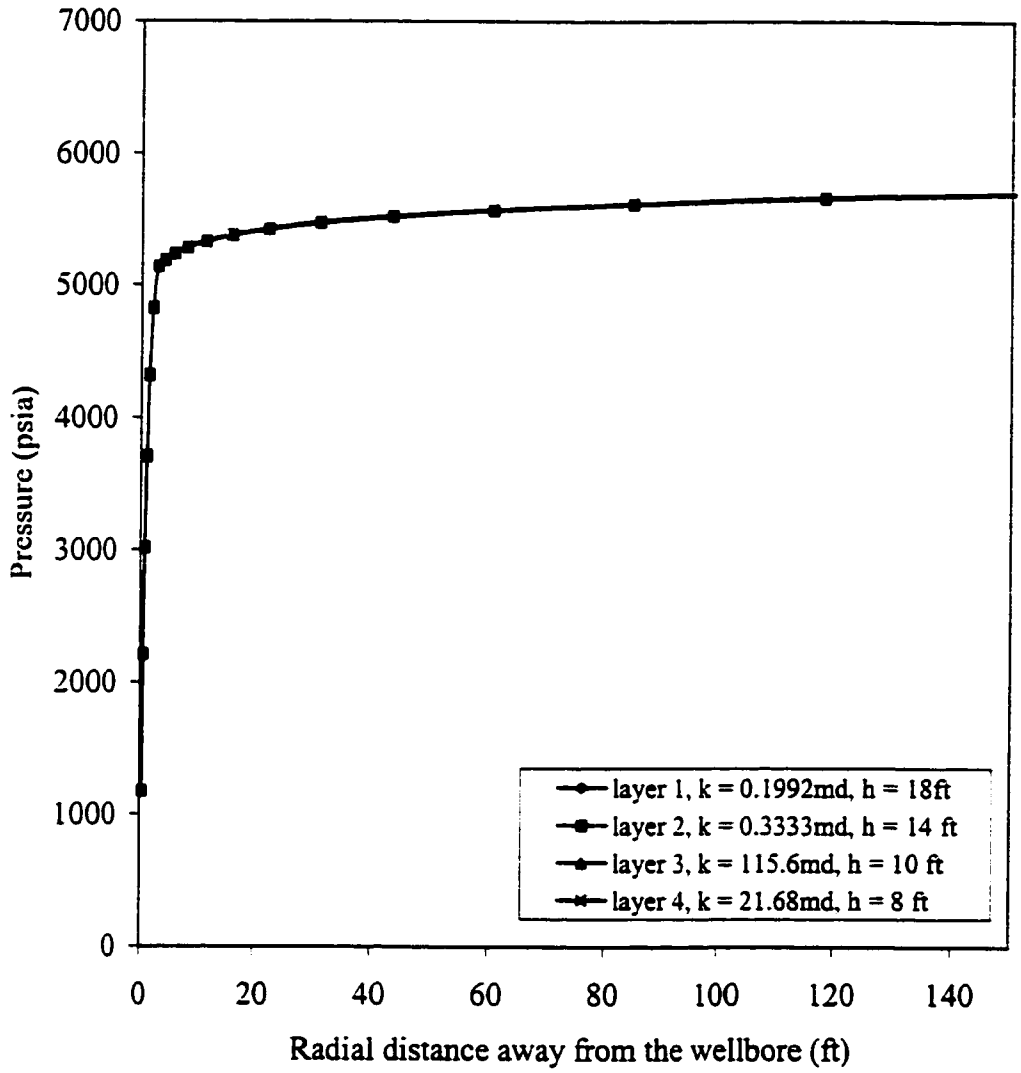

Fig 6.56: Pressure distribution away from the wellbore at 2 years when the maximum gas production constraint is 40 MMSCF/D

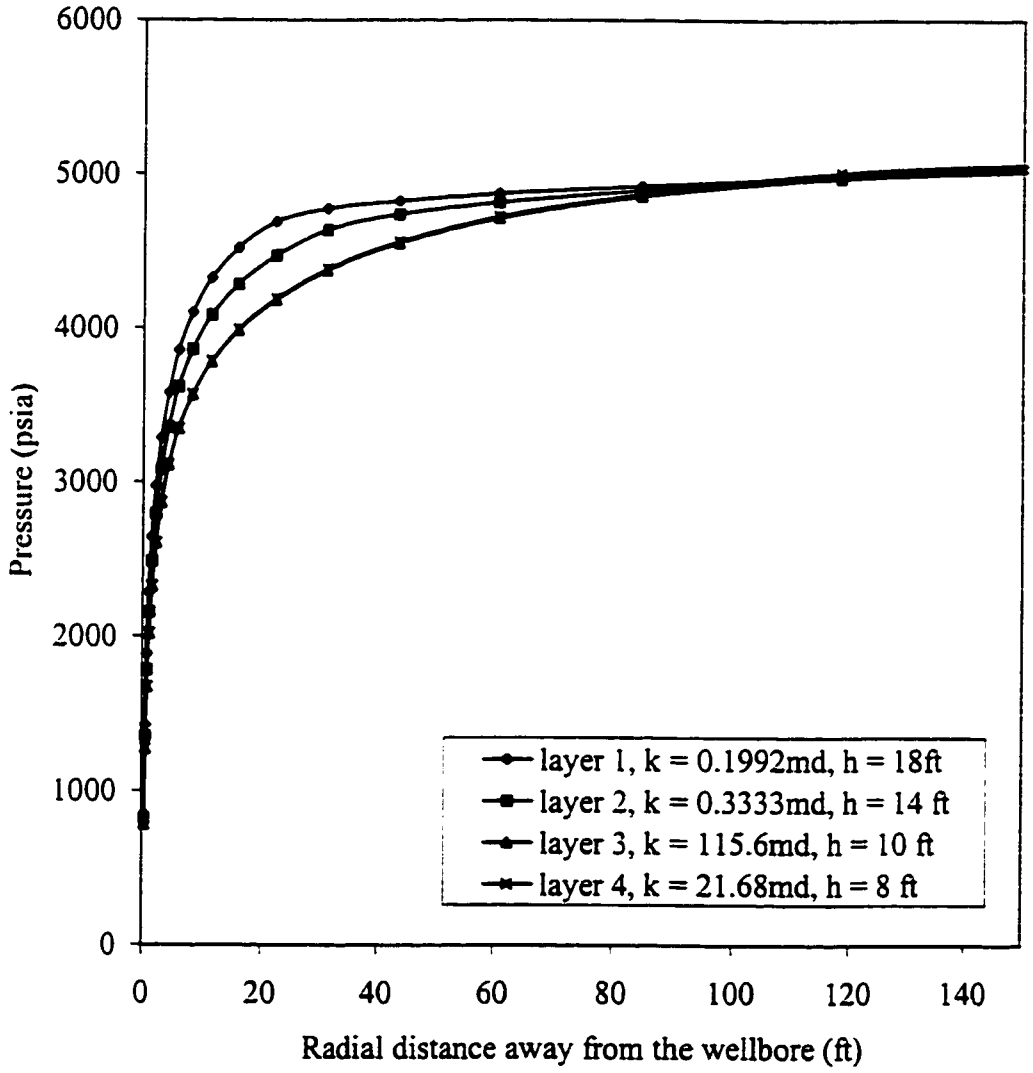

Fig 6.57: Pressure distribution away from the wellbore at 4 years when the maximum gas production constraint is 40 MMSCF/D

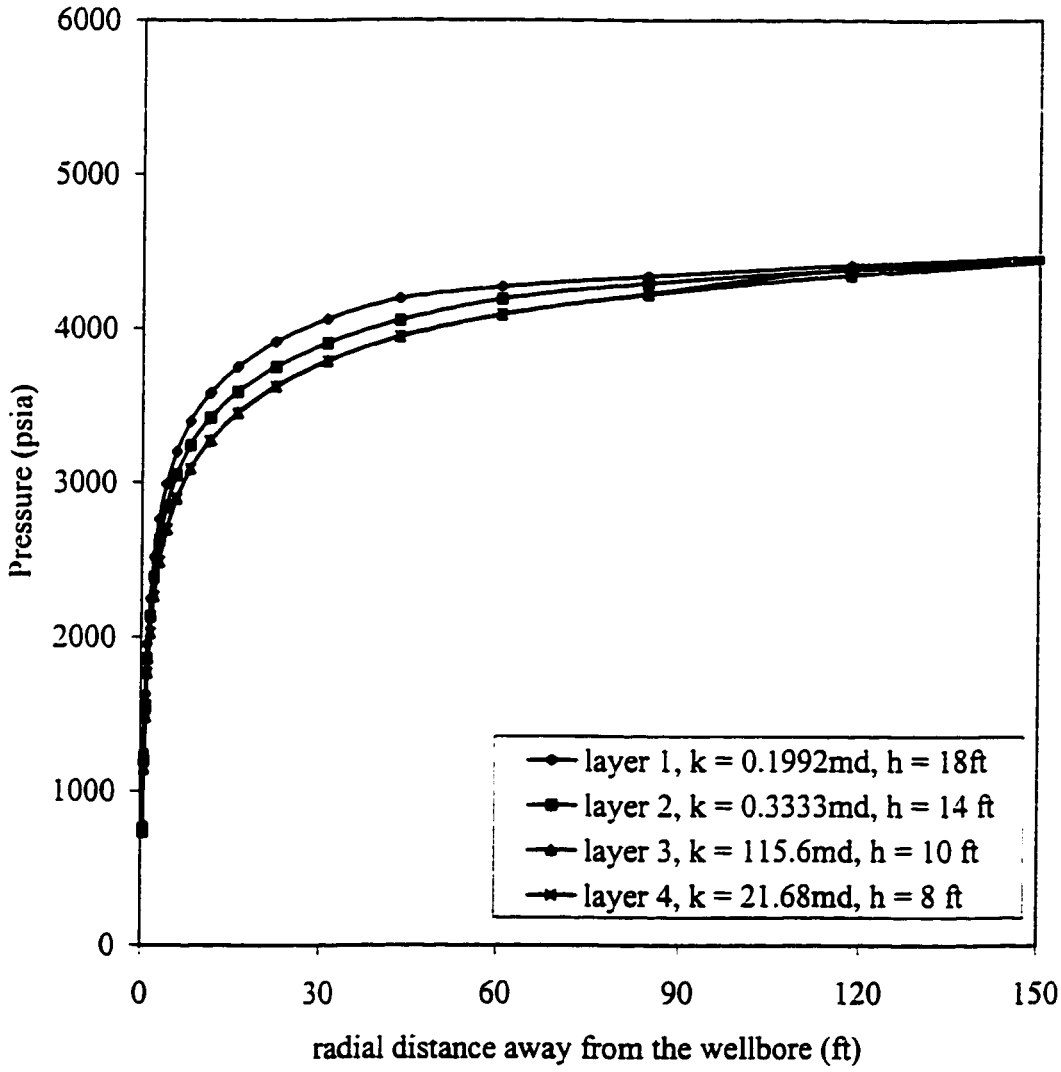

Fig 6.58: Pressure distribution away from the wellbore at 6 years when the maximum gas production constraint is 40 MMSCF/D

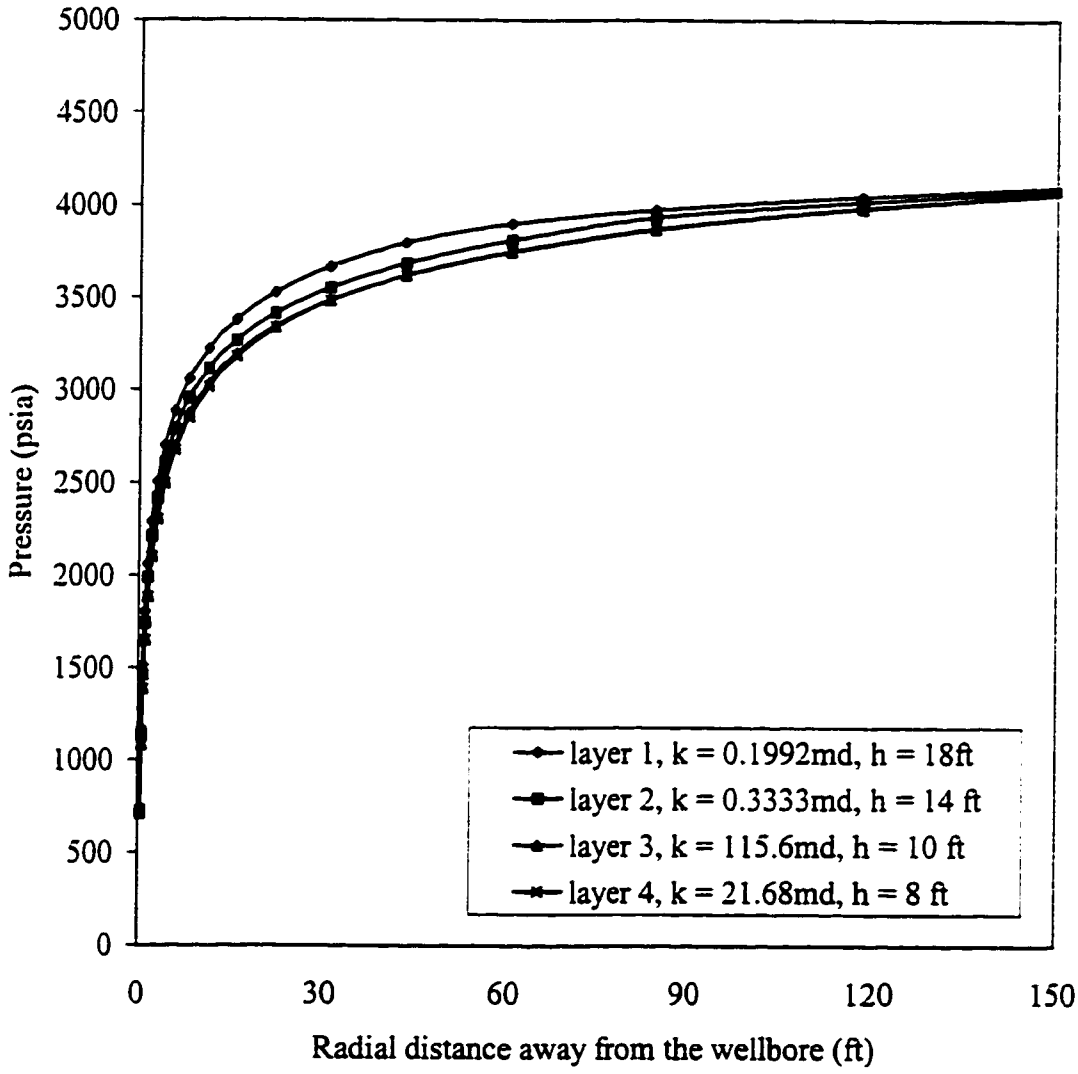

Fig 6.59: Pressure distribution away from the wellbore at 8 years when the maximum gas production constraint is 40 MMSCF/D

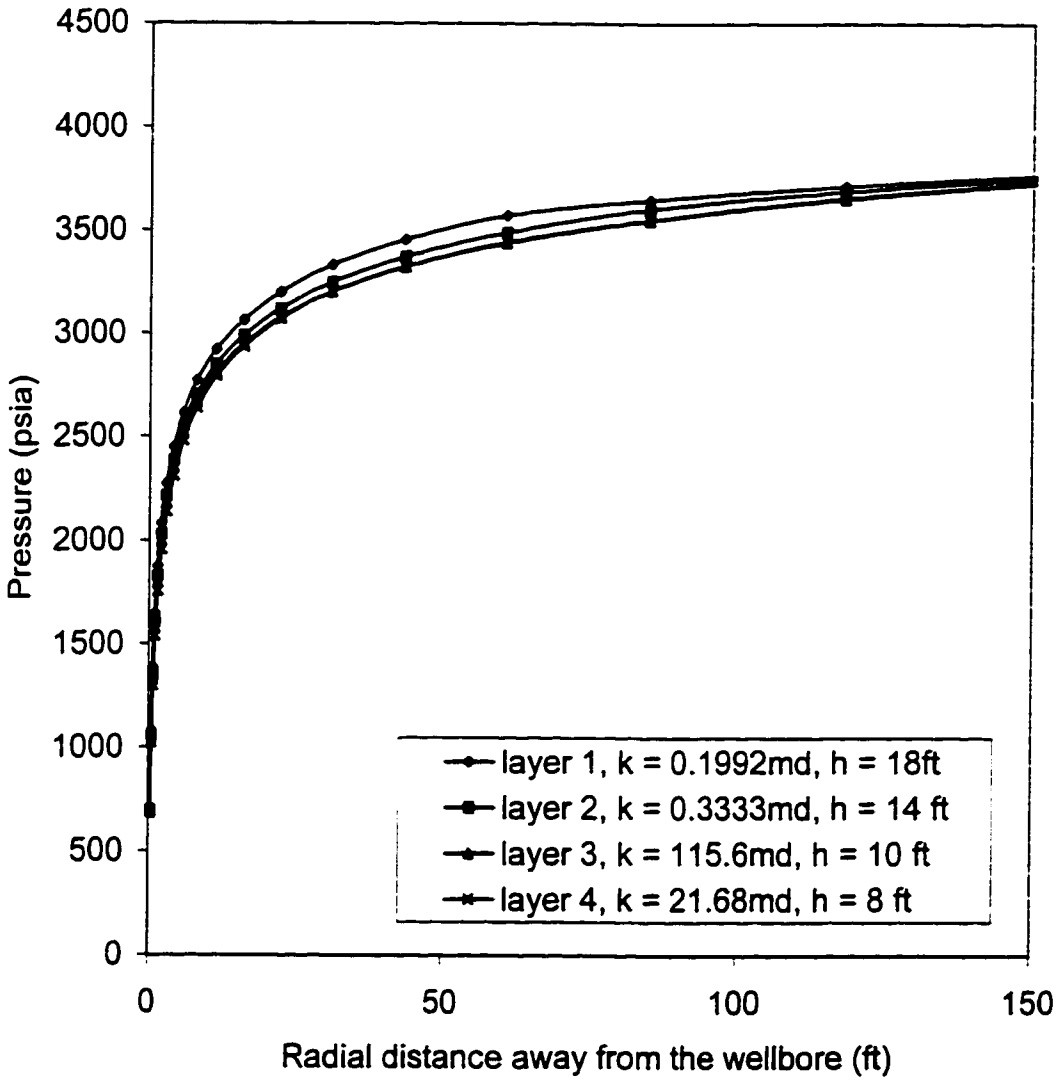

Fig 6.60: Pressure distribution away from the wellbore at 10 years when the maximum gas production constraint is 40 MMSCF/D

CHAPTER SEVEN

CONCLUSIONS AND RECOMMENDATIONS

Based on the results obtained from this study concerning the effect of liquid drop out on the productivity of a gas condensate reservoir undergoing depletion, the following conclusions and recommendations are made.

CONCLUSIONS

1. Sensitivity studies on the effect of critical condensate saturation on well performance indicate that increasing critical condensate saturation reduces the stabilized gas production rates hence reduces well productivity.

2. There is no significant improvement in the cumulative gas and condensate produced if the gas production rate is more than 40 MMSCF/D.

3. The gas condensate well productivity index declines significantly from 23.53, 23.38, 23.16, 22.893 MSCF/D/psia to 2.11MSCF/D/psia when the gas production rates are 20, 30, 40, 50 and 60 MMSCF/D respectively. This is a decline of 91% in productivity index for all rates and this happens immediately when the pressure falls below the dew point pressure.

4. The percent liquid condensed around the wellbore ranges from 37 to 44 % in the four layers depending on the production rate. This accumulation of condensate is

significant within 10 ft of the formation at early time of depletion but when the depletion time reached 6, 8 or 10 years, the liquid has dropped out throughout the reservoir.

5. There exists a difference in pressure distribution in the layers very near the wellbore. At a distance greater than 100-ft from the wellbore, the pressure distribution is the same for all layers.

RECOMMENDATIONS

1. Factors such as reservoir dip and non-Darcy flow were not considered in this study but deserve further investigation.

NOMENCLATURE

GOR	Gas oil ratio scf/bbl
P	Pressure (psi)
P_{sc}	Pressure at standard condition (14.7 psia)
psi	Pound per square inch
psig	Pound per square inch gauge
psia	Pound per square inch absolute
P_i	Initial reservoir pressure
σ	Interfacial tension in mN/m or dyne/cm
ft	Feet
k	Reservoir permeability (md)
k_x	Permeability in the x-direction (md)
k_y	Permeability in the y-direction (md)
k_z	Permeability in the z-direction (md)
°F	Degree Fahrenheit
IFT	Interfacial tension in mN/m or dyne/cm
PVT	Pressure, volume and temperature
HPHT	High pressure high temperature
Eclipse E300	A Schclumberger commercial simulator
β	Non-Darcy coefficient
ccs	Critical condensate saturation (fraction)
S_{cc}	Critical condensate saturation (fraction)

∑CORE	Multipurpose compositional simulator
ϕ	Porosity (fraction)
S_w	Water saturation (fraction)
λ	Pore size distribution index
P_e	Capillary entry pressure, psig
P_c	Capillary pressure, psig
S_{wt}	Wetting phase saturation (fraction)
S_{wtr}	Residual wetting-phase saturation (fraction)
J(Sw)	Leverett J-Function
θ	Contact angle
dz or h	layer thickness
S_{wi}	Initial water saturation (fraction)
DST	Drill Stem Test
S_{gr}	Residual gas saturation (fraction)
k_{rg}	Gas relative permeability
k_{rog}	Oil relative permeability
S_{wir}	Irreducible residual water saturation (fraction)
S_g	Gas saturation (fraction)
Sw	Water saturation (fraction)
CPCP	Chevron phase calculation program
CHEARS	Chevron reservoir simulator
S_{lc}	Critical liquid saturation (fraction)
S_{org}	Residual oil saturation to gas displacement (fraction)

PI	Productivity index (MSCF/D/psia)
P_{wf}	Well flowing bottom hole pressure (psia)
BHFP	Bottom hole flowing pressure (psia)
Q_g	Gas flow rate (MMSCF/D)
P_{avg}	Average reservoir pressure (psia)
V_b	Bulk reservoir volume
GIIP	Gas initially in place
SCF	Standard cubic feet
r_1	First radial grid cell, ft
r_w	Wellbore radius, ft
r_e	Drainage radius, ft
So	Oil saturation (fraction)
B_{gi}	Gas Formation volume factor
GEXP	Power law model gas exponent
WEXP	Power law model water exponent
OEXP	Power law model oil exponent
S_{gc}	Critical gas saturation (fraction)
$V_{roCCE(p)}$	Relative oil volume of the flowing gas during a constant composition expansion
$V_{roCVD(p)}$	Relative volume of the flowing gas during a constant volume depletion
S_{oc}	Critical oil saturation (fraction)
T	Reservoir Temperature
R	Universal gas constant = 10.73
γ_g	Gas gravity

γ	Euler Constant = 0.577215
ρ	Gas density
ρ_{sc}	Gas density at standard condition

Subscripts

sc	Standard condition
o	Oil
w	water
g	Gas
avg	average
x	x-direction
y	y-direction
z	z-direction

REFERENCES

1. Morel, D.C., Nectoux, A, and Danquigny, J.: "Experimental Determination of the Mobility of Hydrocarbon Liquids during Gas Condensate Reservoir Depletion: Three Actual Cases," paper 38922 presented at the 1997 SPE Annual Technical Conference and Exhibition, San Antonio, Texas, October 5-8 1997.

2. Barnum, R. S., Brinkman, F.P., Richardson, T.W., and Spillette, A.G.: " Gas Condensate Reservoir Behaviour: Productivity and Recovery Reduction Due to Condensation," SPE Paper 30767 presented at the SPE Annual Technical Conference & Exhibition, Dallas, October 22-25, 1995.

3. Morel, D.C., Lomer, J-F., Morineau, Y.M., Putz, A.G.: " Mobility of Hydrocarbon Liquids in Gas Condensate Reservoirs: Interpretation of Depletion Laboratory Experiments," SPE Paper 24939 presented at the SPE 67th Annual Technical Conference and Exhibition, Washington, D.C., October 4-7, 1992.

4. Boom, W., Wit, K., Schulte, A.M., Oedai, S., Zeelenberg, J.P.W and Maas, J.G.: "Experimental Evidence for Improved Condensate Mobility at Near-wellbore Flow Conditions," SPE Paper 30766 presented at the SPE Annual Technical & Exhibition, Dallas, October 22-25, 1995.

5. Robert Mott.: "Calculating Well Productivity in Gas Condensate Reservoirs," presented at the IBC Technical Services Conference on Optimisation of Gas Condensate Fields, Aberdeen, June 26-27,1997.

6. Pope, G. A., Wu, W., Delshad, M., Sharma, M., and Wang, P.: " Modeling Relative Permeability Effects in Gas-Condensate Reservoirs," SPE Paper 49266 presented at the 1998 SPE Annual Technical Conference and Exhibition, New Orleans, Louisiana, September 27-30, 1998.

7. Fussel, D. D.: "Single-Well Performance Predictions for Gas Condensate Reservoirs ", Journal of Petroleum Technology, (July 1973) 860-870.

8. Leemput, L.E.C., Bertram, D.A., Bentley, M.R. and Gelling, R.: "Full Field Reservoir Modeling of Central Oman Gas/ Condensate Fields, SPE Paper 30757 presented at the Annual Technical Conference & Exhibition held in Dallas, USA, October 22-25,1995.

9. Boom, W., Wit, K., Zeelenberg, J.P.W., and Maas., J.G.: "On the Use of Model Experiments for Assessing Improved Gas-Condensate Mobility Under Near-

Wellbore Flow Conditions," SPE Paper 36714 presented at the 1996 SPE Annual Technical Conference and Exhibition, Denver, Colorado, October 6-9, 1996.

10. Malachowski, M.A., Yanosik, J.L., Saldana, M.A., and Batten, A.H.: "Simulation of Well Productivity Losses Due to Near Well Condensate Accumulation in Field Scale Simulations," SPE Paper 30715 presented at the SPE Annual Technical Conference & Exhibition, Dallas, October 22-25,1995.

11. Fevang, Ø and Whitson,C.H.: "Modeling Gas Condensate Well Deliverability," paper SPE 30714 presented at the SPE Annual Technical Conference & Exhibition, Dallas, October 22-25,1995.

12. Clark, T.J.: "The Application of a 2-D Compositional, Radial Model to Predict Single Well Performance in a Rich Gas Condensate Reservoir," paper SPE 14413 presented at the 60th Annual Technical and Exhibition of the SPE, Las Vegas, NV, September 22-25,1985.

13. Novosad, Z .: " Composition and Phase Changes in Testing and Producing Retrograde Gas Wells," SPE paper 35645 presented at the Gas Technology Conference held in Calgary, Alberta, Canada, April 28 – May 1st, 1996.

14. Mohammadi, S., Sorbie, K.S., Danesh, A., and Peden, J.M.: " Pore Level Modelling of Gas Condensate Flow Through Horizontal Porous Media," SPE paper 20479 presented at the 65th Annual Technical Conference and Exhibition of the Society of Petroleum Engineers held in New Orleans, LA, September 23-26,1990.

15. Dyung, T. V., Jack, R.J., and Raghavan, R.: " Performance Predictions for Gas Condensate Reservoirs," SPE Formation Evaluation, (December 1989)576-584.

16. Hidde, R.: " Effect of Low Interfacial Tensions on Relative Permeabilities in Some Gas Condensate Systems," SPE paper 25072 presented at the European Petroleum Conference held in Cannes, France, 16-18 November 1992.

17. Kim, J.S.: "Compositional Simulation of the Coyanosa Wolfcamp Field Gas Cycling Operation," SPE/DOE paper 20130 presented at the SPE/DOE Seventh Symposium on Enhanced Oil Recovery held in Tulsa, Oklahoma, April 22-25,1990.

18. Lindeberg, E.G.B., BjØrkvik, B.J.A., and Strand, K.A.: " Interface Light Scattering Measurement of Low Interfacial Tension on a Gas Condensate System at High Pressure and Temperature," SPE/DOE paper 35427 presented at the 1996 SPE/DOE Tenth Symposium on improved Oil Recovery held in Tulsa, OK, 21-24 April 1996.

19. Philip, L. M.: "Engineering Applications of Phase Behavior of Crude Oil and

Condensate Systems," Journal of Petroleum Technology (July 1986) 715-723.

20. Henderson, G.D., Danesh, A., Tehrani, D.H. and Peden, J.M.: " An Investigation into the Processes Governing Flow and Recovery in Different Flow Regimes Present in Gas Condensate Reservoirs", SPE paper 26661 presented at the 68th Annual Technical Conference and Exhibition of the Society of Petroleum Engineers held in Houston, Texas, 3-6 October 1993.

21. Gerard, M., Claire, B., Emmanuelle, T., Patrick, G., and Nicolas, C.: " Early Evaluation of Uncertainties in the Incremental Condensate Recovery Through a Gas Cycling Process," SPE Journal, Volume 2, March 1997, 33-47.

22. Hsu, H.H., and Ponting, D.K.: " Field –Wide Compositional Simulation for HPHT Gas Condensate Reservoirs Using an Adaptive Implicit Method," SPE paper 29948 presented at the International Meeting on Petroleum Engineering Held in Beijing, PR China, 14-17 November 1995.

23. Guo, P., Sun, L., Li, S., and Sun, L.: " Theoretical Study of the Effect of Porous Media on the Dew Point Pressure of a Gas Condensate," SPE paper 35644 presented at the Gas Technology Symposium & Exhibition held in Calgary, Alberta, Canada, 28 April- 1 May,1996.

24. Kalaydjian, F.J-M., Bourbiaux, B.J., and Lombard, J-M.: "Predicting gas Condensate Reservoir Performance: how flow parameters are altered when approaching production wells," SPE paper 36715 presented at the 1996 SPE Annual Technical Conference held in Denver, Colorado, U.S.A., 6-9 October 1996.

25. Henderson, G.D., Danesh, A., Tehrani, D.H., Al-shadi, S., and Peden, J.M.: " Measurement and Correlation of Gas Condensate Relative Permeability by the Steady-State Method," SPE paper 30770 presented at the SPE Annual Technical Conference & Exhibition held in Dallas, U.S.A., 22-25 October, 1995.

26. Ali, J.K., McGauley, P.J., and Wilson, C.J.: " The Effects of High – Velocity Flow and PVT Changes Near Wellbore on Condensate Well Performance," SPE paper 38923 presented at the 1997 SPE Annual Technical Conference and Exhibition held in San Antonio,Texas,5-8 October 1997.

27. Thomas, F.B., Dedora, N., Zhou, X., and Bennion, D.B.: " Optimizing Production from Gas Condensate Reservoirs," Journal of Canadian Petroleum Technology (October 1997) 43-49.

28. Thomas, F.B., Anraku, T., Bennion, D.B., Bennion, D.W.: "Optimizing Production From a Rich Gas Condensate Reservoir," SPE/DOE paper 35455 presented at the 1996 SPE/DOE Tenth Symposium on Improved Oil Recovery held in Tulsa OK, 21-24 April 1996.

29. Chen, H.L., Wilson, S.D., and Monger-Mcclure, T.G.: " Determination of Relative Permeability and Recovery for North sea Gas Condensate Reservoirs," SPE paper 30769 presented at the SPE Annual Technical Conference & Exhibition held in Dallas, U.S.A., 22-25 October,1995.

30. Narayanaswamy, G., Sharma, M.M., and Pope, G.A.: " Effect of Heterogeneity on the Non-Darcy Flow Coefficient," SPE paper 39979 presented at the 1996 SPE Gas Technology symposium held in Calgary, Alberta, Canada, 15-18 March 1996.

31. Coats, K.H.: " Simulation of Gas Condensate Reservoir Performance," Journal of Petroleum Technology (October 1985)1870-1886.

32. Bourbiaux, B.J., " Parametric Study of Gas condensate Reservoir Behavior During Depletion: A Guide for Development planning," SPE paper 28848 presented at the European Petroleum Conference held in London, U.K., 25 October 1994.

33. Al-Majed, A.A., and Dougherty, E.L.: " A Variable Cell Model for Simulating Gas Condensate Reservoir Performance," SPE paper 21428 presented at the SPE Middle East Oil Show held in Bahrain, 16-19 November 1991.

34. Sanger, P.J., and Hagoort, J.: " Recovery of Gas-condensate by Nitrogen Injection compared with methane injection," SPE paper 30795 presented at the SPE Annual Technical Conference & Exhibition held in Dallas, U.S.A., 22-25 October, 1995.

35. Delshad, M., Delshad, M., Bhuyan, D., Pope, G.A., and Lake, L.W.: " Effect of Capillary Number on the Residual Saturation of a Three Phase Micellar Solution," SPE/DOE Fifth Symposium on Enhanced Oil Recovery of the Society of Petroleum Engineers and the Department of Energy held in Tulsa, Ok, April 20-23,1986.

36. Wu Wei-Jr., Wang, P., Delshad, M., Wang, C., Pope, G.A., and Mukul, M.S.: "Modelling Non-Equilibrium Mass Transfer Effects for a Gas Condensate Field," SPE paper 39764 presented at the 1996 SPE Asia Pacific Conference on Integrated Modeling for Asset Management, 23-24 March 1998, Kuala Lumpur, Malaysia.

37. Asar, H., and Handy, L.L.: " Influence of Interfacial Tension on Gas-oil Relative Permeability in a Gas Condensate System," SPE paper 11740 presented at the 1983 California Regional Meeting held in Ventura, California, March 23-25,1983.

38. Bardon, C.P., and Longeron, D.: " Influence of Very Low Interfacial Tensions on Relative Permeability," SPE paper 7609 presented at the 53rd Annual Fall

Technical Conference and Exhibition of the Society of Petroleum Engineers of AIME, held in Houston,Texas, Oct 1-3, 1978.

39. Kenyon, D., and Behie, G.A.: " Third SPE Comparative Solution Project: Gas Cycling of Retrograde Condensate Reservoirs," Journal of Petroleum Technology (August 1987) 981-996.

40. Killough, J.E., and Kossack, C.A.: " Fifth Comparative Solution Project: Evaluation of Miscible Flood Simulators," SPE paper presented at the Ninth SPE Symposium on Reservoir Simulation held in San Antonio, Texas, February 1-4,1987.

41. Al-Majed, A.A.: " A Variable Cell Model for Simulating Gas Condensate Reservoir Performance," Ph.D. Dissertation, University of Southern California, U.S.A (July 1988).

42. Al-Marry, J.A.S.: " Prediction of Liquid Recovery From a Gas Condensate Reservoir," Ph.D. Dissertation, West Virginia University, U.S.A (1983).

43. Al-Shadi, S.M.: " Modelling of Gas Condensate Flow in Reservoir at Near Wellbore Conditions," Ph.D. Dissertation, Heriot-Watt University, Edinburgh, U.K (August 1997).

44. Afidick, D., Kaczorowski, N.J., and Asrinivas, B.: "Production Performance of a Retrograde Gas Reservoir: A Case Study of the Arun Field", SPE paper presented at the Asia pacific oil & Gas conference held in Melbourne, Australia, 7-10 November 1994.

45. Settari. A, Bachman, R.C., Hovem, K. and Paulsen, S.G.:" Productivity of Fractured Gas Condensate Wells- A Case Study of the Smorbukk Field", SPE paper 35604 presented at the Gas Technology conference held in calgary, Alberta, Canada, 28 April- 1 May 1996.

46. Christie, M.A and Clifford, P.J.: " Fast procedure for Upscaling Compositional Simulation", SPE paper 50992 presented at the SPE Reservoir Simulation Symposium held in Dallas, 8-11 June 1977.

47. Al-kaabi, U.A.: "Open-hole well log interpretation class note", KFUPM, 1998.

48. Chevron Phase Calculation Program Manual

49. Burdine, N.T.: " Relative Permeability Calculations from Pore Size Distribution Data," Trans., AIME 198, 1953, 71-78.

50. Brooks, R.H. and Corey, A.T.: "Properties of Porous Media Affecting Fluid Flow," J.Irrigation and Drainage Division, Proc., ASCE (1996), 81-88.

51. "Petrophysical Evaluation of Pore Resistivity Gas Sand", 2nd progress report, February 1999, KFUPM-RI.

52. "Effect of Condensate Drop-out on the Productivity of Hawiyah Jauf Gas Condensate Wells", Annual report, July 1998, KFUPM-RI

53. Roebuck, I.F., Jr., Ford, W.T., Henderson, G.E. and Douglas, Jim, Jr.: " The compositional Reservoir Simulator: Case I- The Linear Model," Soc. Pet Eng. J. (March 1969) 115-130; Trans., AIME, 246.

54. Roebuck, I.F., Jr., Ford, W.T., Henderson, G.E. and Douglas, Jim, Jr.: " The compositional Reservoir Simulator: Case II- The Two Dimensional Model," Paper SPE 2235 presented at SPE-AIME 43rd Annual Fall Meeting, Houston, Sept. 29-Oct. 2, 1968.

55. Roebuck, I.F., Jr., Ford, W.T., Henderson, G.E. and Douglas, Jim, Jr.: " The compositional Reservoir Simulator: Case III - The Radial Geometry," unpublished paper, available from Core Laboratories, Inc., Dallas, Texas.

56. Evinger, H.H. and Muskat, M.: " Calculation of Theoretical Productivity Factor," Trans., AIME (1942) 146,126.

57. Jones, J.R. and Raghavan, R.: " Interpretation of Flowing Well responses in Gas-Condensate Wells," SPEFE (Sept. 1998) 578-94.

58. Wilke, C.R. and Lee, C.Y.: Ind. Eng. Chem., 47:1253 (1955)

59. Wilkins, M.D., L.M. Abriola, and K.D. Pennell.: "An Experimental investigation of Rate-Limited Nonaqeous Phase Liquid Volatilization in Unsaturated Porous Media: Steady State Mass Transfer," water resources research, vol. 31, no. 9, 2159-2172 (Sept. 1995).

60. CHEARS 94A Vol. 1A & B, User's Guide-Initialization Data, Chevron Petroleum Technology, October 1996.

61. O'Dell, H.G. and Miller, R.N.: " Successfully Cycling a Low permeability, High Yield Gas Condensate Reservoir," J.Pet. Tech. (Jan., 1967) 41-44.

APPENDIX-A

EFFECT OF GAS PRODUCTION RATE ON CONDENSATE SATURATION DISTRIBUTION IN LAYERS 2 to 4.

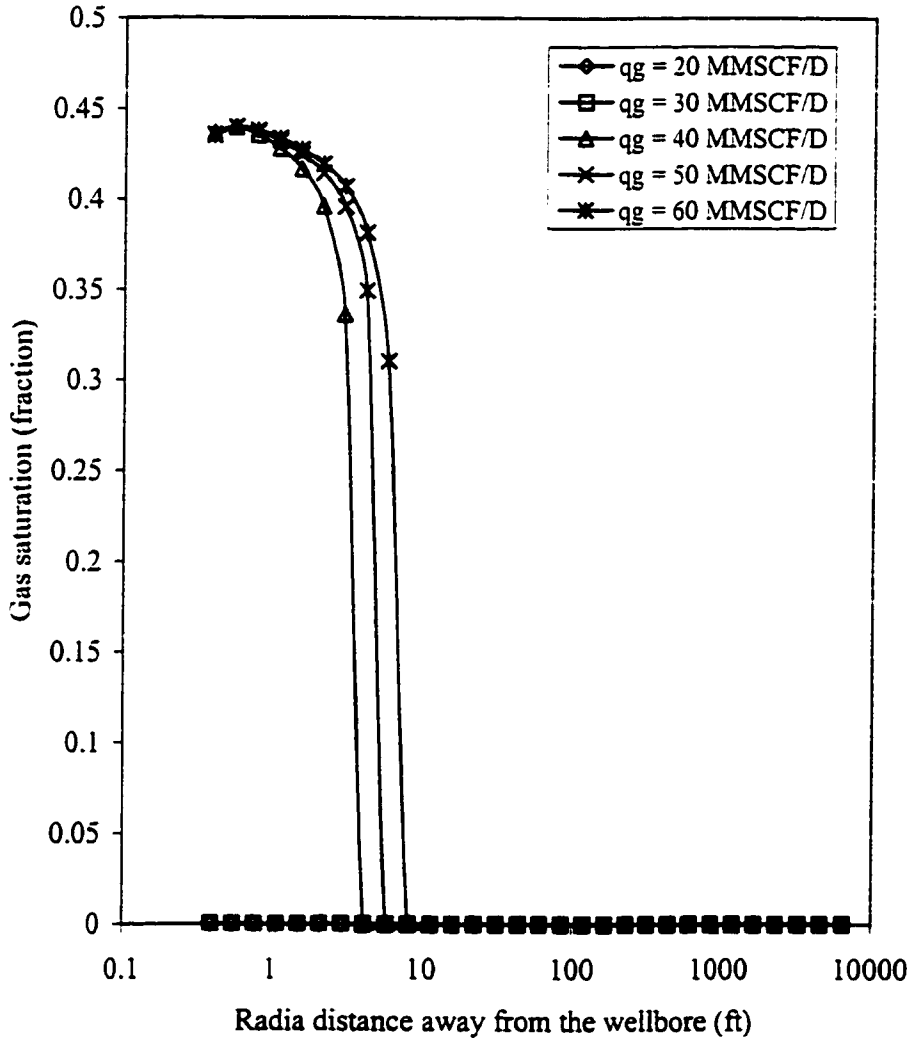

Fig A-1: Effect of gas production rate on condensate saturation distribution in layer 2 at 2 years

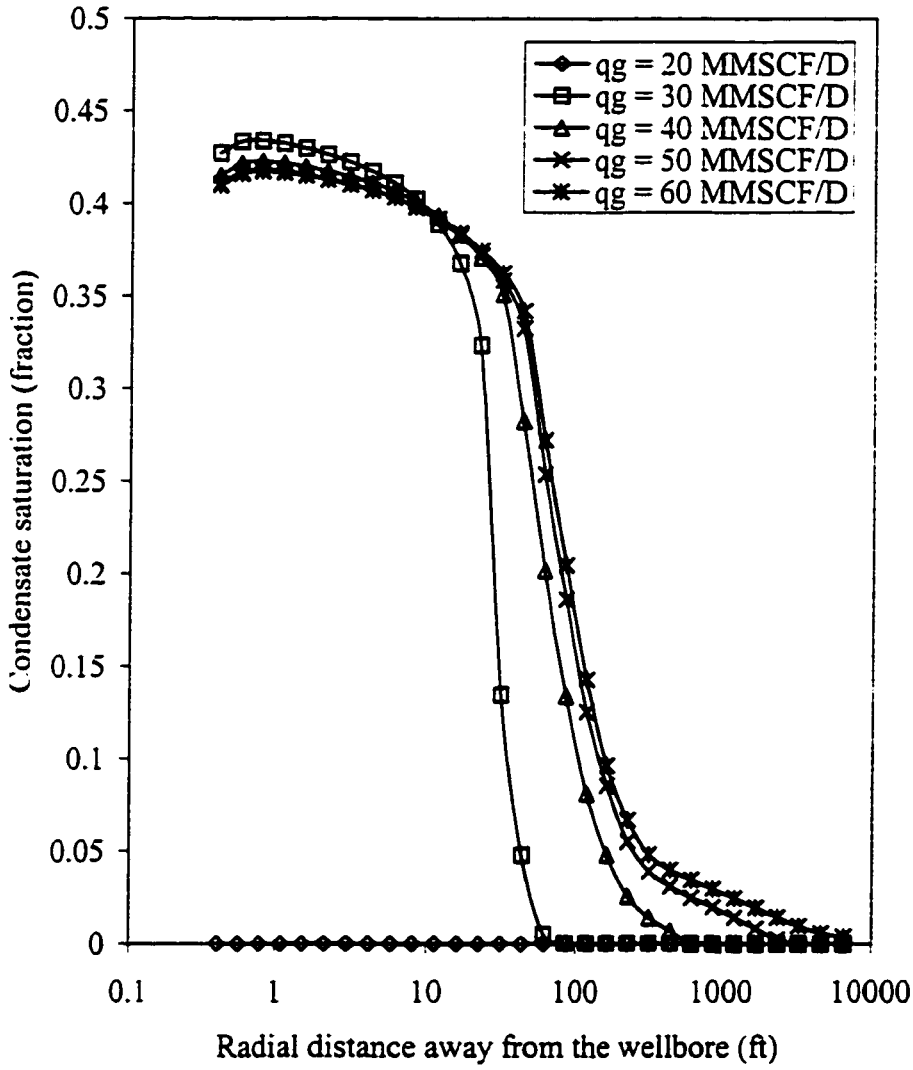

Fig A-2: Effect of gas production rate on condensate saturation distribution in layer 2 at 4 years

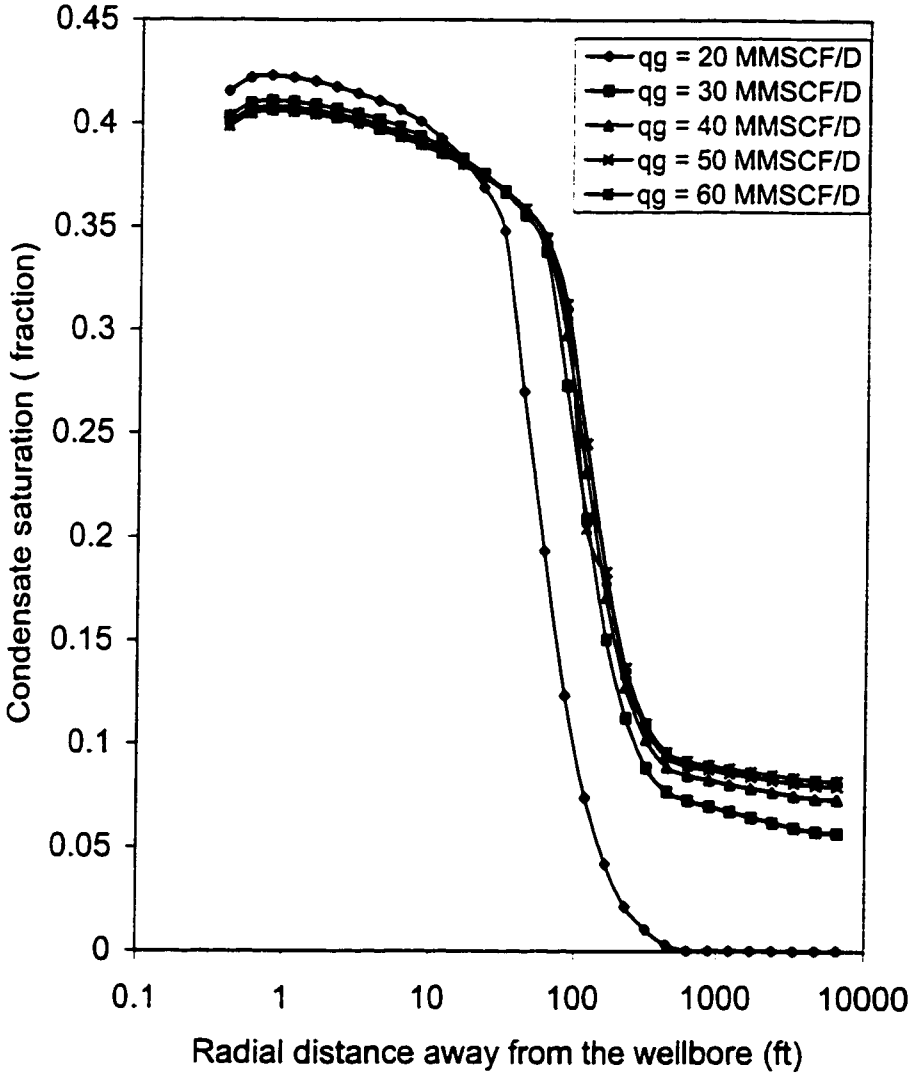

Fig A-3: Effect of gas production rate on condensate saturation distribution in layer 2 at 6 years

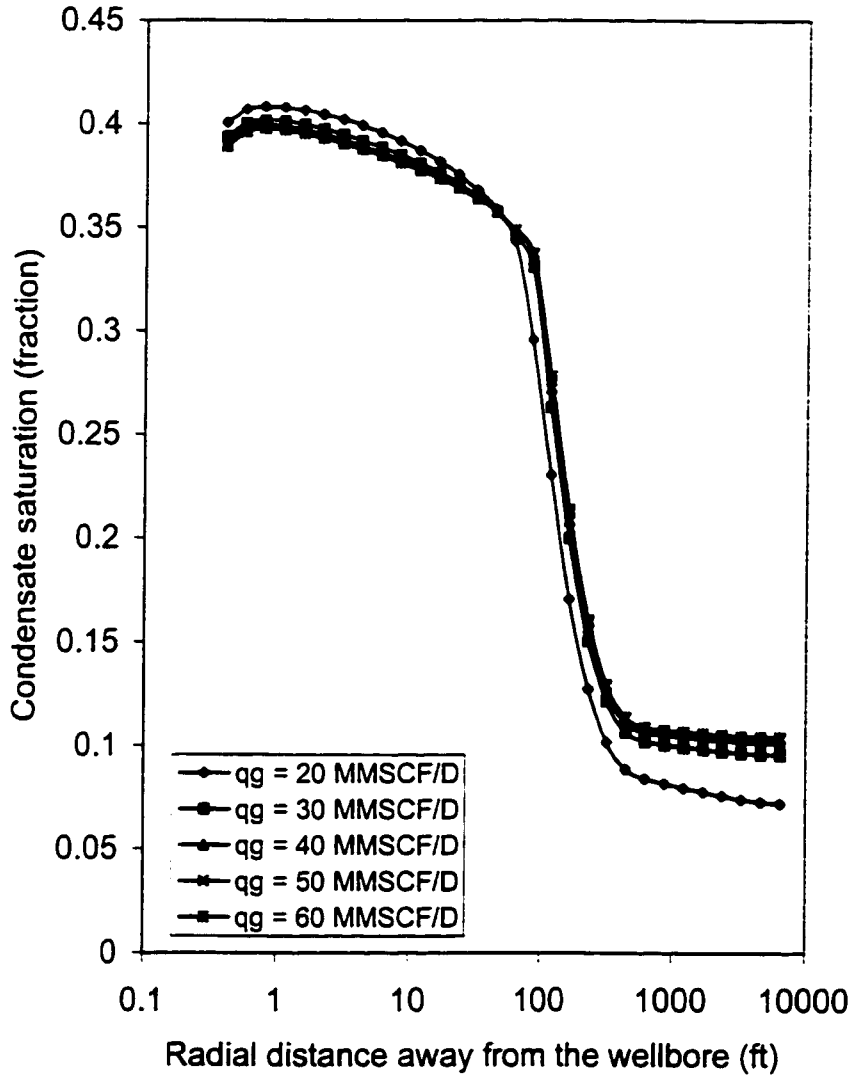

Fig A-4: Effect of gas production rate oncondensate saturation distribution in layer 2 at 8 years

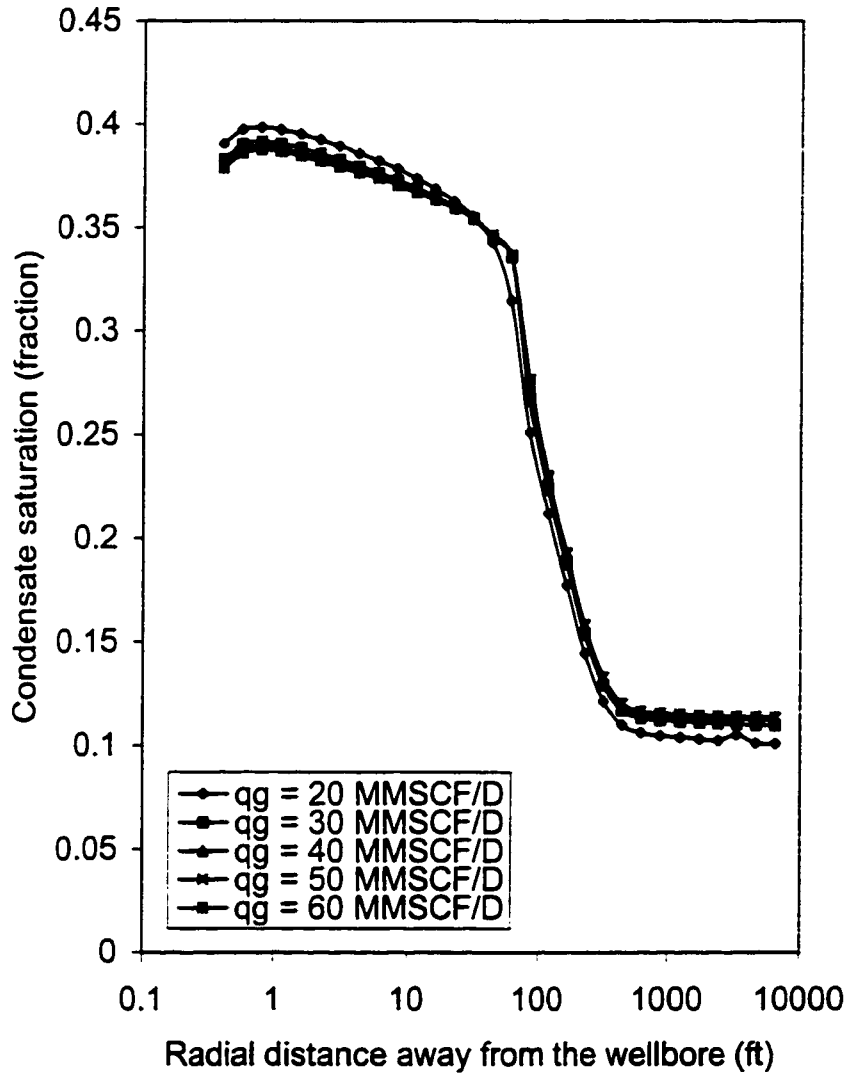

Fig A-5: Effect of gas production rate on condensate saturation distribution in layer 2 at 10 years

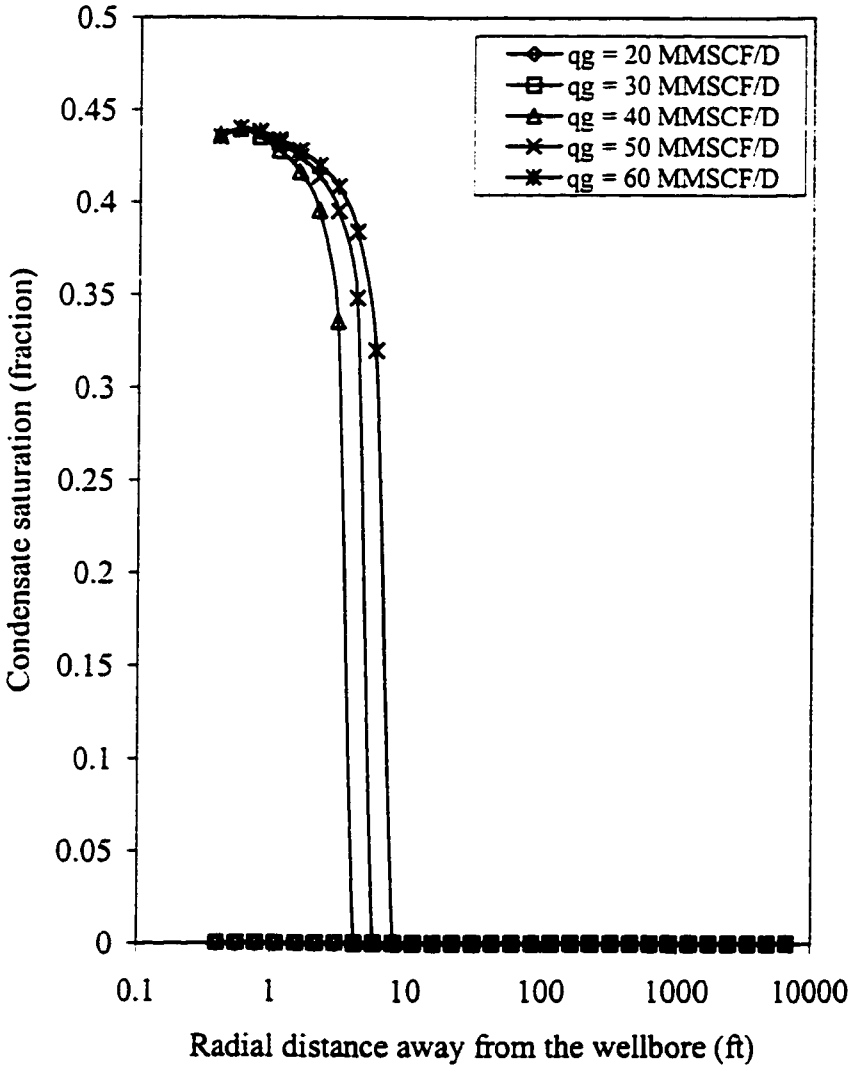

Fig A-6: Effect of gas production rate on condensate saturation distribution in layer 3 at 2 years.

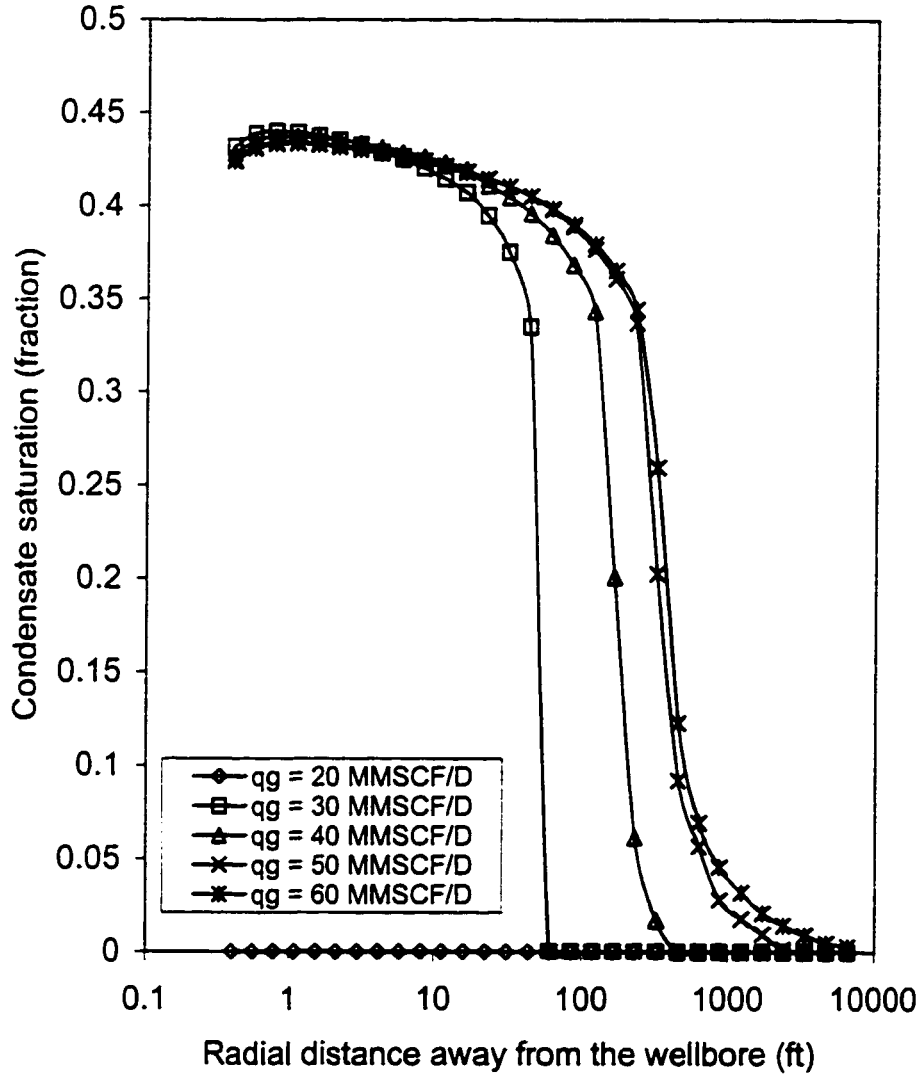

Fig A-7: Effect of gas production rate on condensate saturation distribution in layer 3 at 4 years

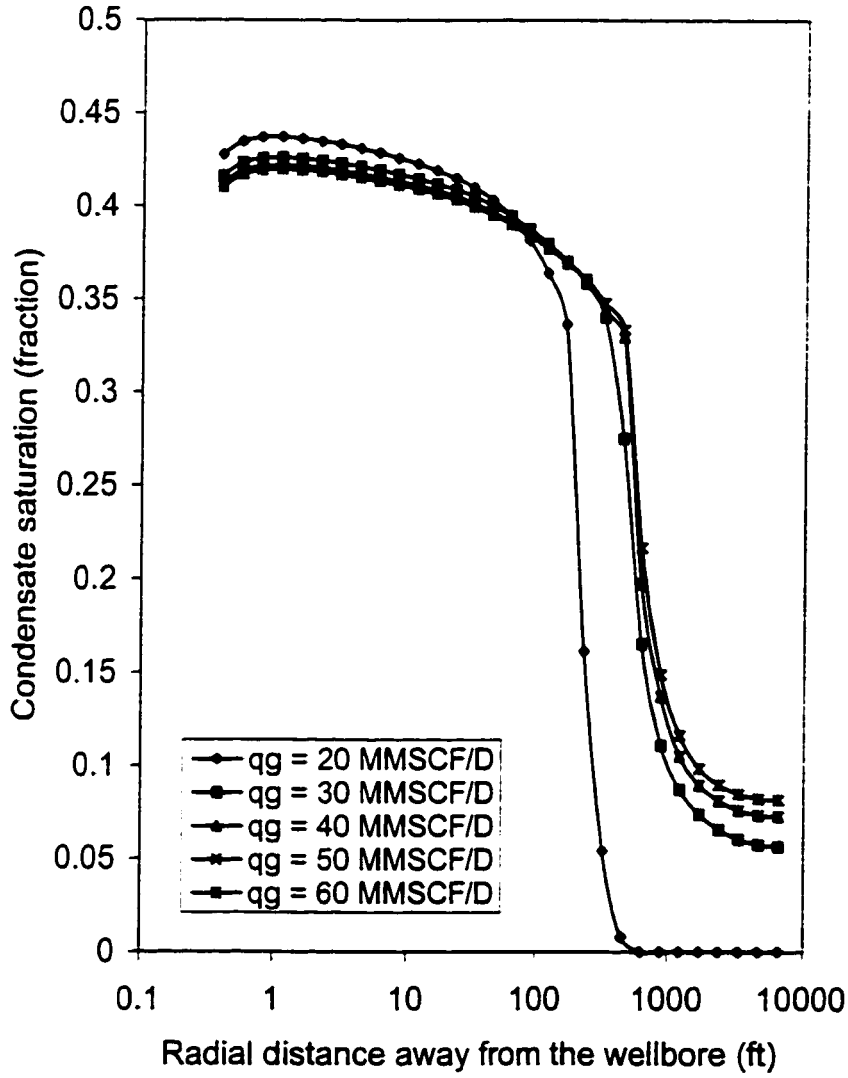

Fig A-8: Effect of gas production rate on condensate saturation distribution in layer 3 at 6 years

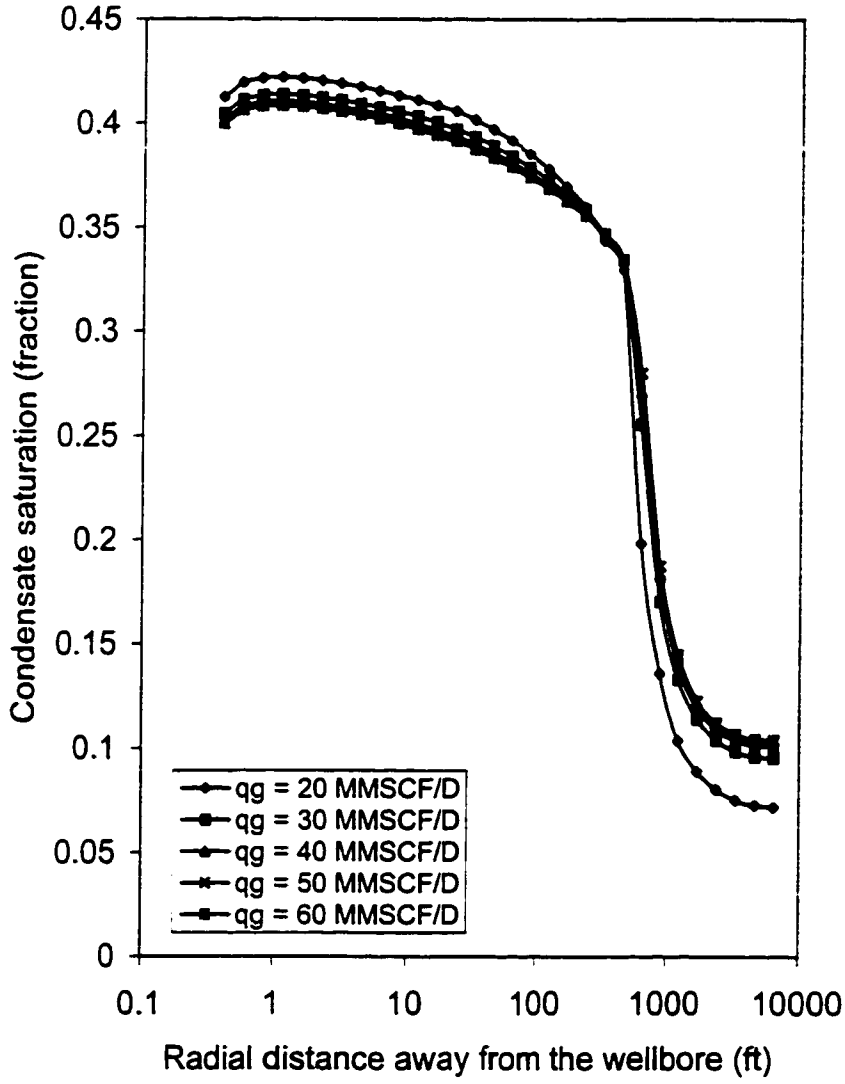

Fig A-9: Effect of gas production rate on condensate saturation distribution in layer 3 at 8 years

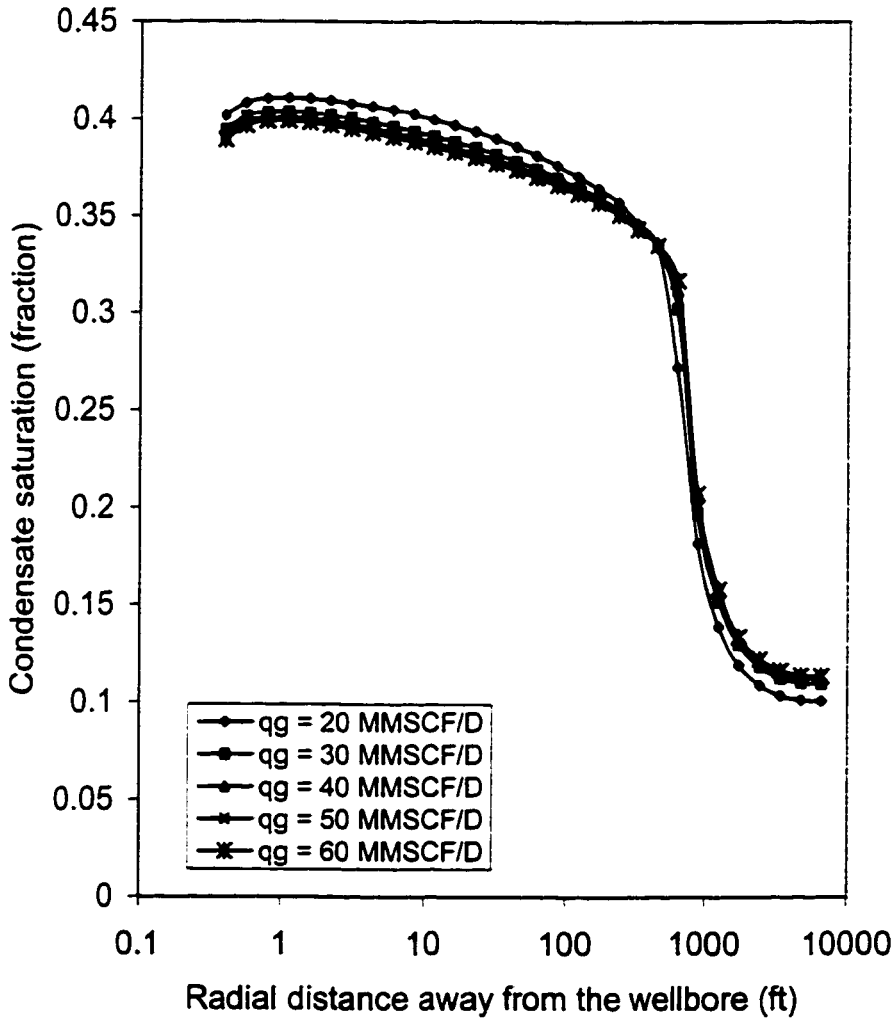

Fig A-10: Effect of gas production rate on condensate saturation distribution in layer 3 at 10 years

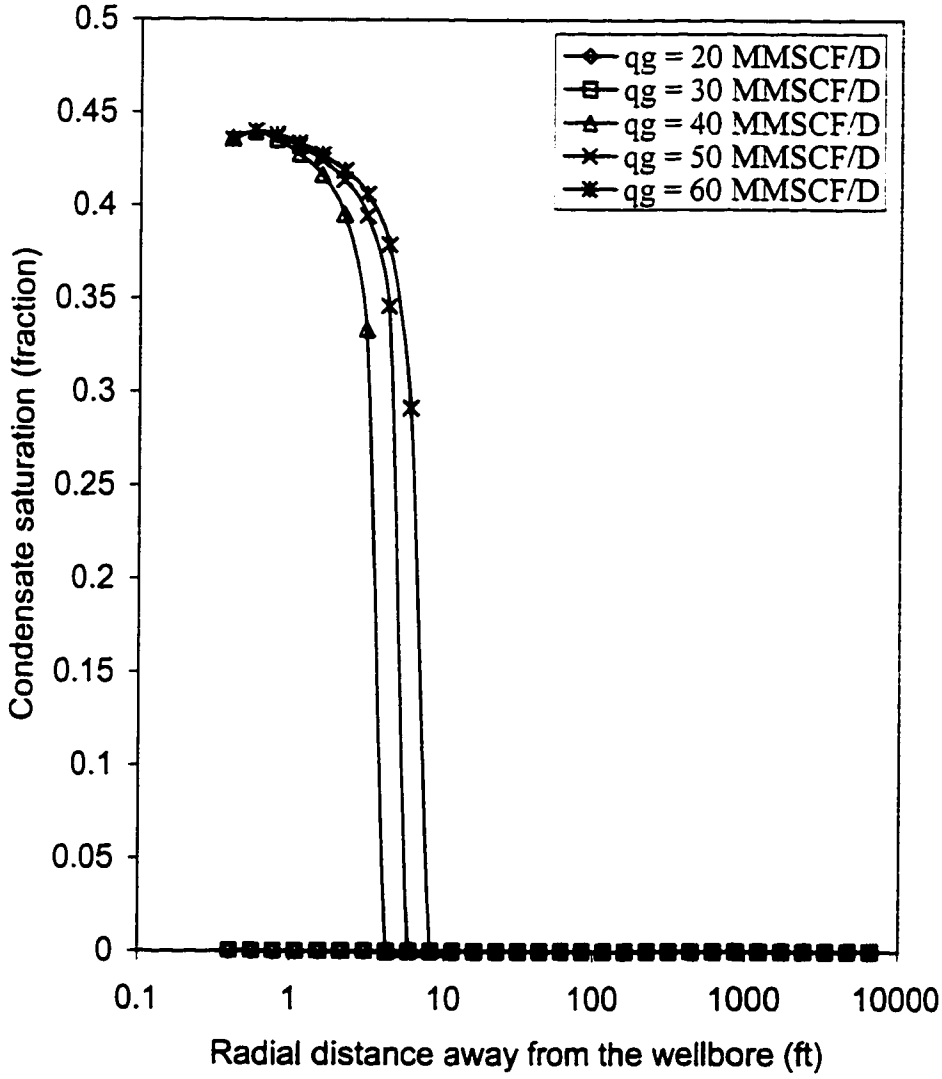

Fig A-11: Effect of gas production rate on condensate saturation distribution in layer 4 at 2 years

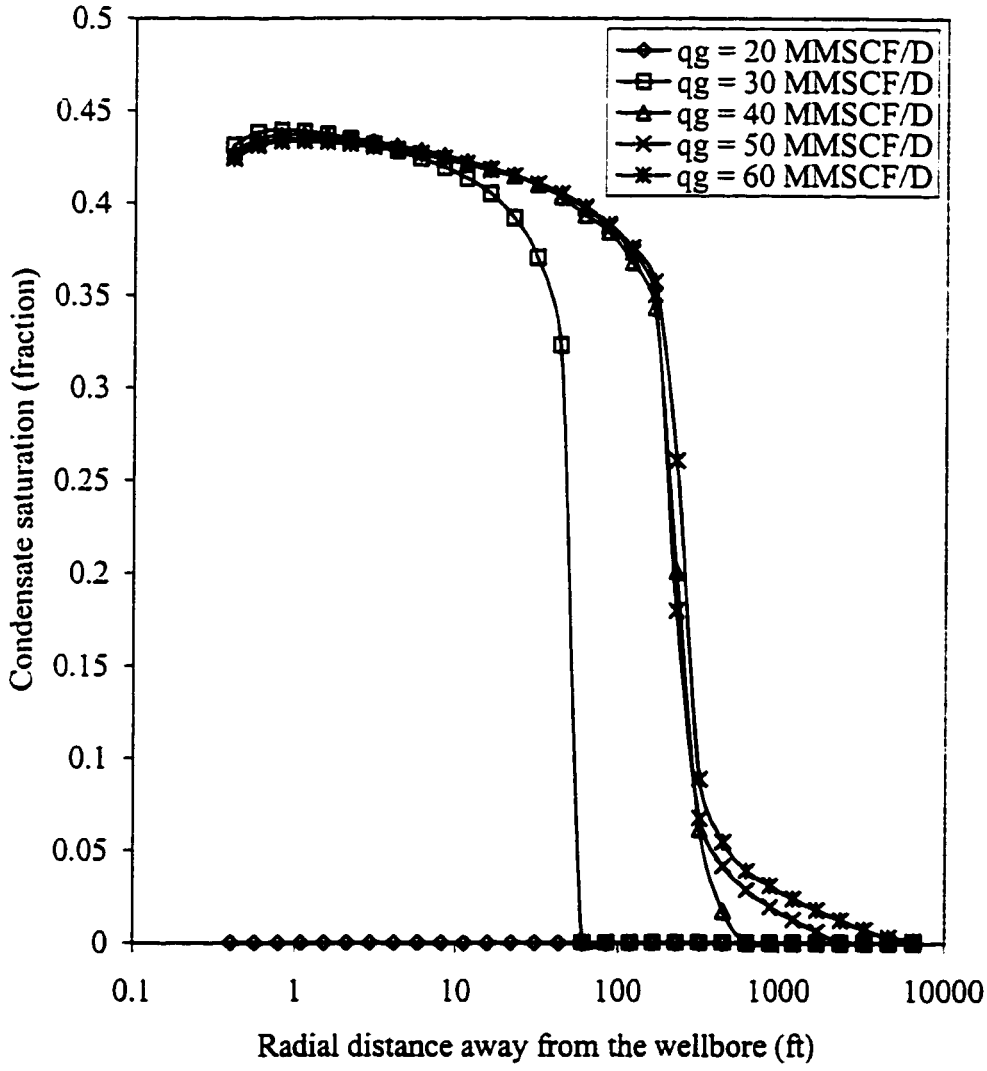

Fig A-12: Effect of gas production rate on condensate saturation distribution in layer 4 at 4 years

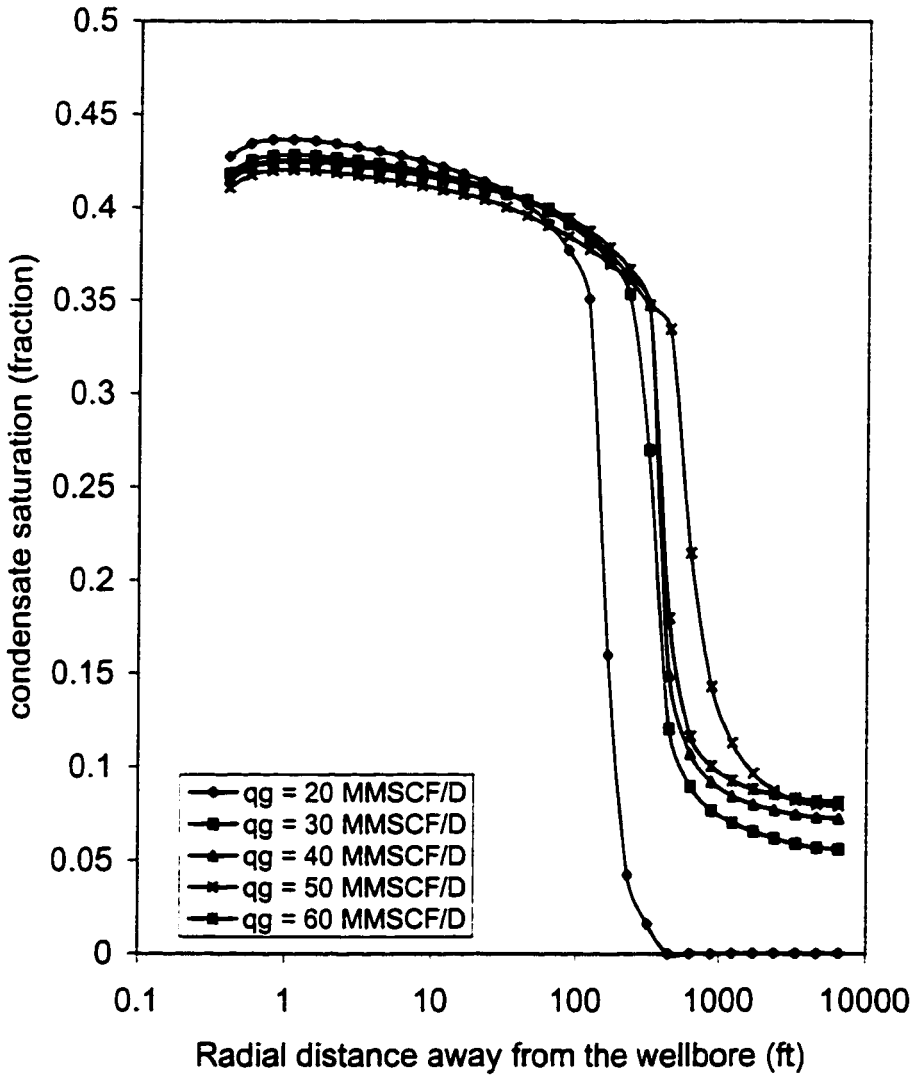

Fig A-13: Effect of gas production rate on condensate saturation distribution in layer 4 at 6 years

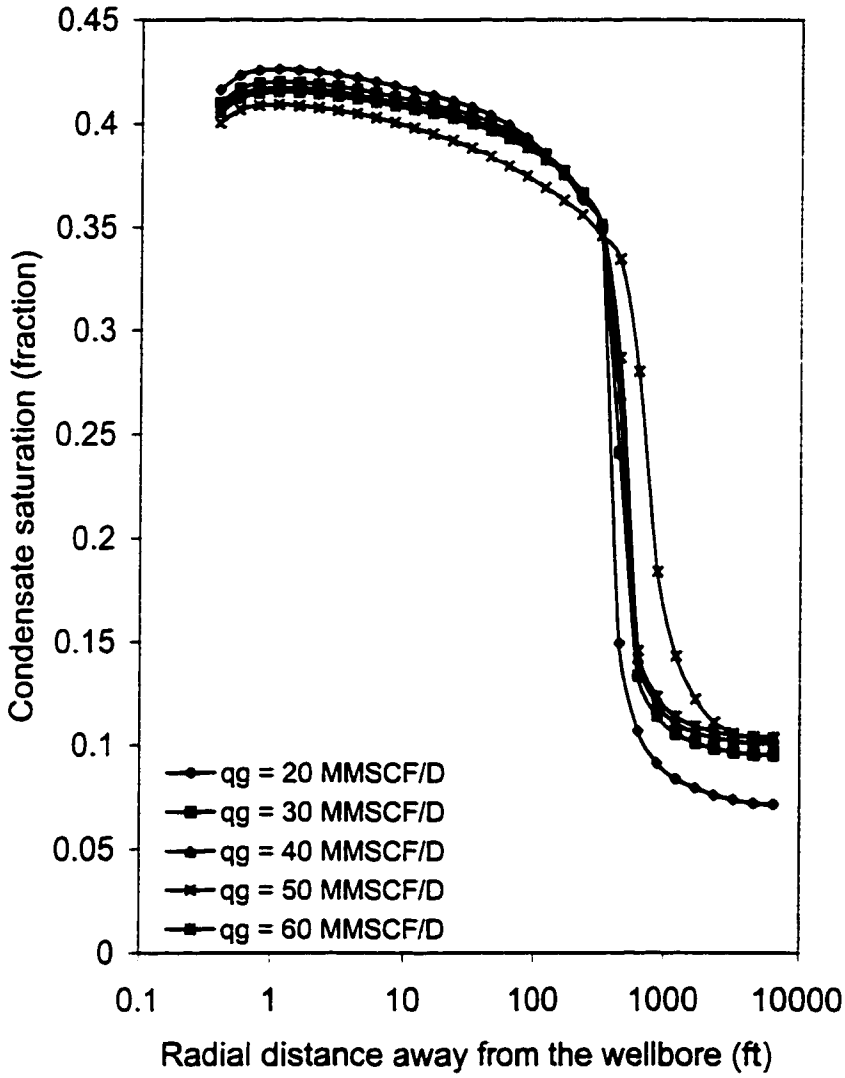

Fig A-14: Effect of gas production rate on condensate saturation distribution in layer 4 at 8 years

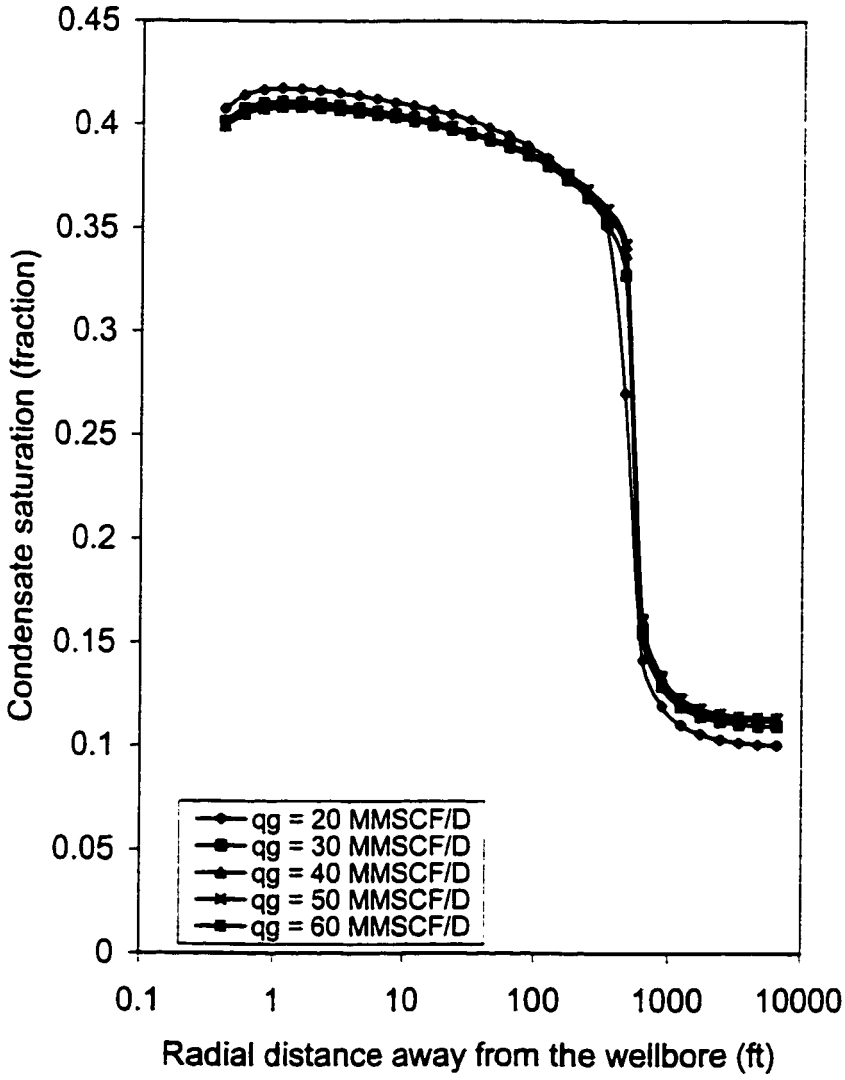

Fig A-15: Effect of gas production rate on condensate saturation distribution in layer 4 at 10 years

APPENDIX-B

INPUT DECK FILE FOR COMPOSITIONAL SIMULATOR

"CHEARS"

```
MEGAWORDS 15.0
*
*----------------------------------------
* PROBLEM DESCRIPTION
*----------------------------------------
*
SIMULATOR CHEARS COMPOSITIONAL
*
*
*TITLE : COMPOSITIONAL SIMULATION STUDIES OF RICH GAS CONDENSATE

*RESERVOIR USING SINGLE WELL MODEL

*****TWO PHASE RELATIVE PERMEABILITY USED IN THIS MODEL.*************
*
********INITIAL WATER SATURATION IS IMMOBILE*****************************
*
START 06-OCT-1999
*
EQNSOLVER DIRECT
*
EXCELFILE
*          RECNUM  IFLAG
RESTART TIMESTEP -1     1
*
FORMULATION  OWG  IMPLICIT
*
*     WELLS   TOTCOMP  WELCOMP
MAXWELL  1      4       4
*   SEPS  STAGES
MAXSEPS 1     3
*      NKR NEQL NMTBLU  NPVTRG MAXPI
NREGIONS  1   1    0     1     1
*
NCOMPONENTS 12
*
*          NR  NTHETA NZ
MODELSIZE  30  1    4
*
*    MTAB  MINIT
MAXTABL 400
*
*NORMSATENDPT
*
*
*----------------------------
* OUTPUT SPECIFICATION
*----------------------------
MAPORIENT XY
*
```

```
MAPSINITIAL PRINT
*
PORVOL
*
MAPSRECUR FILE
 PRESS
 OSAT
 GSAT
 WSAT
 ORELPERM
 GRELPERM
*
GRAPHOUTPUT ISG
*
GRAPHINITIAL
*
PERMX
*
GRAPHRECUR
 ORELPERM
 GRELPERM
*
XYPLOT
 WELLS
*
XYPOUTPUT  ECL  XYP
*
MAPFREQ  2
*
GRAPHFREQ 2
*
XYPLOTFREQ  2
*
WELLFREQ  2
*
IDEBUG  -50
*
COMPFREQ  2
*
WMSOUTPUT 0 2 0
*
*----------------------------
* FLUID PROPERTIES
*----------------------------
*
COMPONENTS
*   NAME        MOL WT
    CO2          44.0100
    N2           28.0130
    METHANE      16.0430
    ETHANE       30.0690
```

```
   PROP          44.0960
   I-C4          58.1230
   N-C4          58.1230
   I-C5          72.1500
   N-C5          72.1500
   N-C6          86.1770
   C10          131.5630
   C25          343.7043
*
OILVISC   LBC  0.0233640  0.0585330 -0.0407580  0.0093324
*
GASVISC   LBC  0.0233640  0.0585330 -0.0407580  0.0093324
*
PARACHOR
        49.0  35.0  71.0  111.0  151.0  191.0  191.0  231.0
231.0 271.0  512.1 1253.4
*
EOSPARMS
* NAME   PC(PSIA)   TC(F)  VC(ft3/lbmol)  W      SC    OMEGAA  OMEGAB
 CO2       1070.6036   87.8720  1.5058   0.2276  0.0000  0.457240  0.077800
 N2         492.3160 -232.6900  1.4433   0.0403  0.0000  0.457240  0.077800
 METHANE 667.8010 -116.6260  1.5899   0.0108  0.0000  0.457240  0.077800
 ETHANE    707.8034   90.0860   2.3696   0.0990  0.0000  0.457240  0.077800
 PROP      616.2915  206.0060  3.2500   0.1517  0.0000  0.457240  0.077800
 I-C4      529.1001  274.9820  4.2082   0.1770  0.0000  0.457240  0.077800
 N-C4      550.6885  305.6540  4.0849   0.1931  0.0000  0.457240  0.077800
 I-C5      490.4055  369.1040  4.8992   0.2275  0.0000  0.457240  0.077800
 N-C5      488.6126  385.7000  5.0034   0.2486  0.0000  0.457240  0.077800
 N-C6      436.8974  453.7039  5.9292   0.3047  0.0000  0.457240  0.077800
 C10       356.5999  652.0421 10.2718  0.4062  0.0000  0.457240  0.077800
 C25       176.6897 1049.6464 28.1453  0.9255  0.0000  0.457240  0.077800
*
BININTCOEF
*
-0.0200
 0.1000 0.0360
 0.1300 0.0500 0.0020
 0.1350 0.0850 0.0070 0.0010
 0.1300 0.0950 0.0120 0.0030 0.0000
 0.1300 0.0950 0.0120 0.0030 0.0000 0.0000
 0.1250 0.0950 0.0170 0.0040 0.0010 0.0000 0.0000
 0.1250 0.0950 0.0180 0.0050 0.0020 0.0000 0.0000 0.0000
 0.1250 0.1000 0.0240 0.0070 0.0030 0.0010 0.0010 0.0000 0.0000
 0.1250 0.1000 0.0230 0.0100 0.0100 0.0000 0.0000 0.0000 0.0000 0.0000
 0.1250 0.1000 0.0373 0.0100 0.0100 0.0000 0.0000 0.0000 0.0000 0.0000 0.000
*
*          BGNPRESS ENDPRESS PINCR
KVALUES PREOS  14.700  9014.700 50.0
*
WATPROP 14.7  3.467  0.7  1.0  3.628E-06  0.0
*
```

```
RESTEMP   301.000
*
*-----------------------------------
* RELATIVE PERMEABILITY
*-----------------------------------
WATEROILPOWER   1
*SW          SORW        KRWRO       KROCW       WEXP  OEXP
0.33         0.1         0.0         1.0         2.0    2.0
*
*            REGNUM
OILGASPERM   1
*SG                KRG                KROG               PCOG
0.0                0.0                1.00               0.0
0.1                0.0                2.59E-01           0.0
0.15               5.53E-03           1.18E-01           0.0
0.2                2.56E-02           4.86E-02           0.0
0.25               6.25E-02           1.76E-02           0.0
0.3                1.17E-01           5.35E-03           0.0
0.32               1.43E-01           3.12E-03           0.0
0.33               1.57E-01           2.35E-03           0.0
0.40               2.74E-01           2.10E-04           0.0
0.50               4.92E-01           4.21E-07           0.0
0.55               6.23E-01           6.55E-11           0.0
0.60               7.69E-01           0.0                0.0
0.65               9.31E-01           0.0                0.0
0.67               1.0                0.0                0.0
*
* ROCK COMPRESS REF.PRESS  REGNUM
RCOMPRESS  4.58E-06   8714.7     1
*
*
*-------------------------------------------------------------------
* INITIALIZATION
*-------------------------------------------------------------------
*              DEPTH   PRESSURE   WOC     GOC
EQUILIBRIUM   14236.0   8804.7      #       #
* COMPINIT    IDEW        SATP
COMPINIT      DEW         5153.0
EQUILCMP
    0.0270 0.0349 0.65070 0.1050 0.04970 0.00950 0.01870
    0.0077 0.00780 0.0125 0.064446 0.012054
*
SEPSTAGE  FIELD
* PRESSURE  TEMPERATURE
 1014.7    100.0
  214.7    100.0
   14.7     60.0
*
*-----------------------------------
* ARRAY DATA
*-----------------------------------
```

```
*
RADIAL
*
* RWEL  R1   ROUT    ANGLE   DEPTH    DIP
  0.35    0.4   6557.4   360.0     14342.0   0.0
*-------------------------------------
*THICKNESS
DZ
*
18.0 14.0 10.0 8.0
*-------------------------------------
*
TDEPTH
*
LAYER 1 = 14342.0
LAYER 2 = 14370.0
LAYER 3 = 14390.0
LAYER 4 = 14415.0
*
POROSITY
*
LAYER 1 = 0.1256
LAYER 2 = 0.1788
LAYER 3 = 0.1729
LAYER 4 = 0.1757
*
RPERM
*
LAYER 1 = 0.1992
LAYER 2 = 0.3333
LAYER 3 = 115.66
LAYER 4 = 21.68
*
ZPERM
*
LAYER 1 = 0.01992
LAYER 2 = 0.03333
LAYER 3 = 11.566
LAYER 4 = 2.1680
*
*
*-----------------------------------
* RECURRENT DATA
*-----------------------------------
*
TIME    0.000E+0
*
WELLDEF  PRD
*
WELLCOMP  PRD
* I  J  K  PI  RW          STATUS
```

```
 1 1 1 # 0.35        OPEN
 1 1 2 # 0.35        OPEN
 1 1 3 # 0.35        OPEN
 1 1 4 # 0.35        OPEN
*
SEPDEF   SEP
SEPSTAGE  SEP
* PRESSURE  TEMPERATURE
   1014.7            100.0
   214.7             100.0
   14.7              60.0
*
WELLSEP  PRD  SEP
*
MAXGAS   PRD  20000.0
*
MINBHP   PRD   500.0
*
TSLIM   1.0E-8     120
*
TIME          365.0
*
TIME          730.0
*
TIME          1095.0
*
TIME          1460.0
*
TIME          1825.0
*
TIME          2190.0
*
TIME          2555.0
*
TIME          2920.0
*
TIME          3285.0
*
TIME          3650.0
*
*
STOP
```